Lecture 7: InSAR

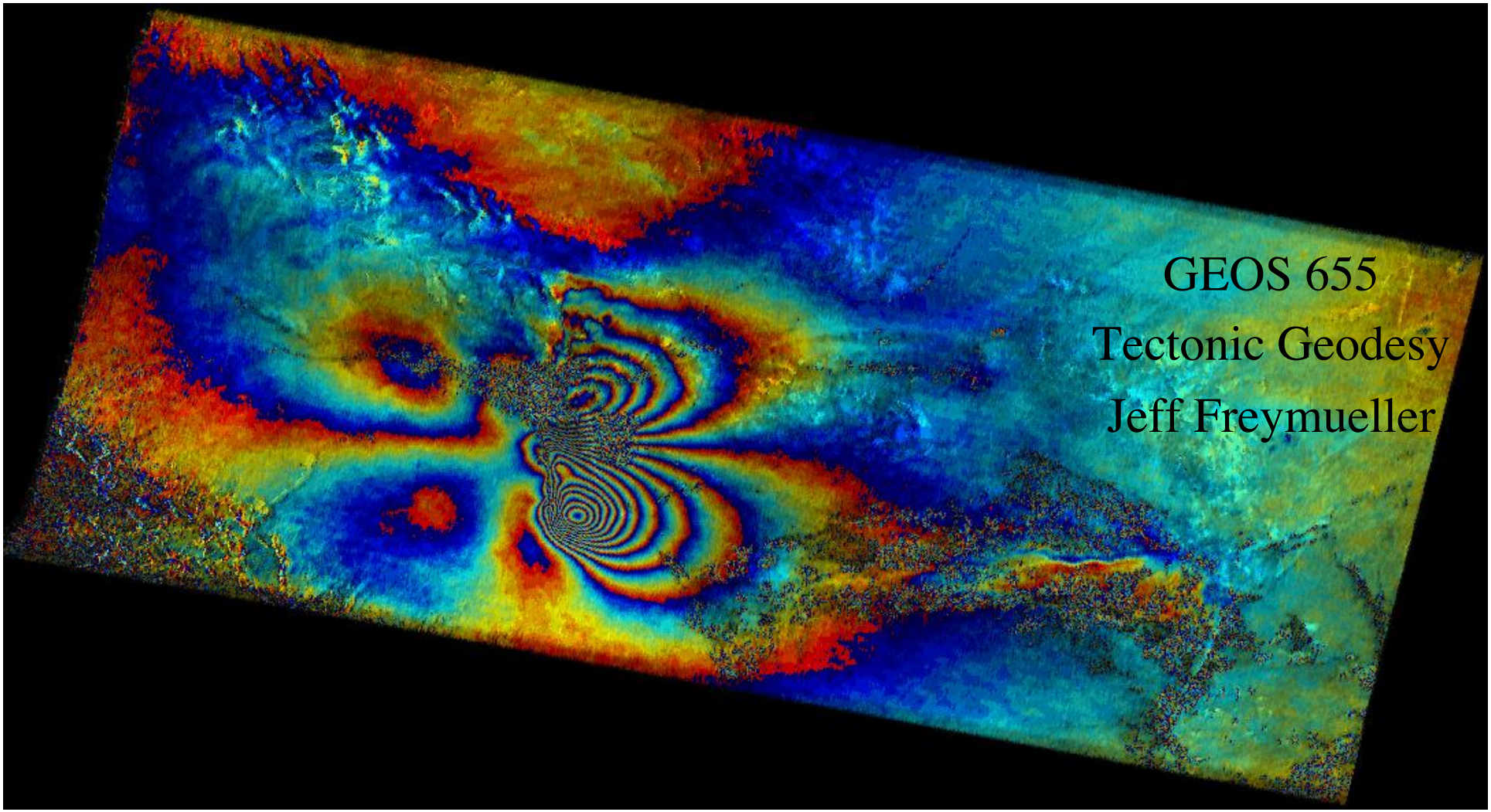

Thanks to Ramón Hanssen, Mark Simons, Dörte Mann, and Howard Zebker for slides and images

The Picture That Started the Excitement

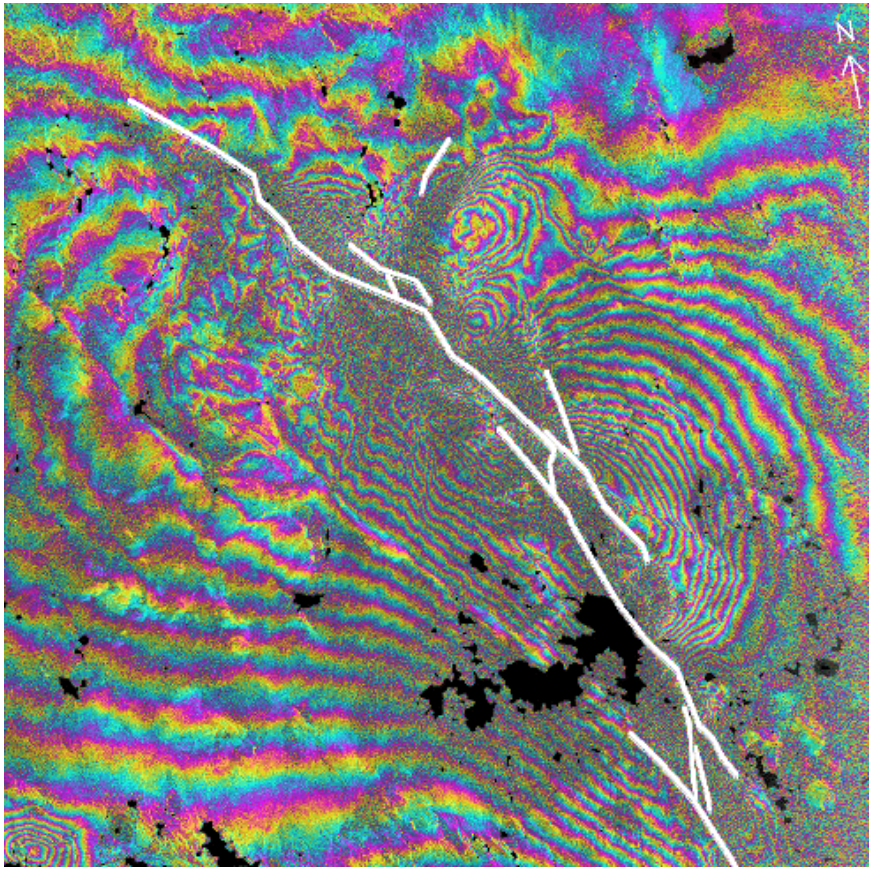

Landers earthquake, first shown by Massennet et al. (1993)

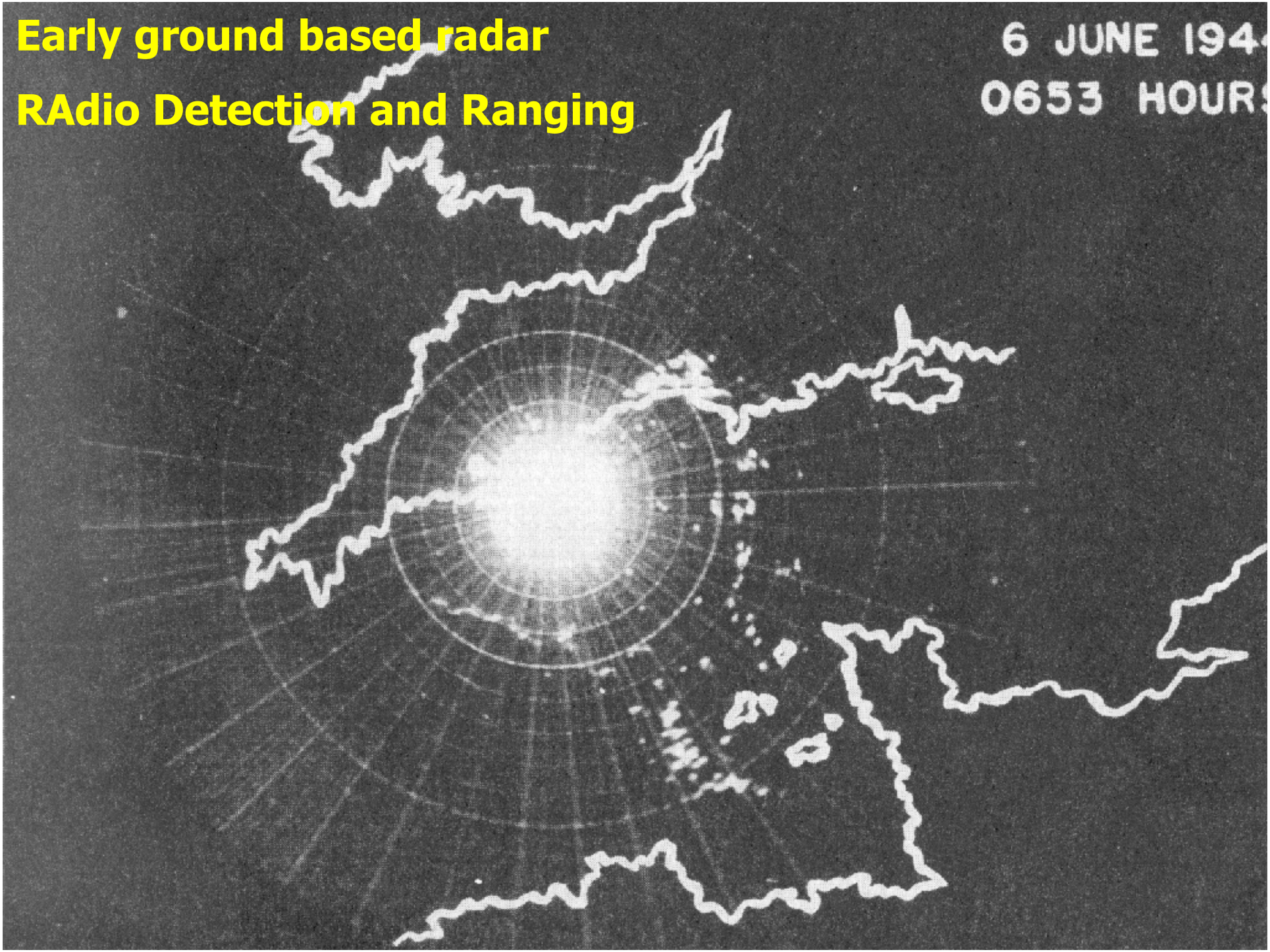
Early ground based radar
RAdio Detection and Ranging
6 JUNE 194
0653 HOUR

Radio waves, active sensor

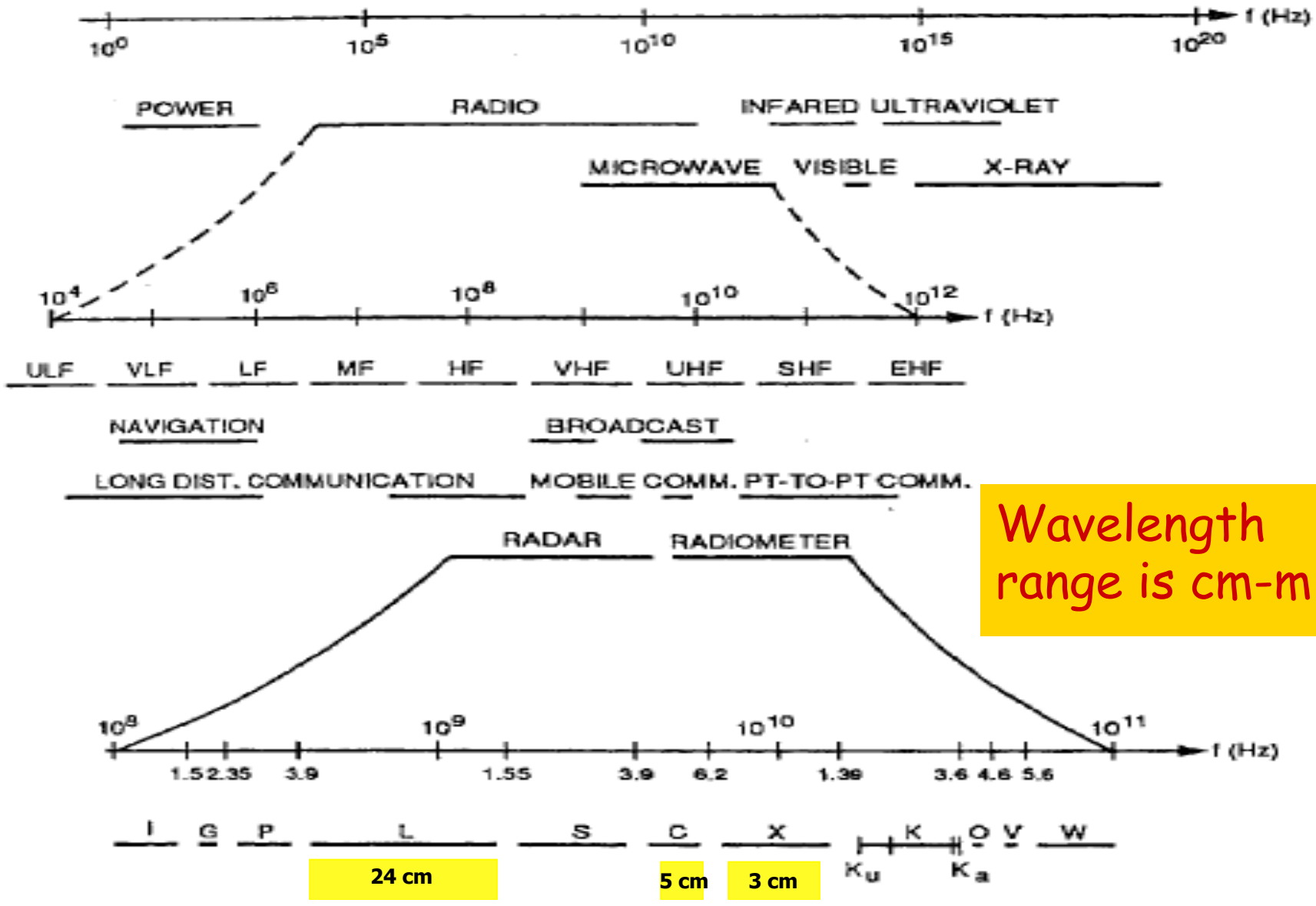

Wavelength range is cm-m

Penetration (weather independent)

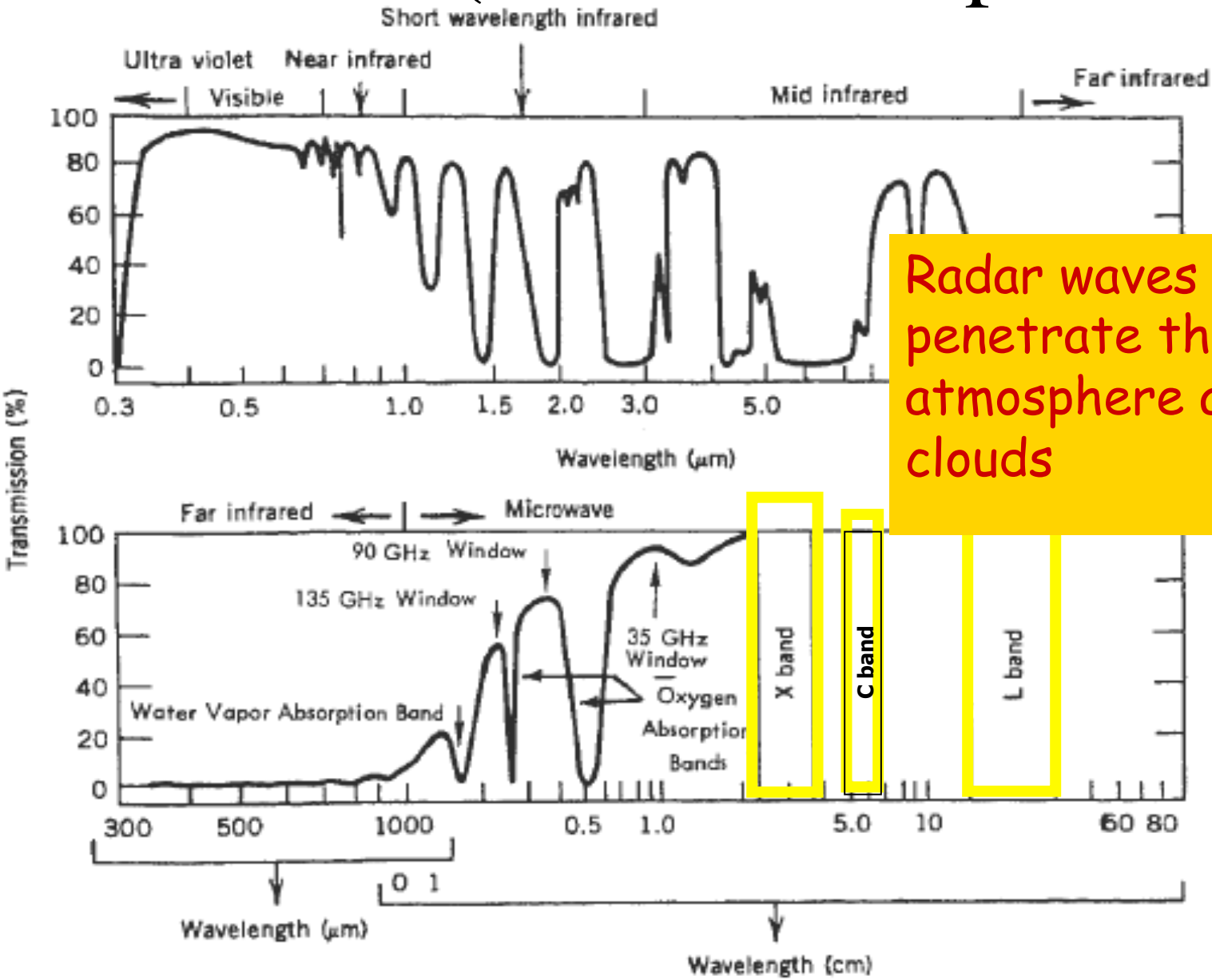

Radar waves penetrate the atmosphere and clouds

InSAR Platforms

Aircraft: Shown here: AIRSAR
Measures topography, ocean currents

Satellites: Repeat pass
Fly over once, repeat days-years later
* Measures deformation and topography

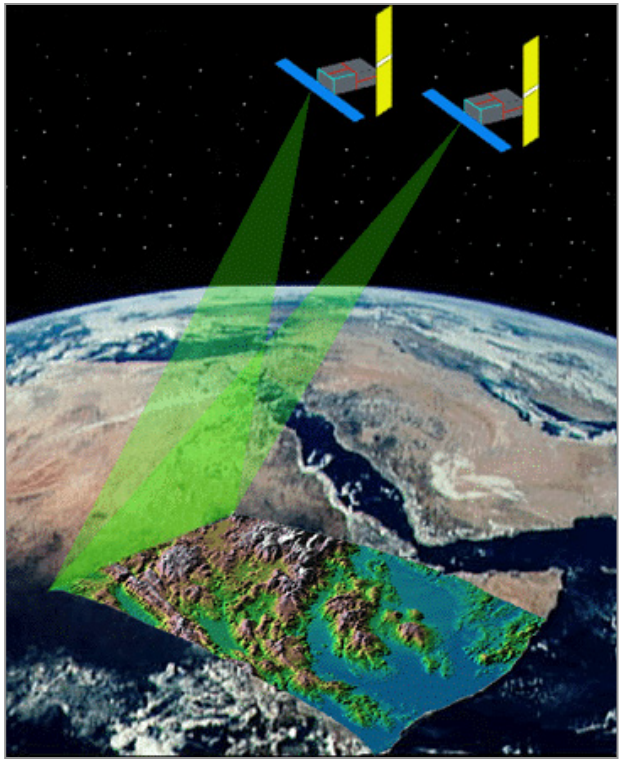

Space shuttle:
Shuttle Radar Topography Mission (SRTM)

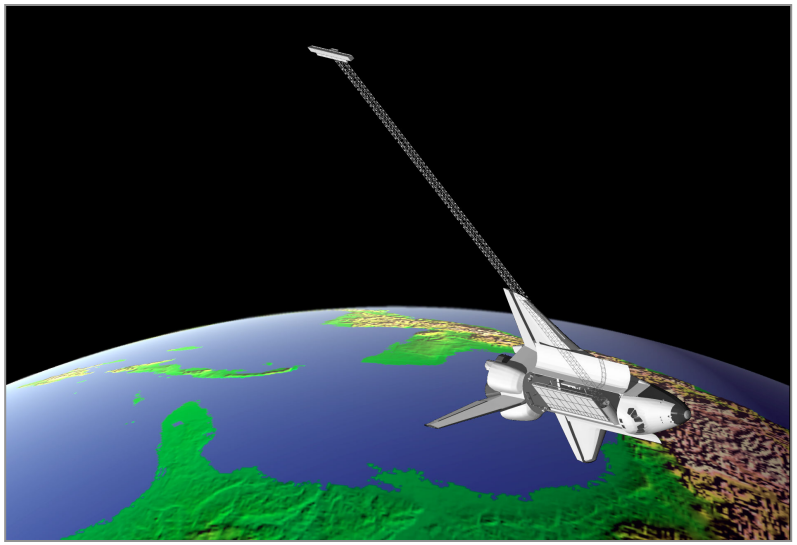

Early SAR/InSAR Missions

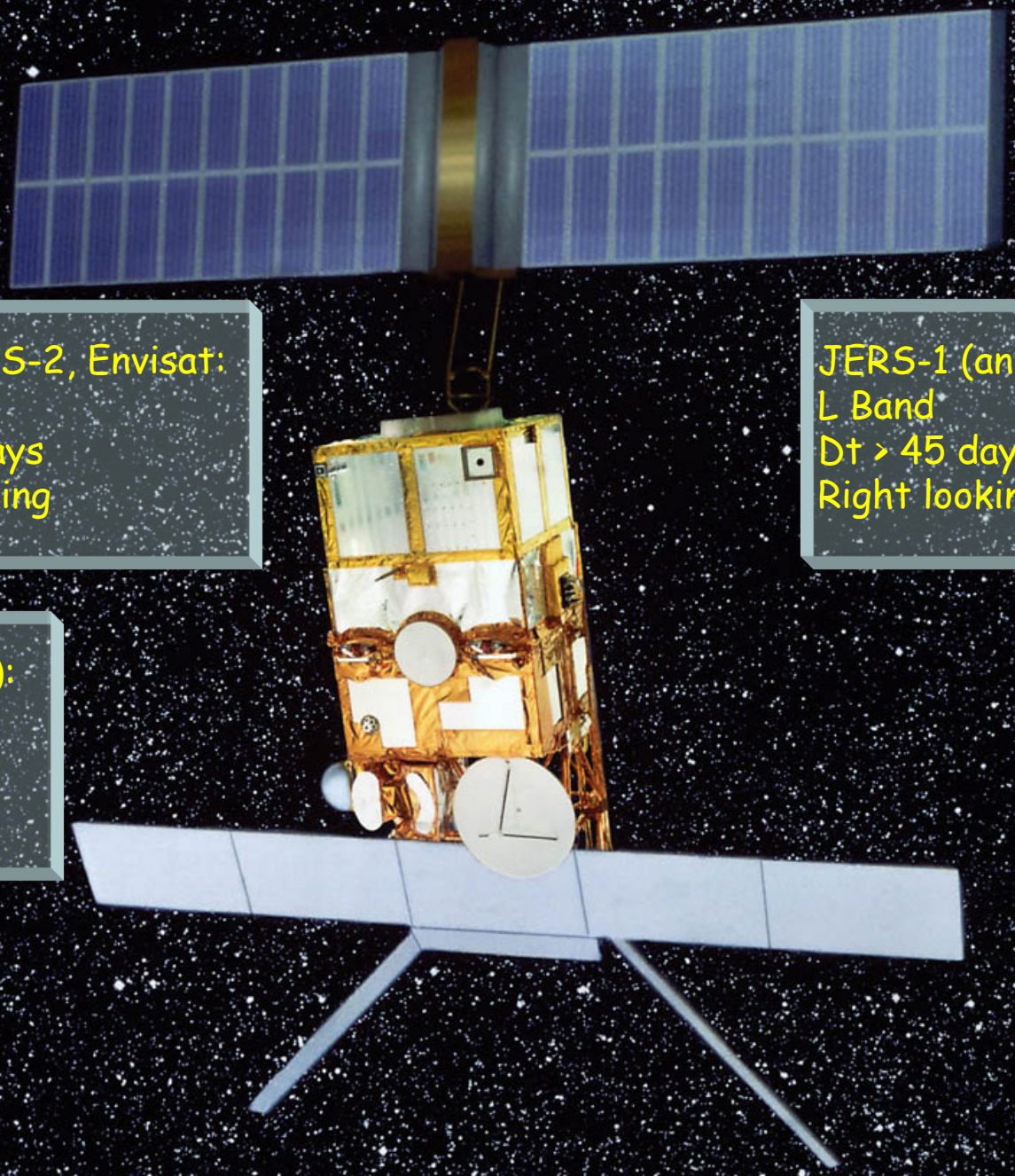

ERS-1, ERS-2, Envisat:
C Band
Dt > 35 days
Right looking

JERS-1 (and ALOS):
L Band
Dt > 45 days
Right looking

Radarsat 1 (and 2):
C Band
DT > 23 days
Right looking

SAR Satellite Timeline

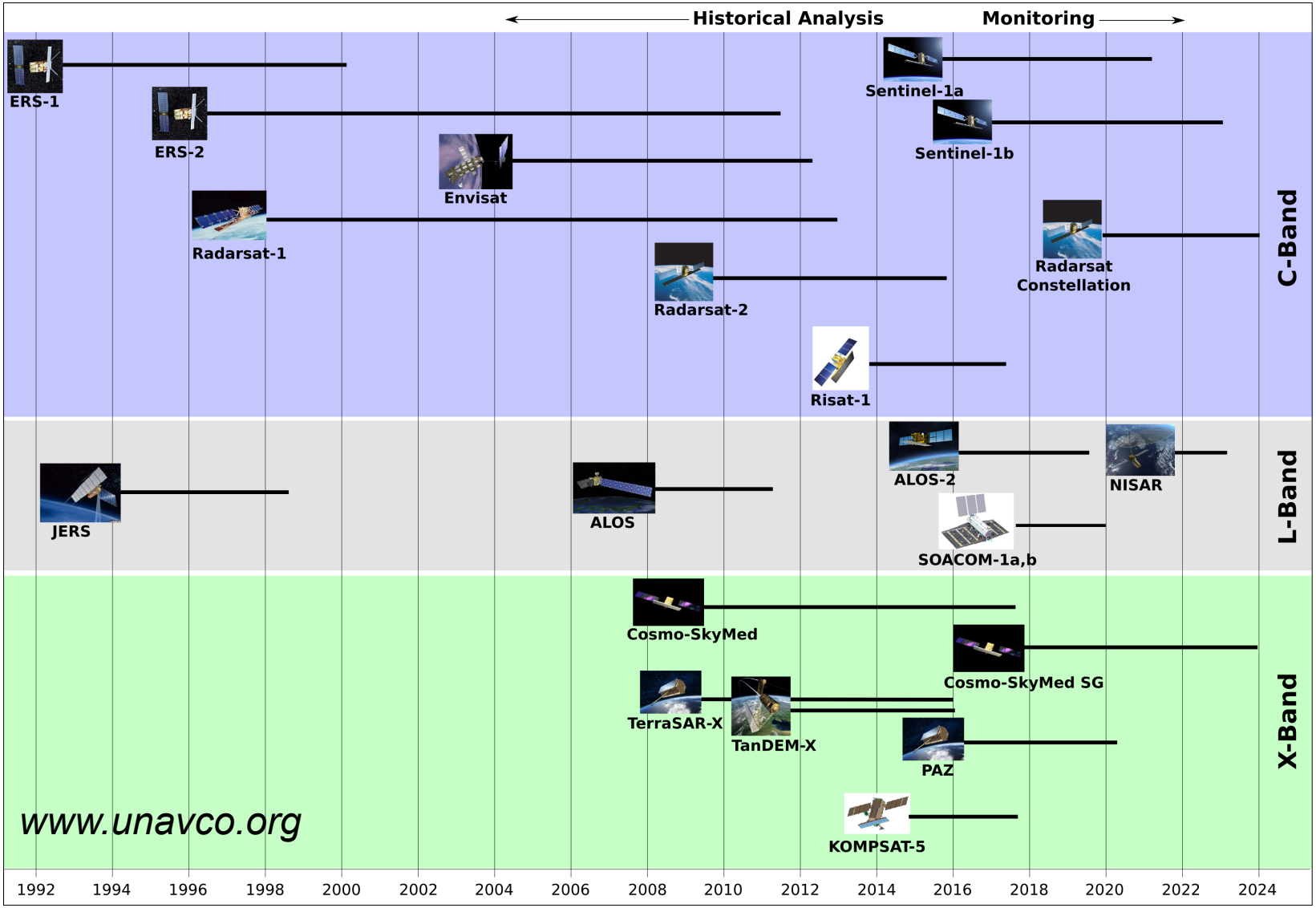

Physics

Sahara, NW Sudan (SIR-A)

- Landsat optical
- Shuttle L-band radar
- What do we see?

Radar penetrates material with a low dielectric constant (dep. on wavelength)

Here about 3 m.

Physics - Scattering

- Scattering is dominated by wavelength-scale structures
- Wavelength shorter: image brighter
- Specular and Bragg scattering
- Speckle

Backscatter

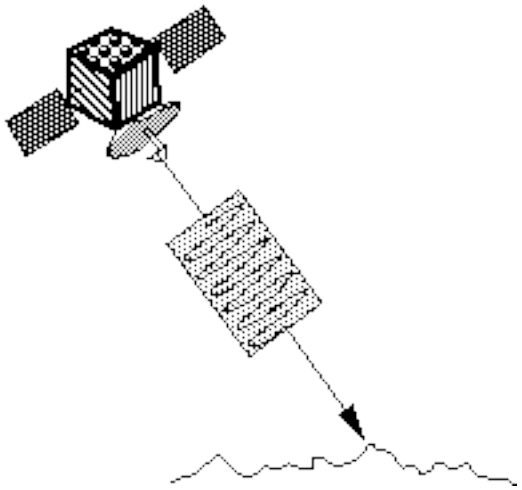

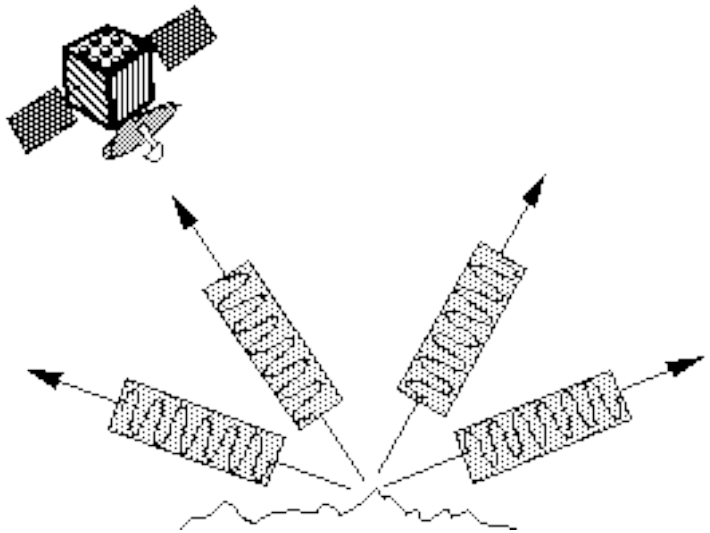

Scattering

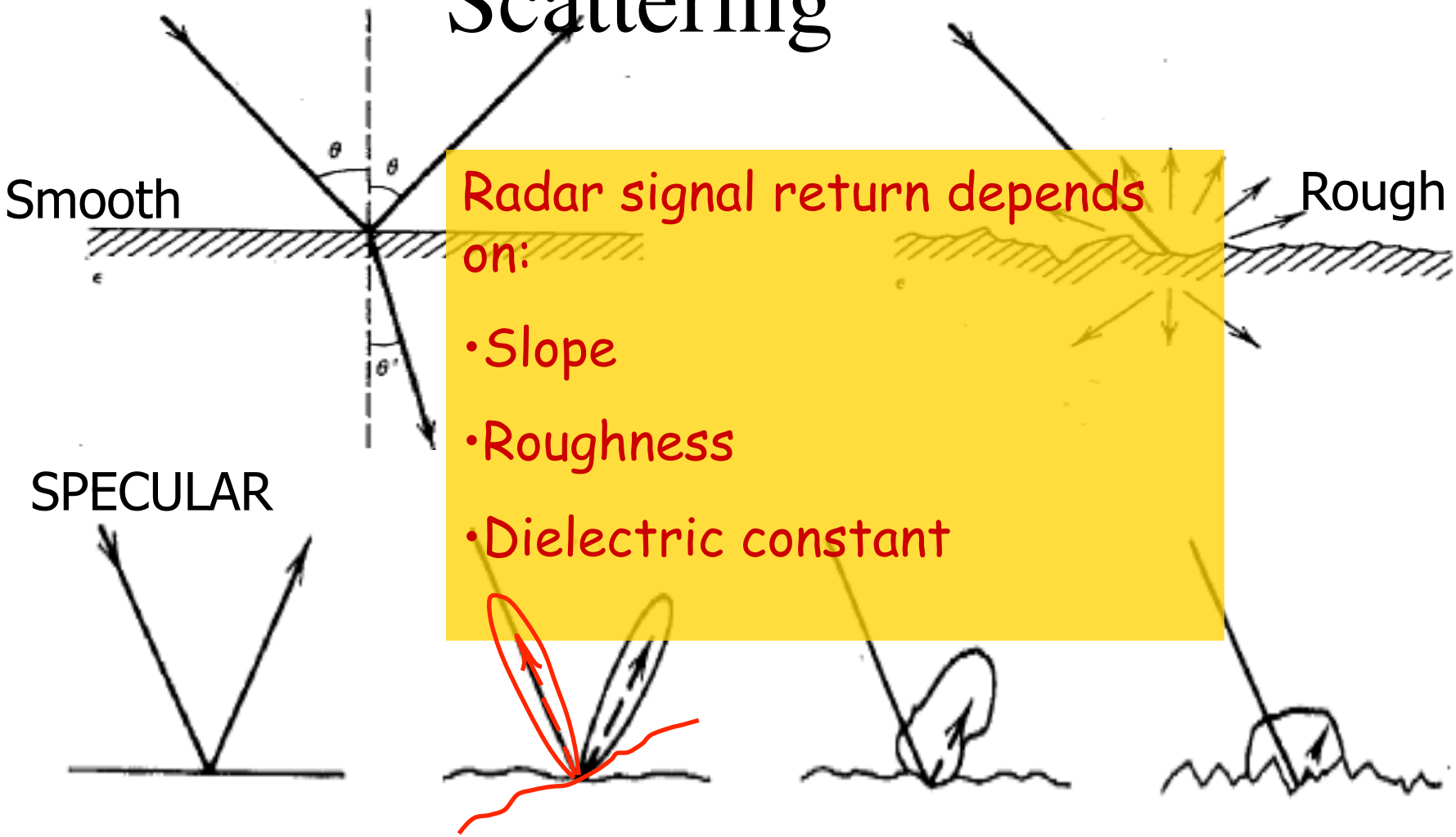

Radar signal return depends on:

- Slope
- Roughness
- Dielectric constant

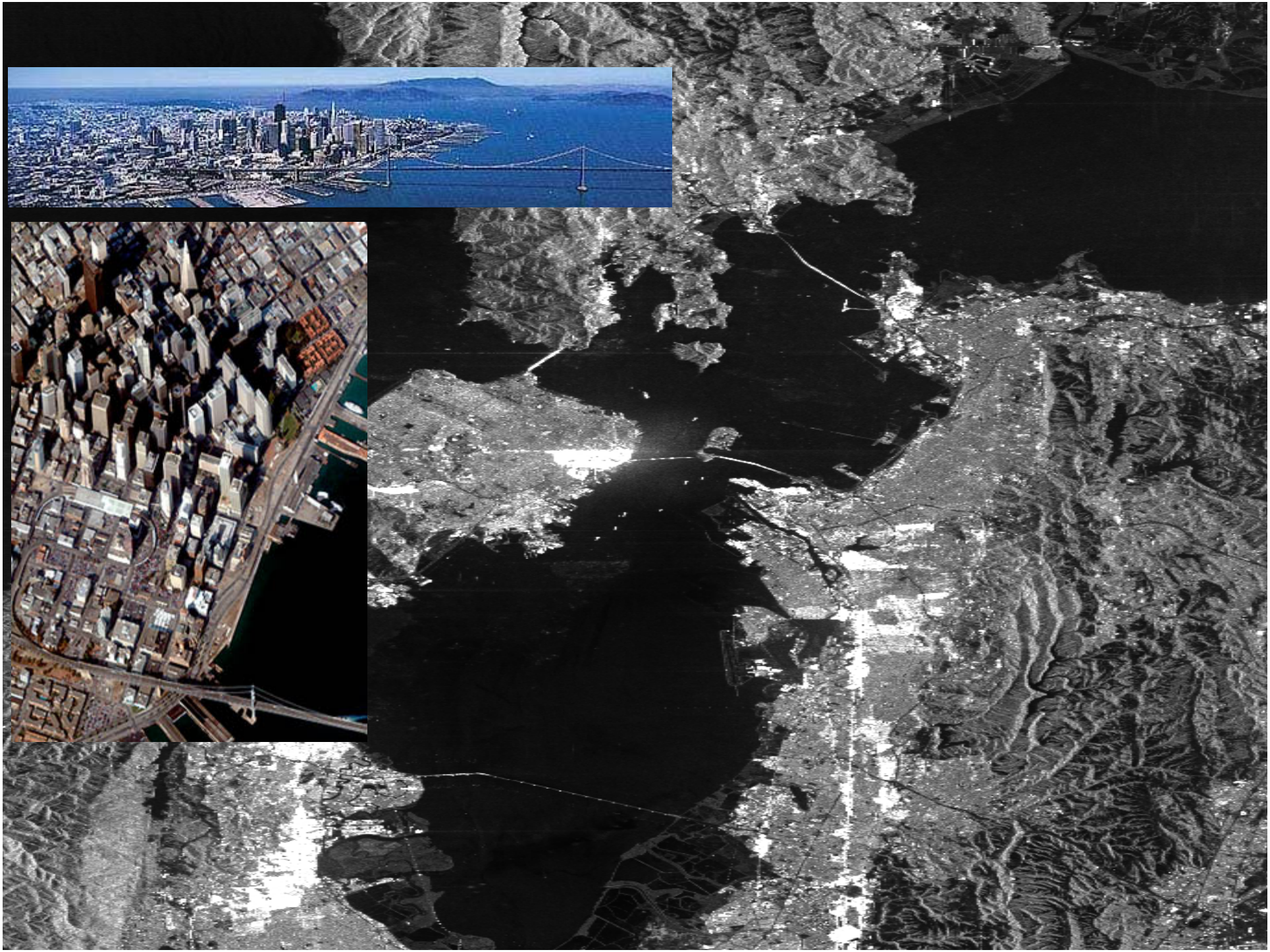

Physics – scattering phase

Radar pixel phase is superposition of near-random scattering elements:

Unpredictable!

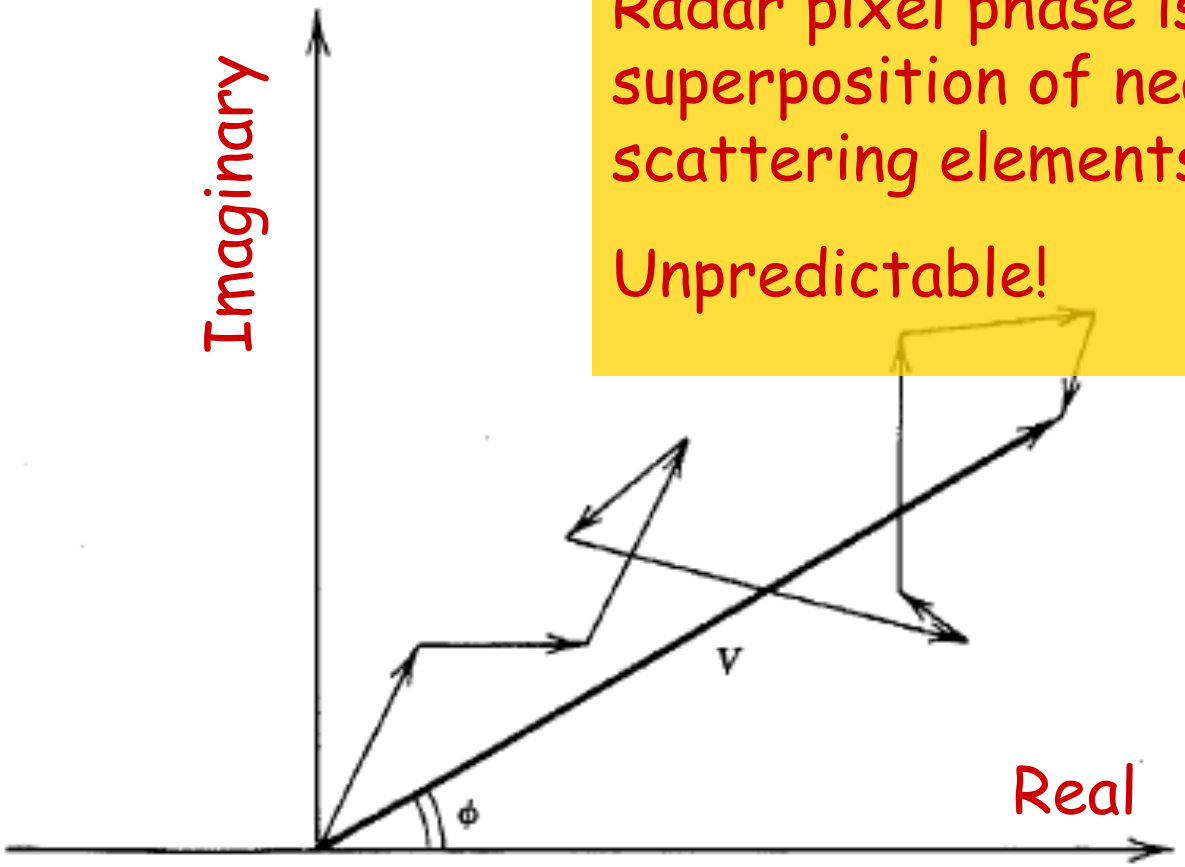

Composite return from an area with multiple scatters.

Scattering Mechanisms

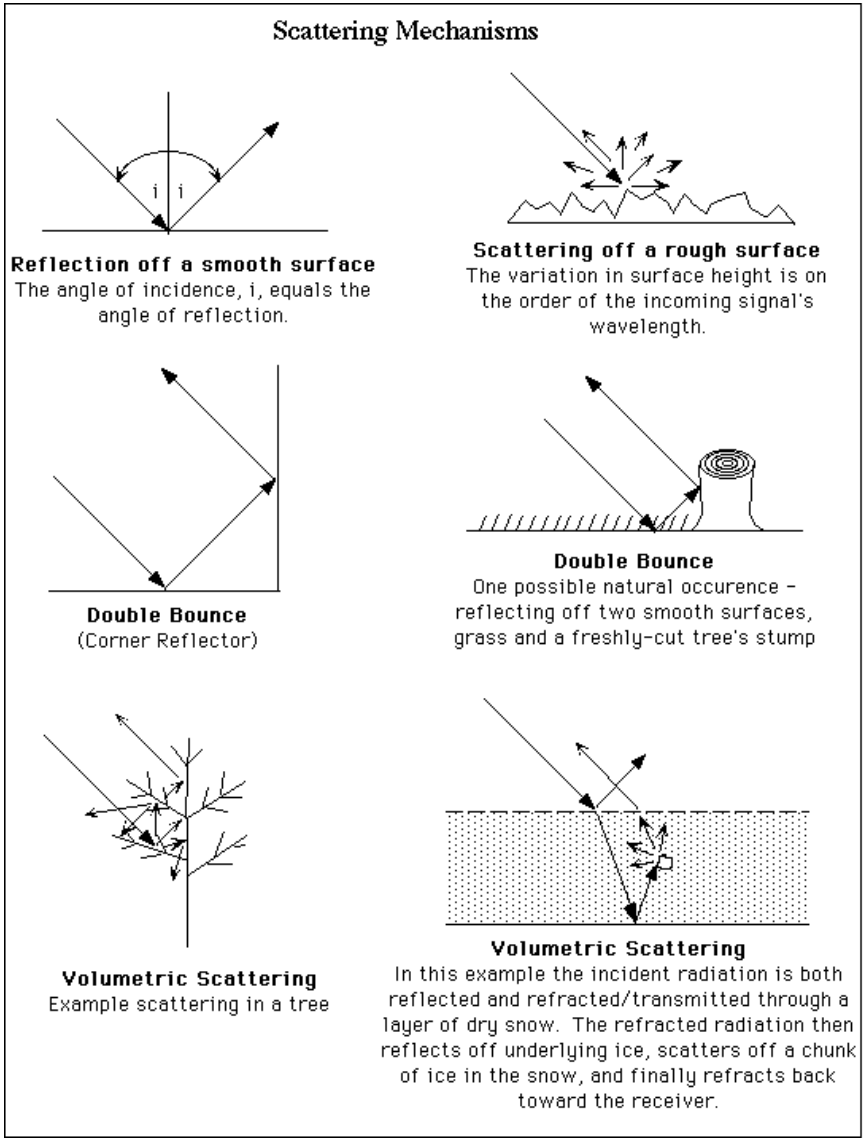

Rule of Thumb in SAR images

•Backscattering Coefficient

•Smooth – Black
•Rough surface – white

•Calm water surface – black
•Water in windy day – white

•Hills and other large-scale surface variations tend to appear bright on one side and dim on the other.

•Human-made objects - bright spots (corner reflector)
•Strong corner reflector- Bright spotty cross (strong sidelobes)

Geometry

Terminology

- Foreshortening, layover, shadow
- Why side-looking?
- Incidence angle,
- Coordinates range, azimuth

Geometry

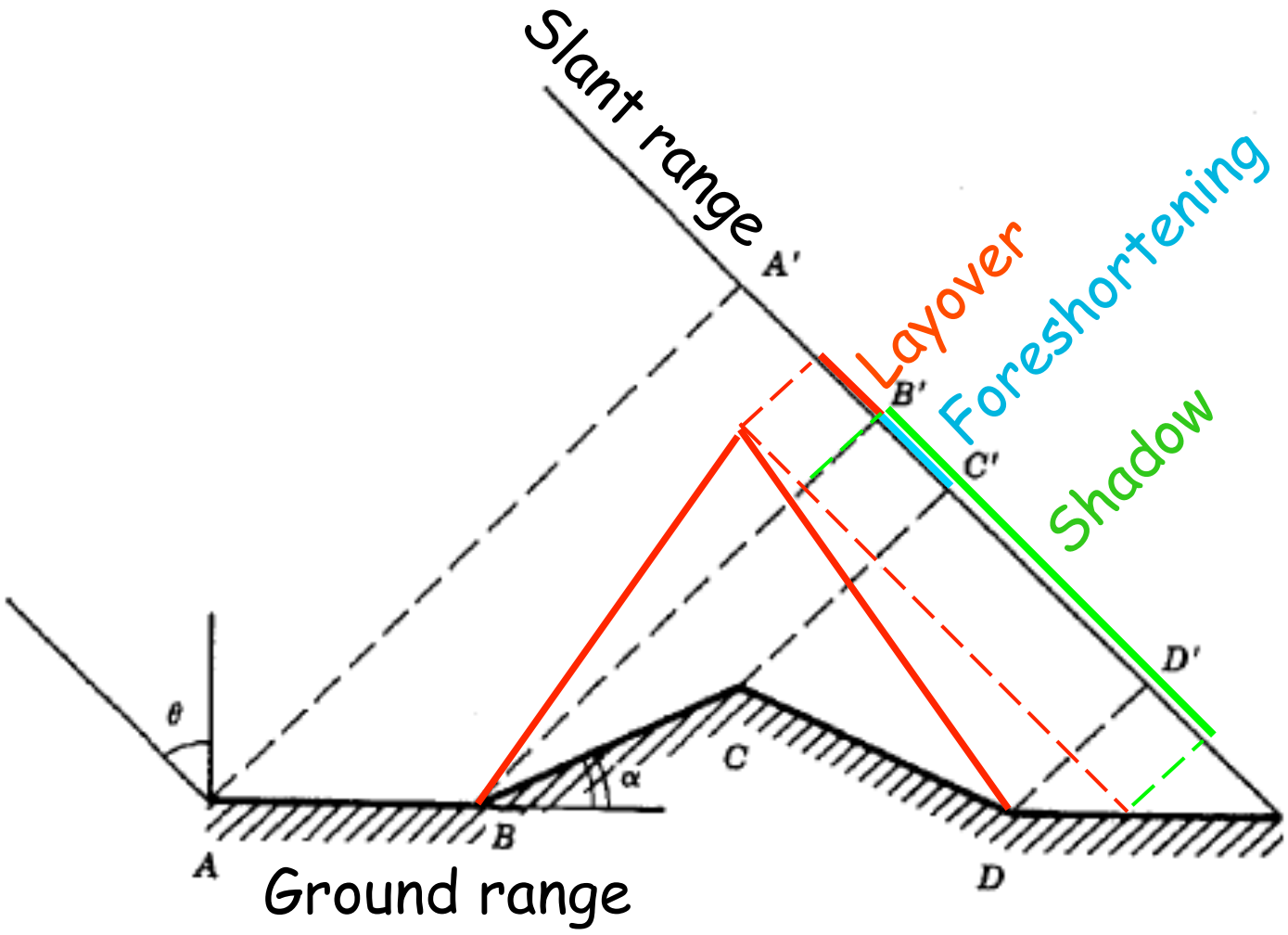
Slant range
A'
Layover
B'
Foreshortening
C'
Shadow
D'
θ
α
C
A
B
D
Ground range

Geometry

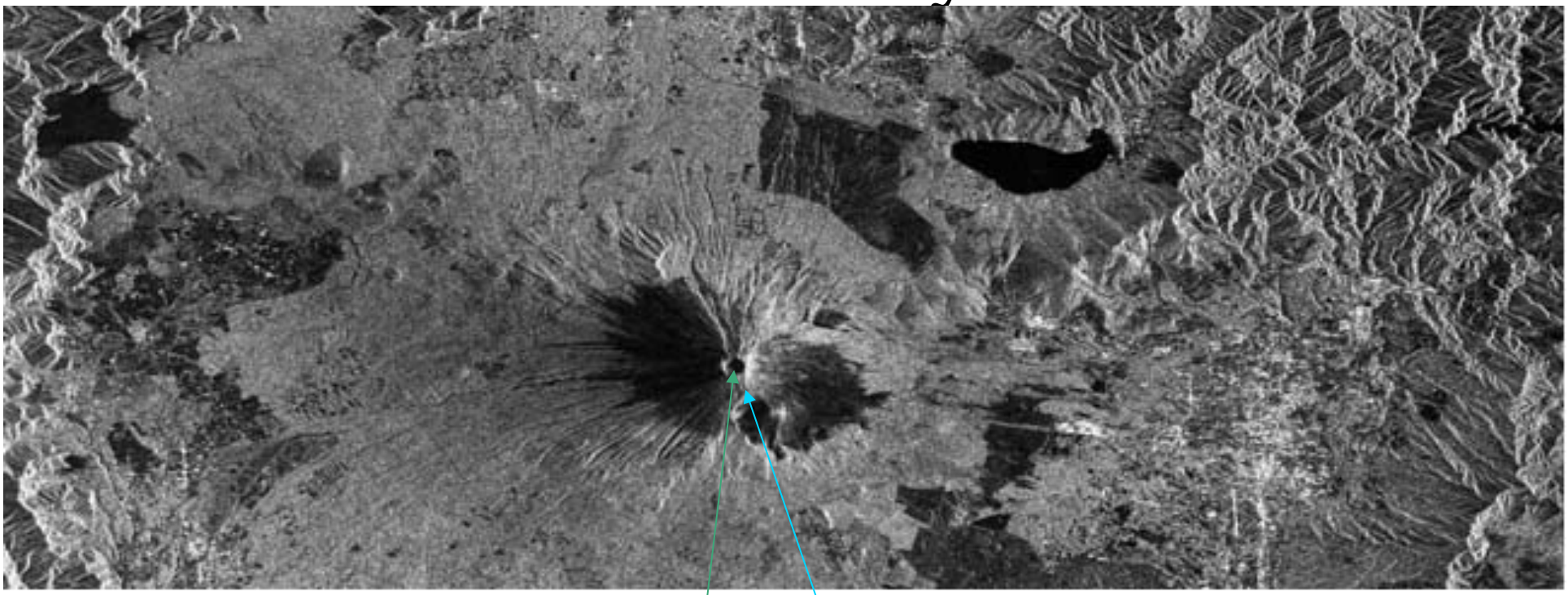

JERS-1 data (M.Shimada)

Shadow

Foreshortening

Layover

Real Aperture vs. Synthetic Aperture

- Real Aperture :
  resolution ~ $R\lambda/L$

- Synthetic Aperture:
  resolution ~ $L/2$

  Irrespective of R
  Smaller, better?!
  - Carl Wiley (1951)

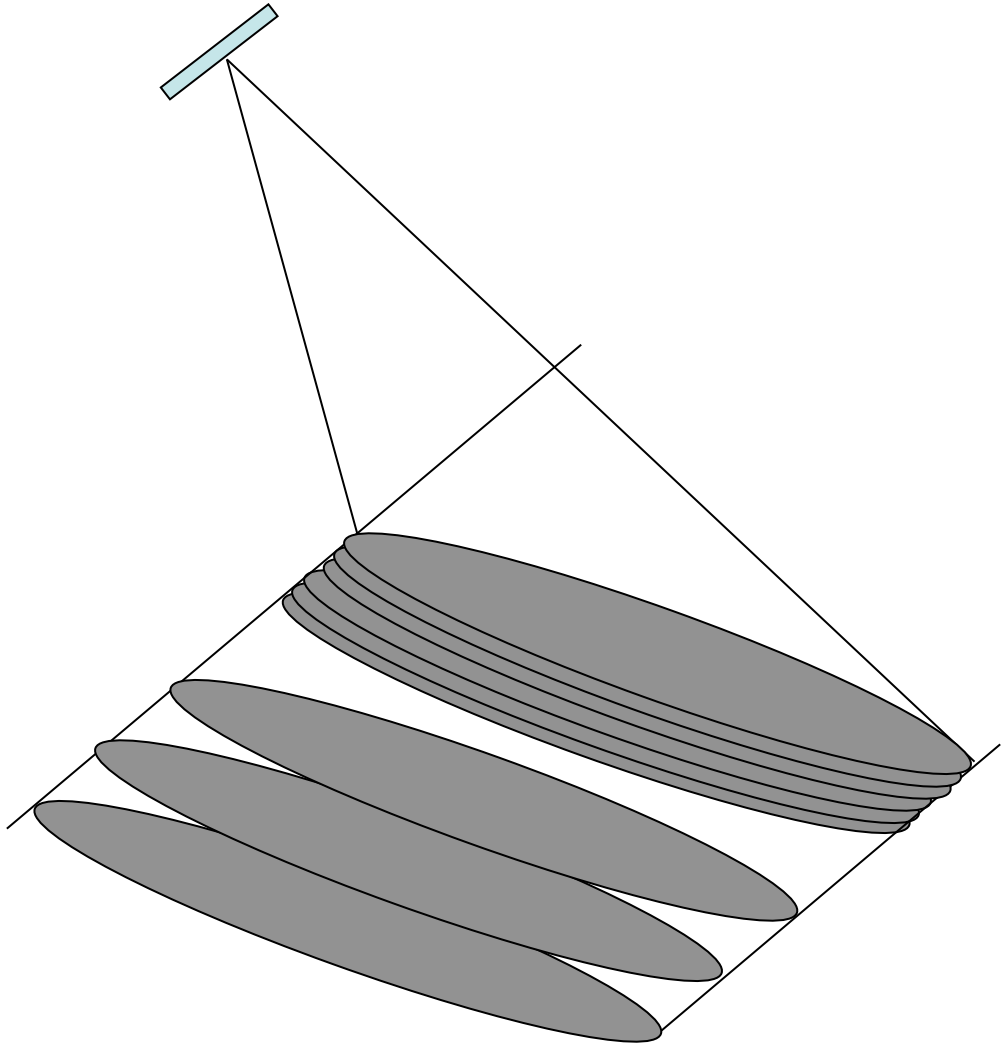

Resolution I: RAR

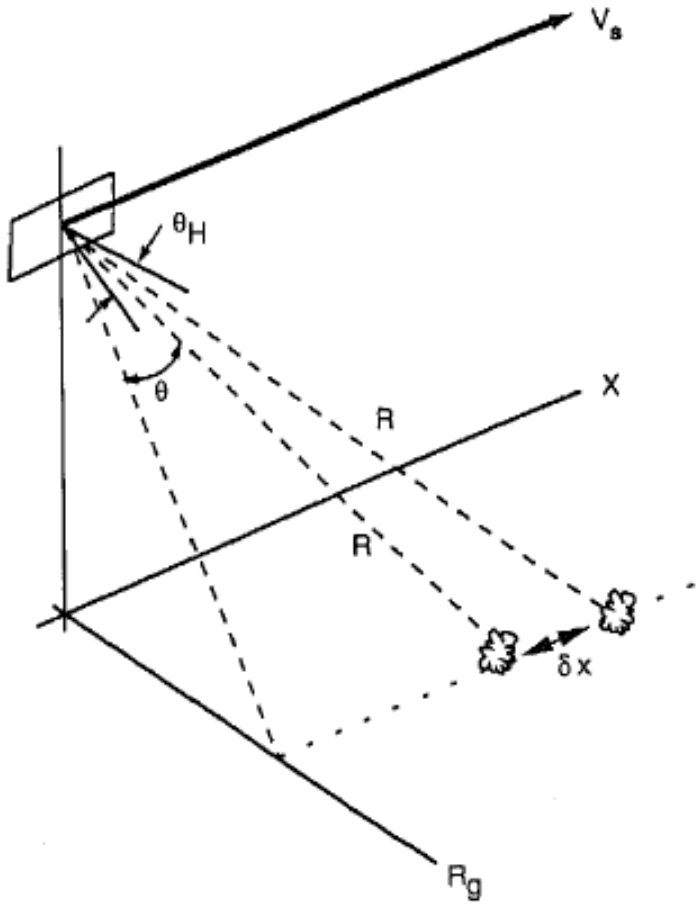

- Real Aperture Radar
- Resolution dependent on antenna dimension/pulse length
- Beam width (half power width) is ratio of wavelength over antenna size:

$$\theta = \alpha \frac{\lambda}{D} \text{ with } 0.9 < \alpha < 1.4$$

Figure 1.8 Illustration of real-aperture radar capability to resolve two targets separated in azimuth.

Calculate Ground Resolution

C-band λ= ~0.05 m

D=10 m antenna

Beam angle = $5.10^{-2}/10 = 5.10^{-3}$ rad

R=850 km

times $8.5.10^{5} = 42.10^{2}$[m] = 4.2 km

Antenna dimensions

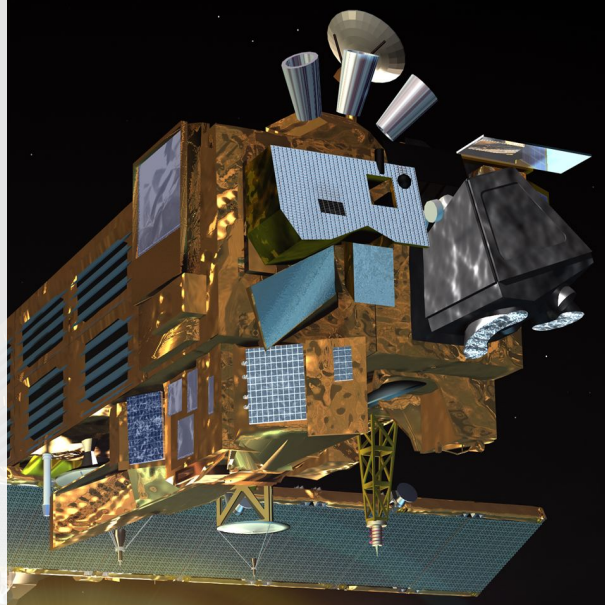

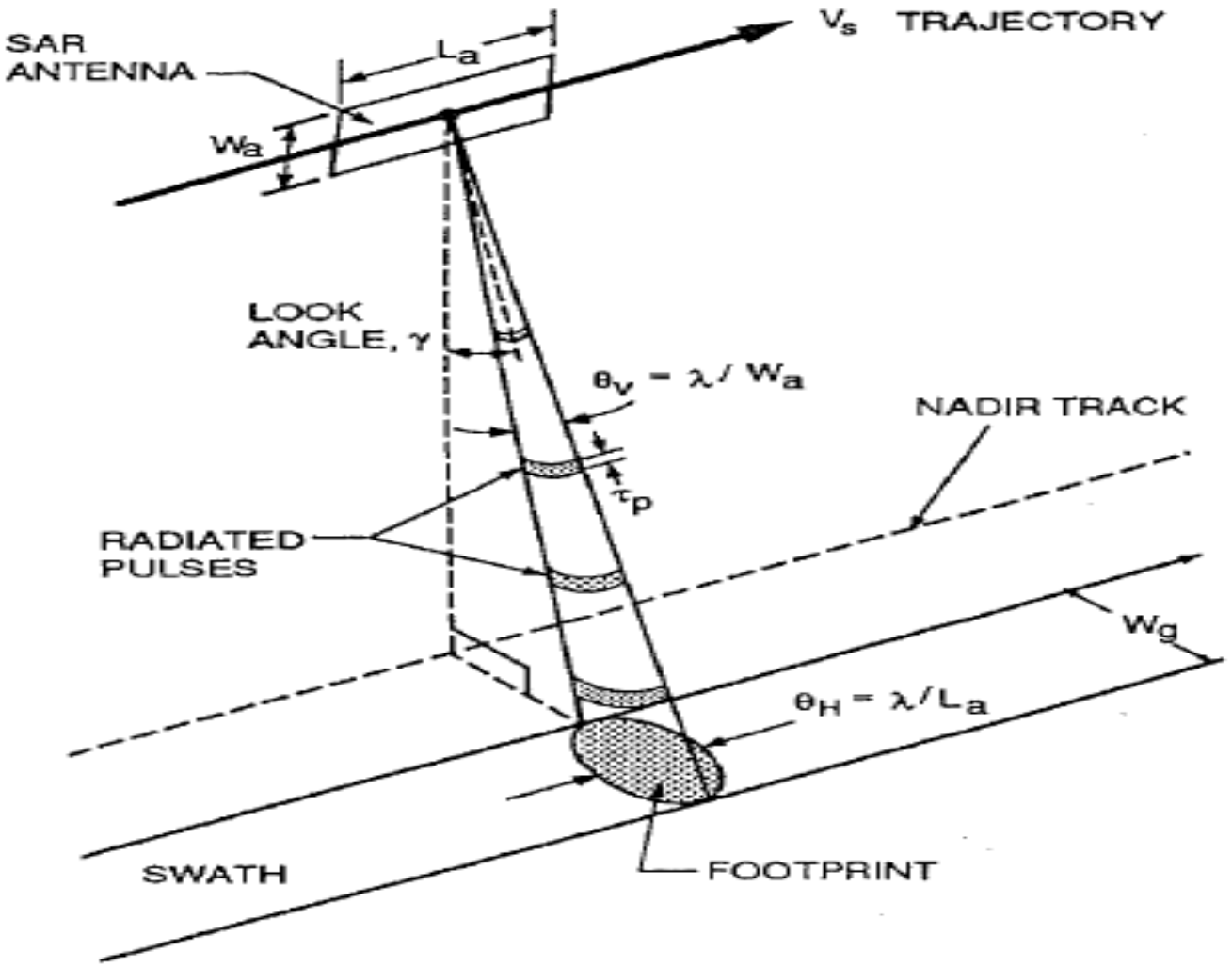
SAR
ANTENNA
L_a
V_s TRAJECTORY
W_a
LOOK
ANGLE, γ
$\theta_v = \lambda / W_a$
NADIR TRACK
τ_p
RADIATED
PULSES
W_g
$\theta_H = \lambda / L_a$
SWATH
FOOTPRINT

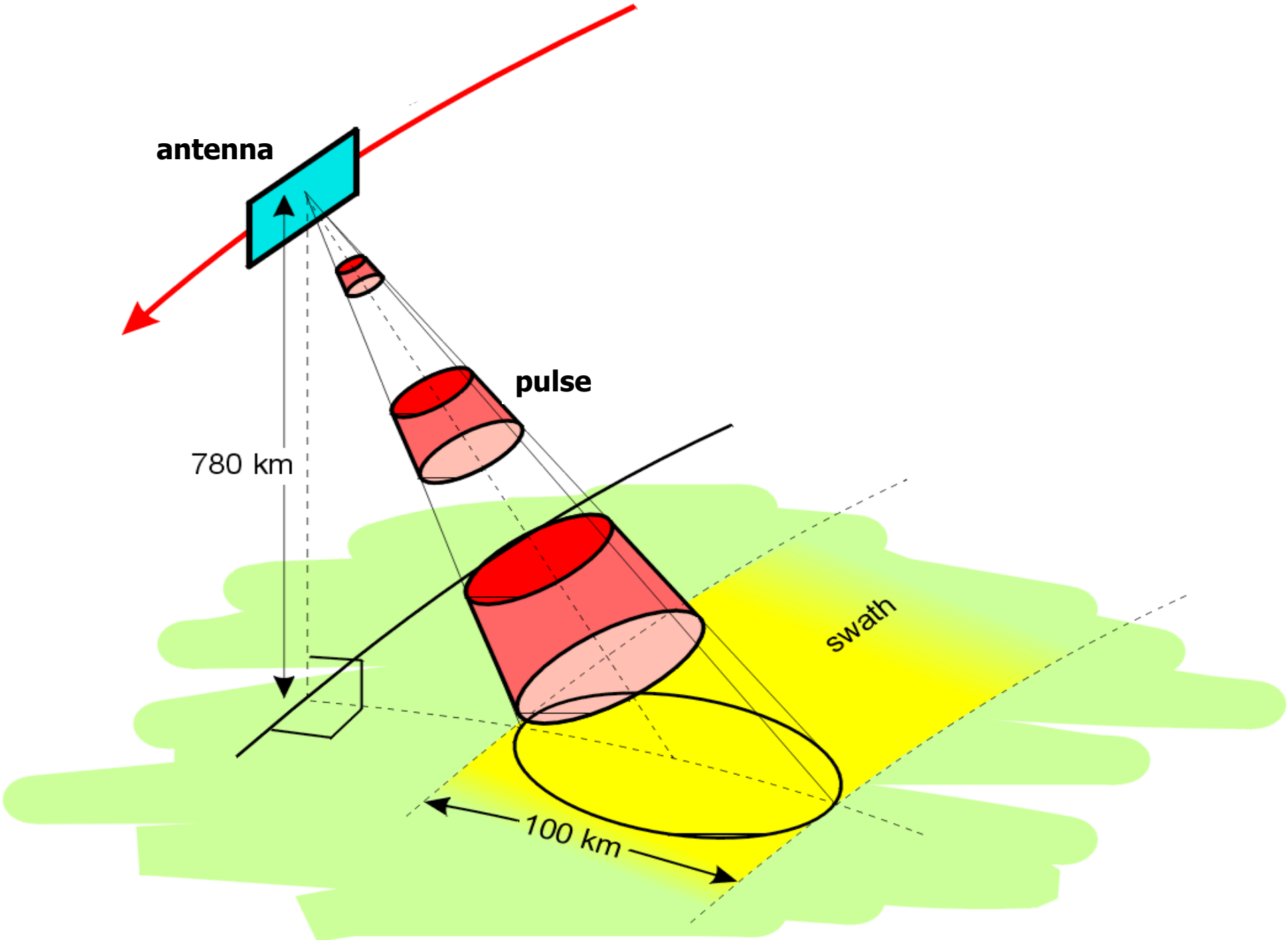
antenna
pulse
780 km
swath
100 km

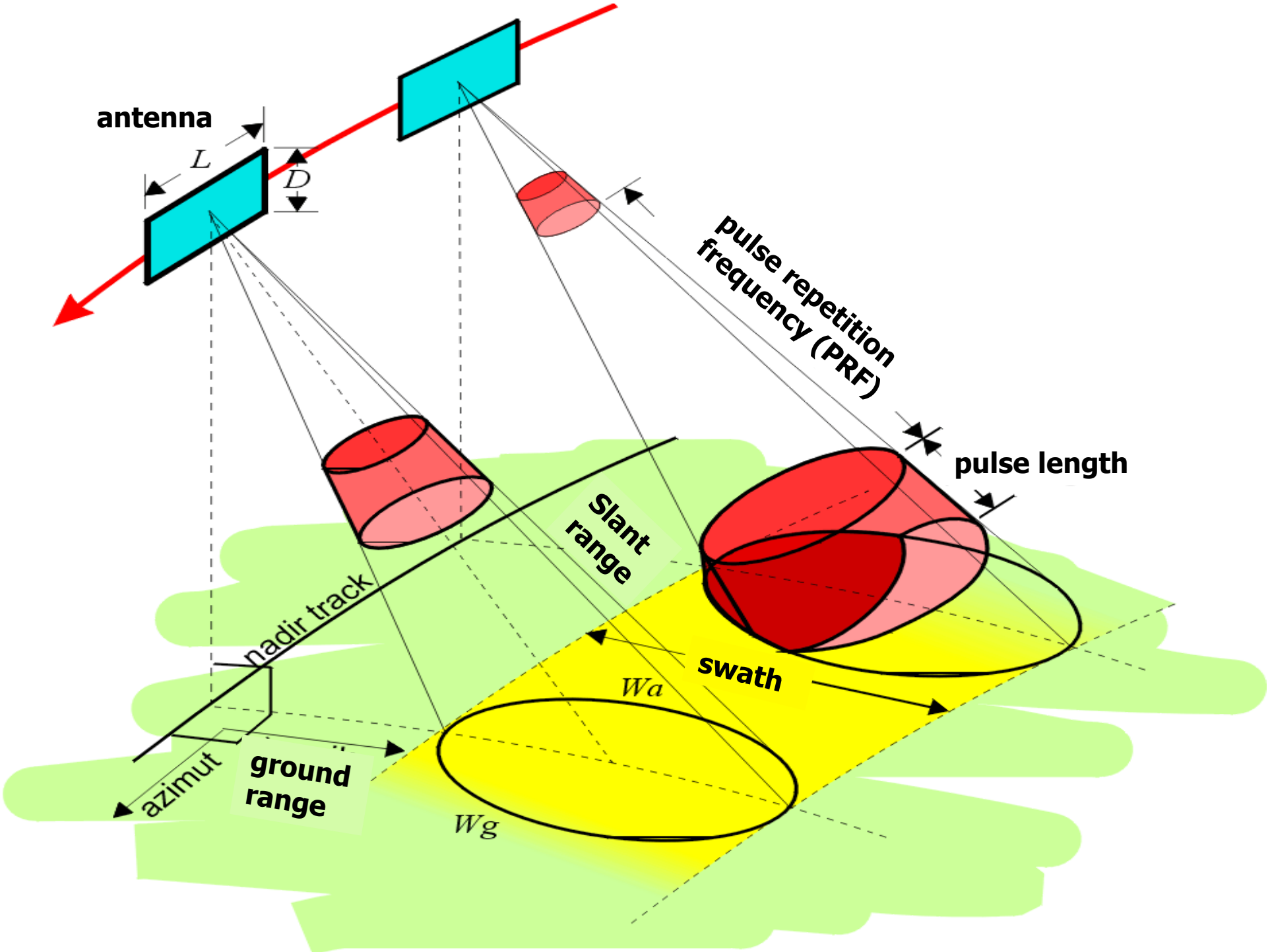
antenna
L
D
pulse repetition
frequency (PRF)
pulse length
Slant
range
nadir track
swath
Wa
azimut
ground
range
Wg

Improvement in Resolution
(Crimea, Ukraine)

Real Aperture Radar

Massonnet and Feigl, 1998

Improvement of along-track resolution

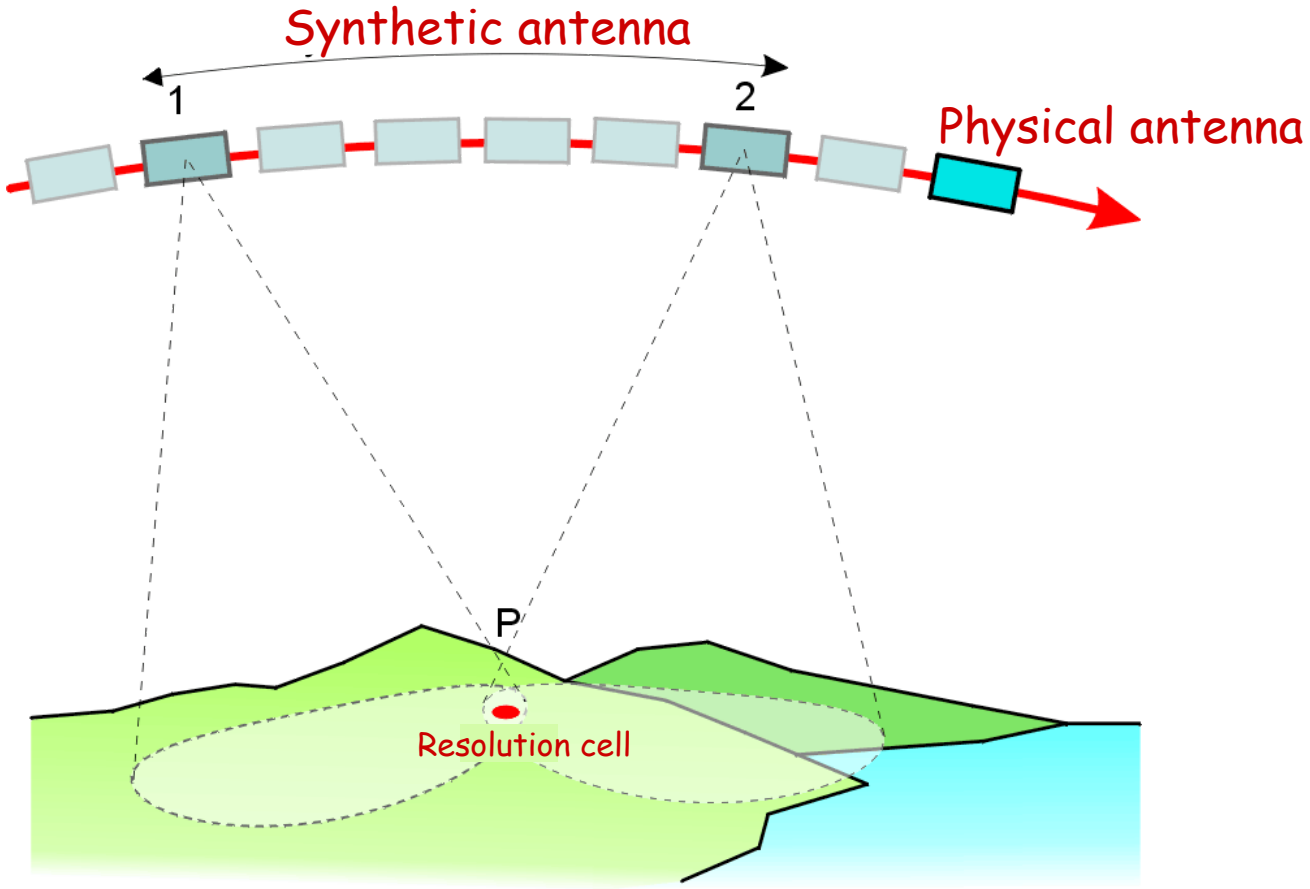

Improvement in Resolution

(Crimea, Ukraine)

Real Aperture Radar

Synthetic Aperture Radar

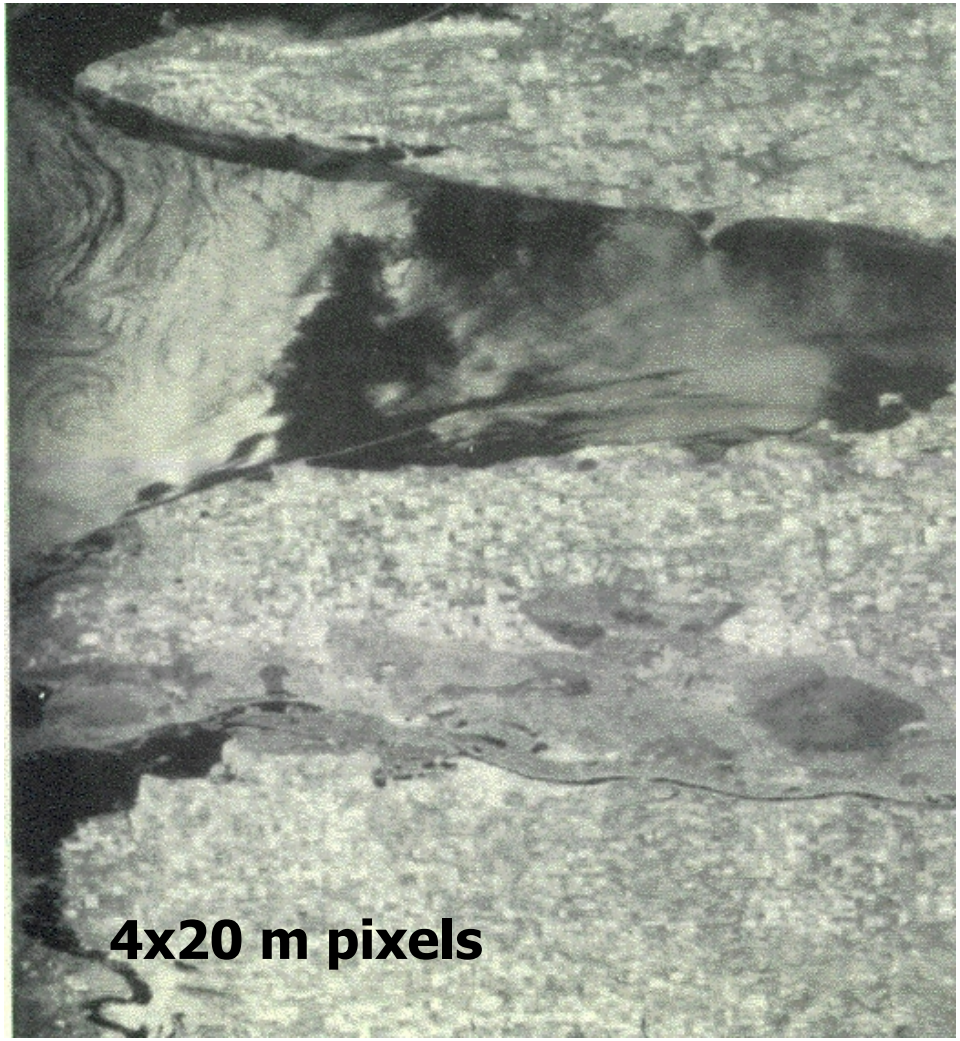

Massonnet and Feigl, 1998

Radar Interferometry

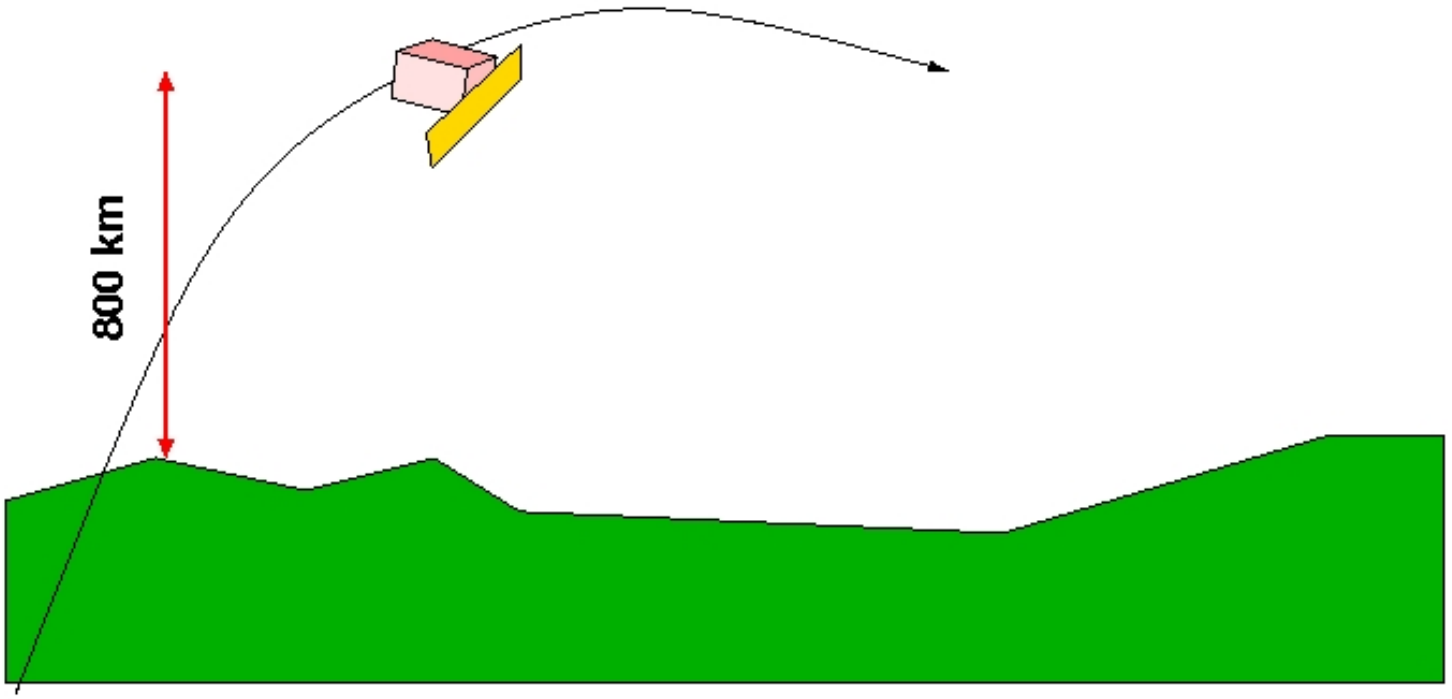

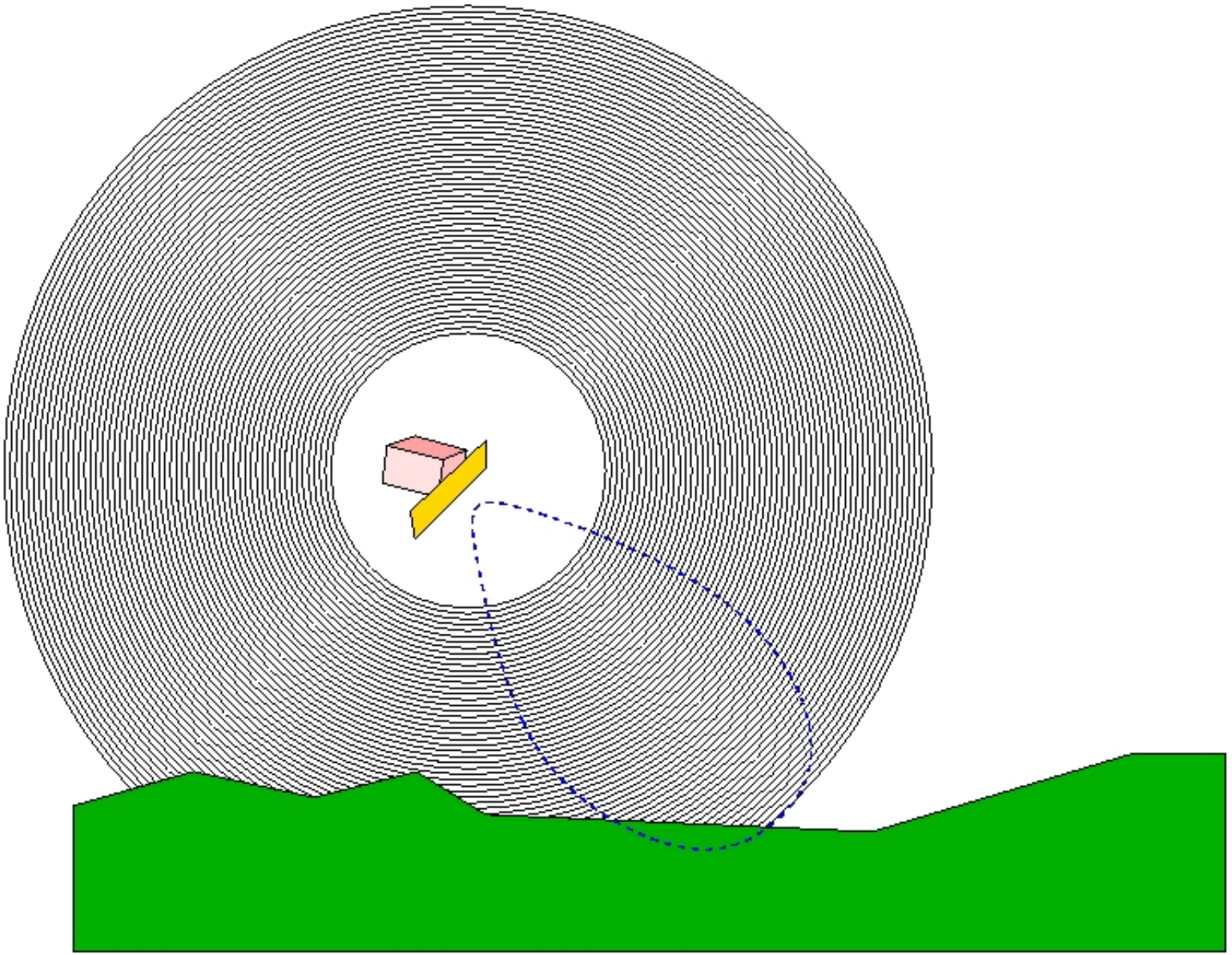

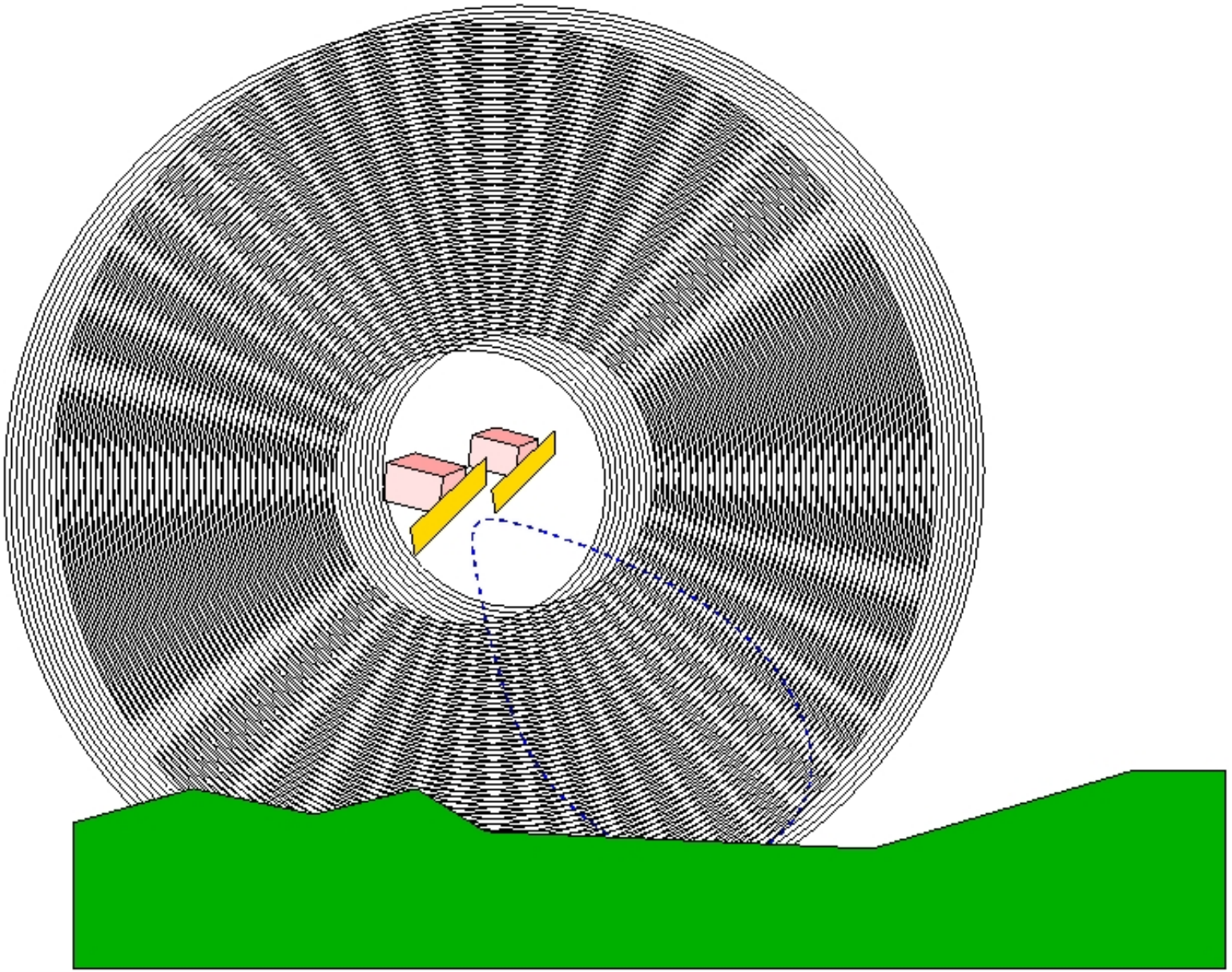

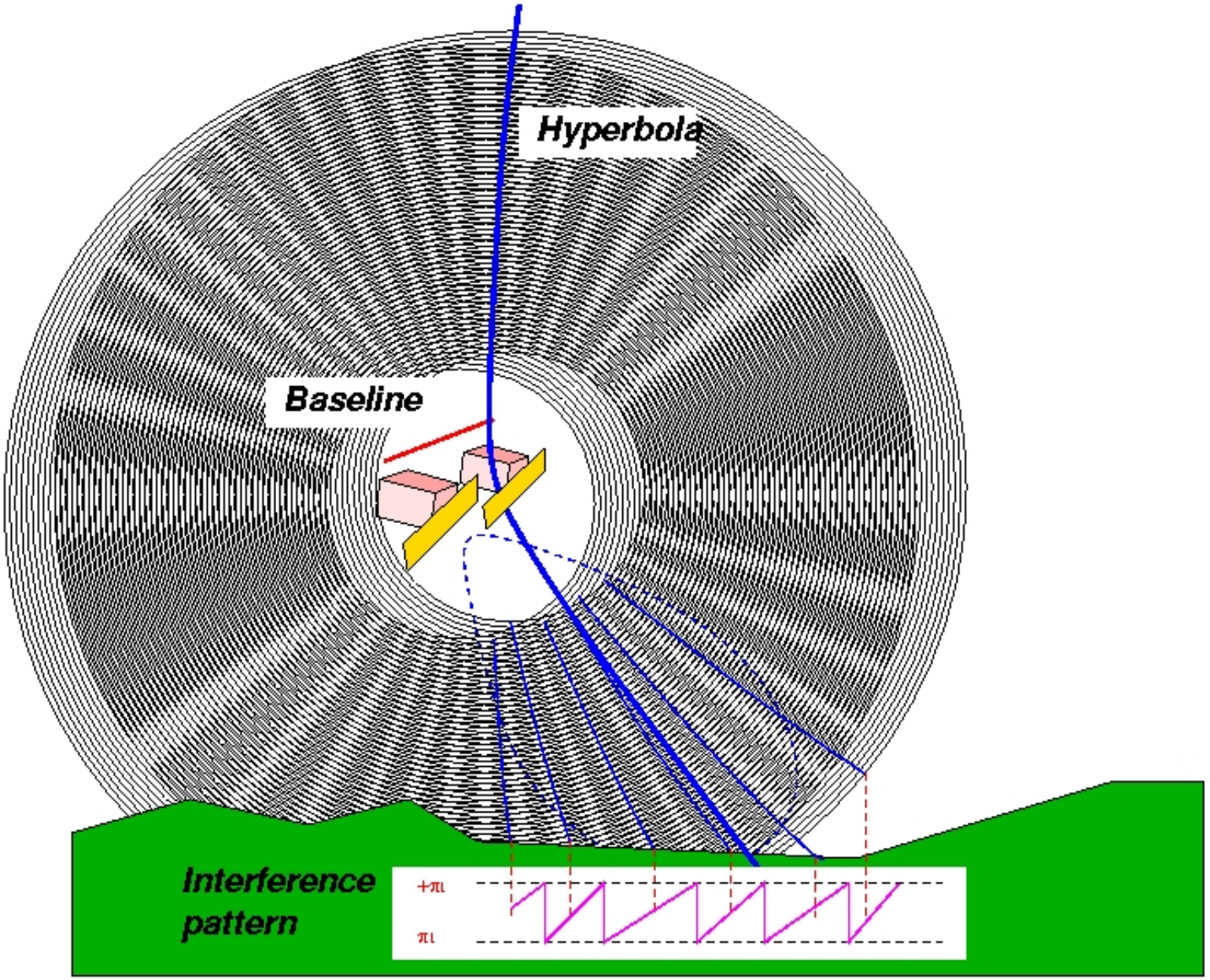
Hyperbola
Baseline
Interference pattern
+πι
πι

Example in 2D: interferogram

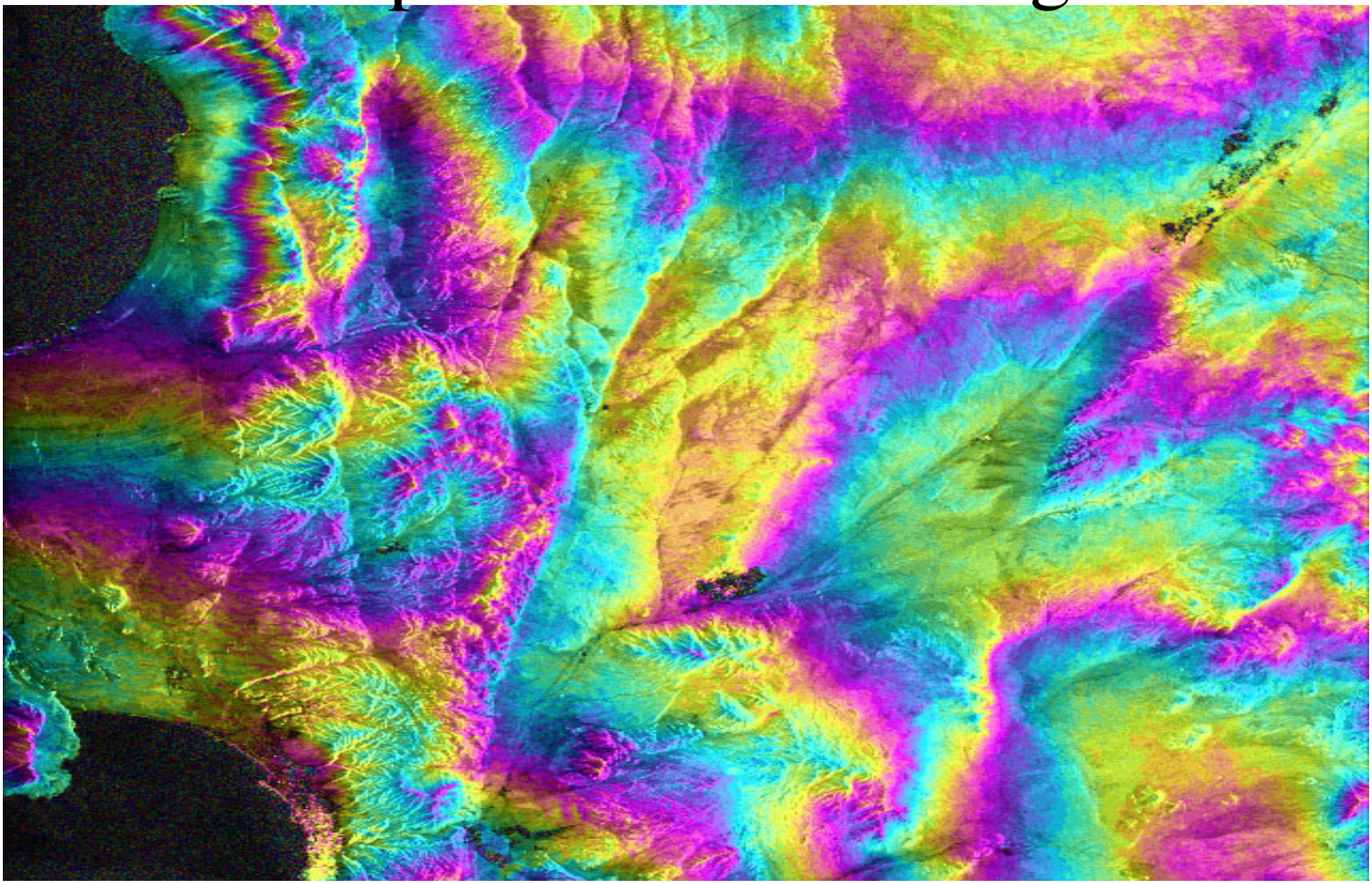

SAR Interferometry (InSAR)

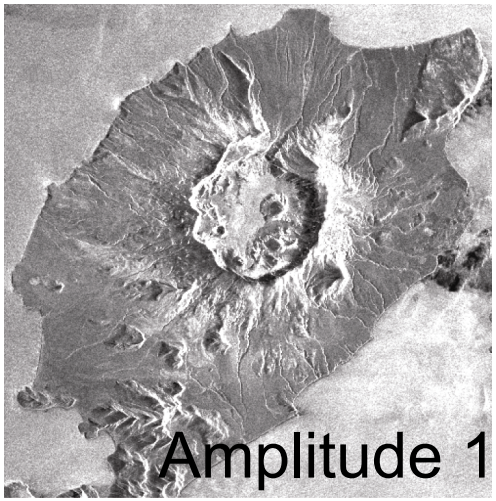

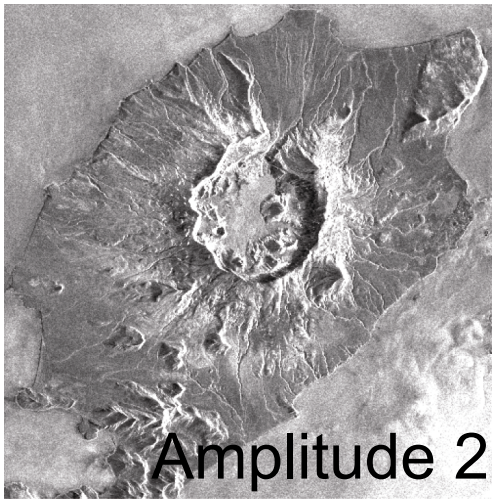

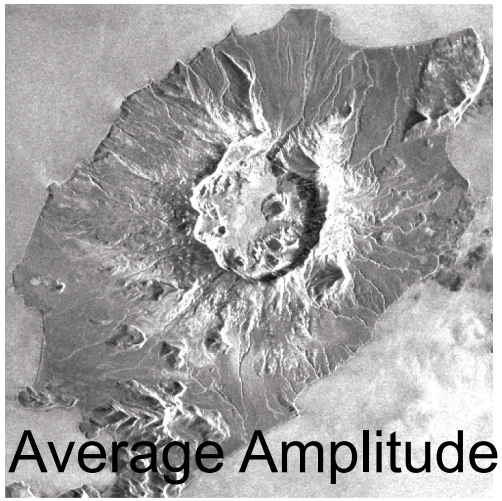

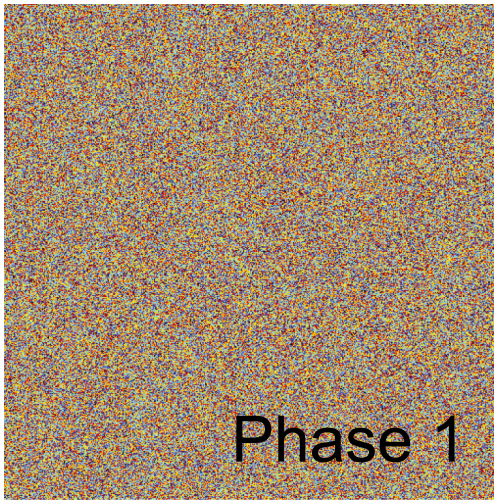

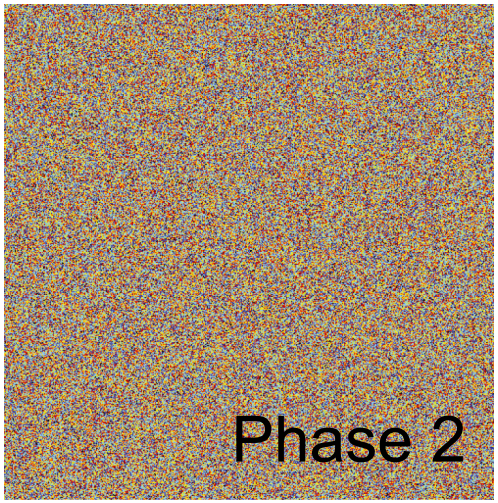

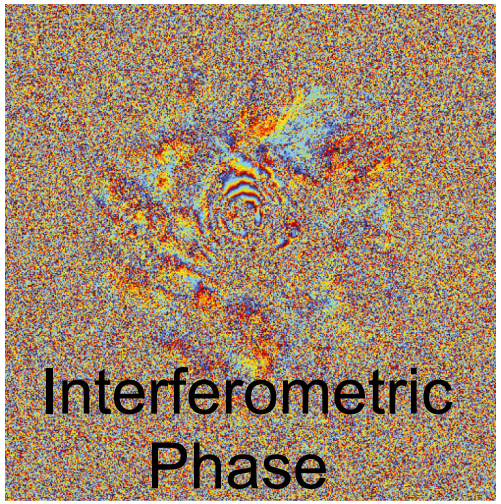

Basics: Interferogram Formation I

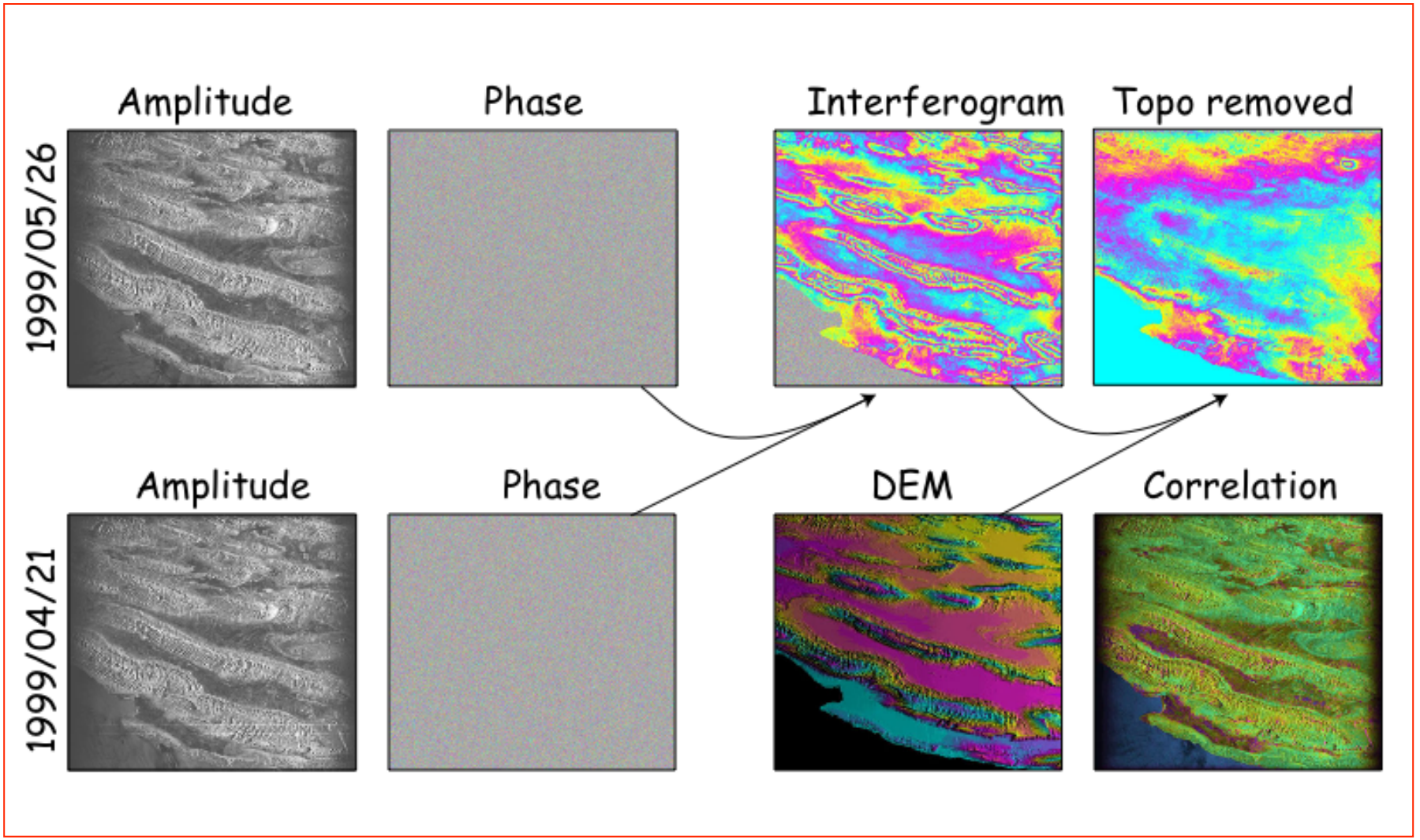

Effect of SAR Frequency

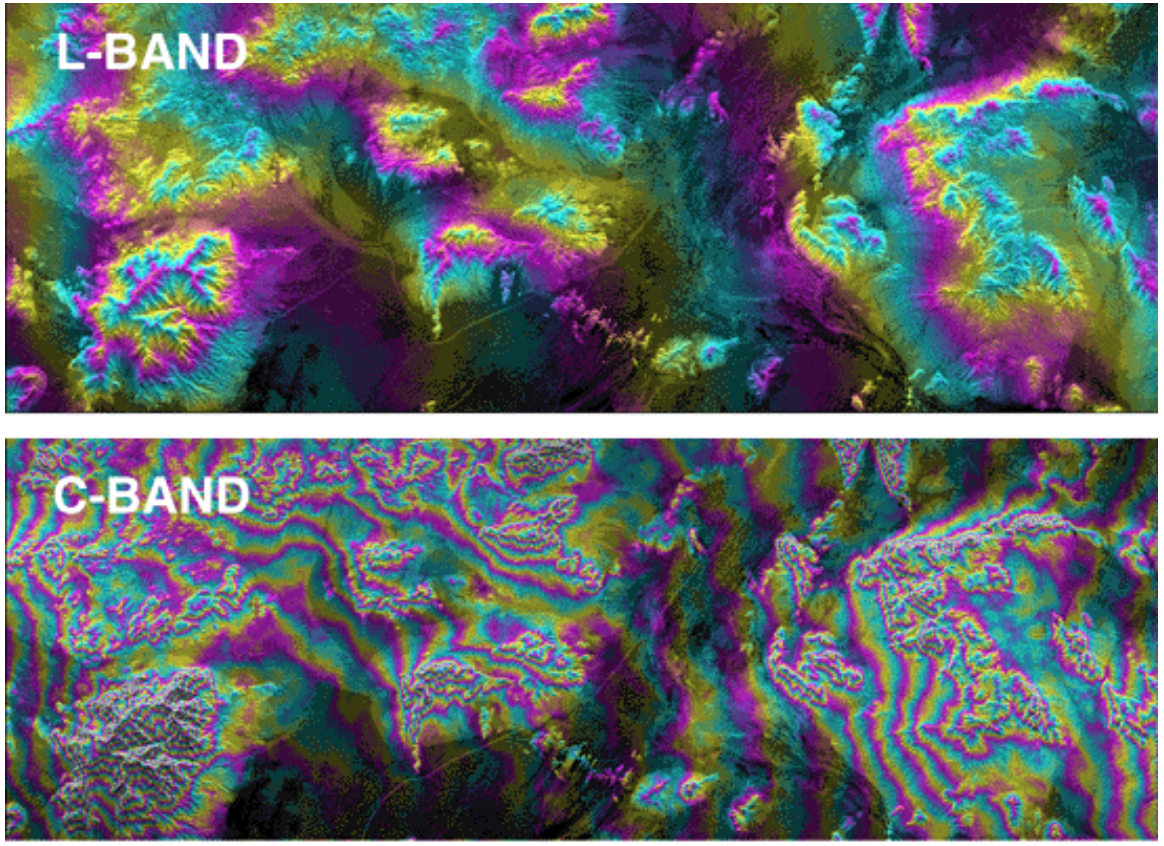

SIR-C L, C BAND INTERFEROGRAMS
FT. IRWIN, CALIFORNIA

L band: longer λ, fewer fringes, better coherence

Why is Coherence Better at L-band?

- Coherence is a measure of how well the phase of adjacent pixels agree with each other
  - Random phase = low or zero coherence
- C-band radars usually have poor coherence in vegetated areas.
  - Leaves on trees tend to have size ~ wavelength
    - Therefore are effective scatterers
    - Leaves move (wind, growth) and change (fall off)
- L-band scattering is dominated by features 20-25 cm in scale
  - More likely to be ground features or unchanging features of vegetation (large branches)
- Some other notes on coherence
  - Plowed fields have bad coherence
  - Permanent structures (buildings, roads) usually have good coherence.
  - Surprisingly, certain kinds of swamps seem to have good coherence with returns that depend on the water level.

Range

Expressed as phase (radians)

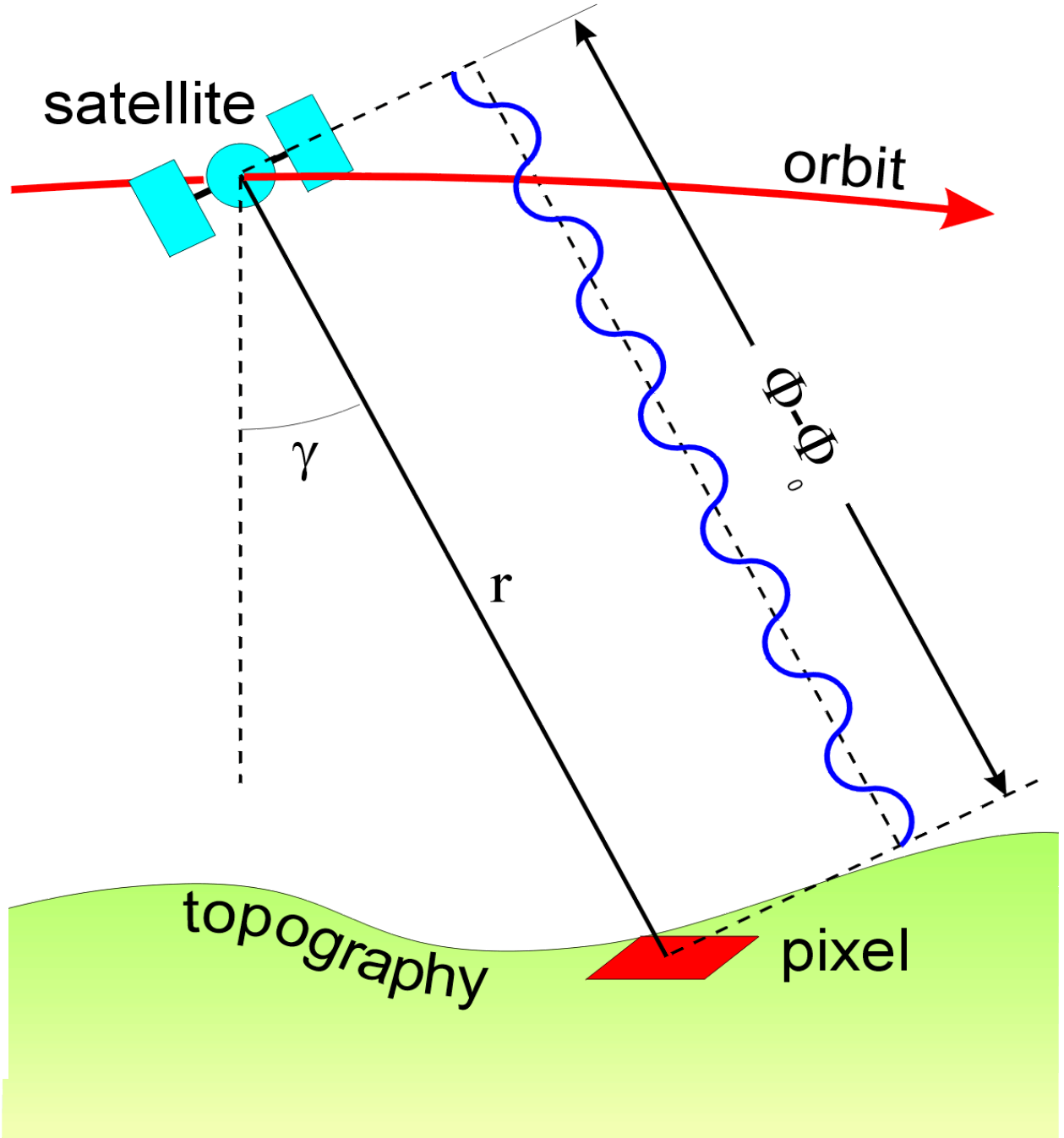

Range

Expressed as integer cycles + fractional phase

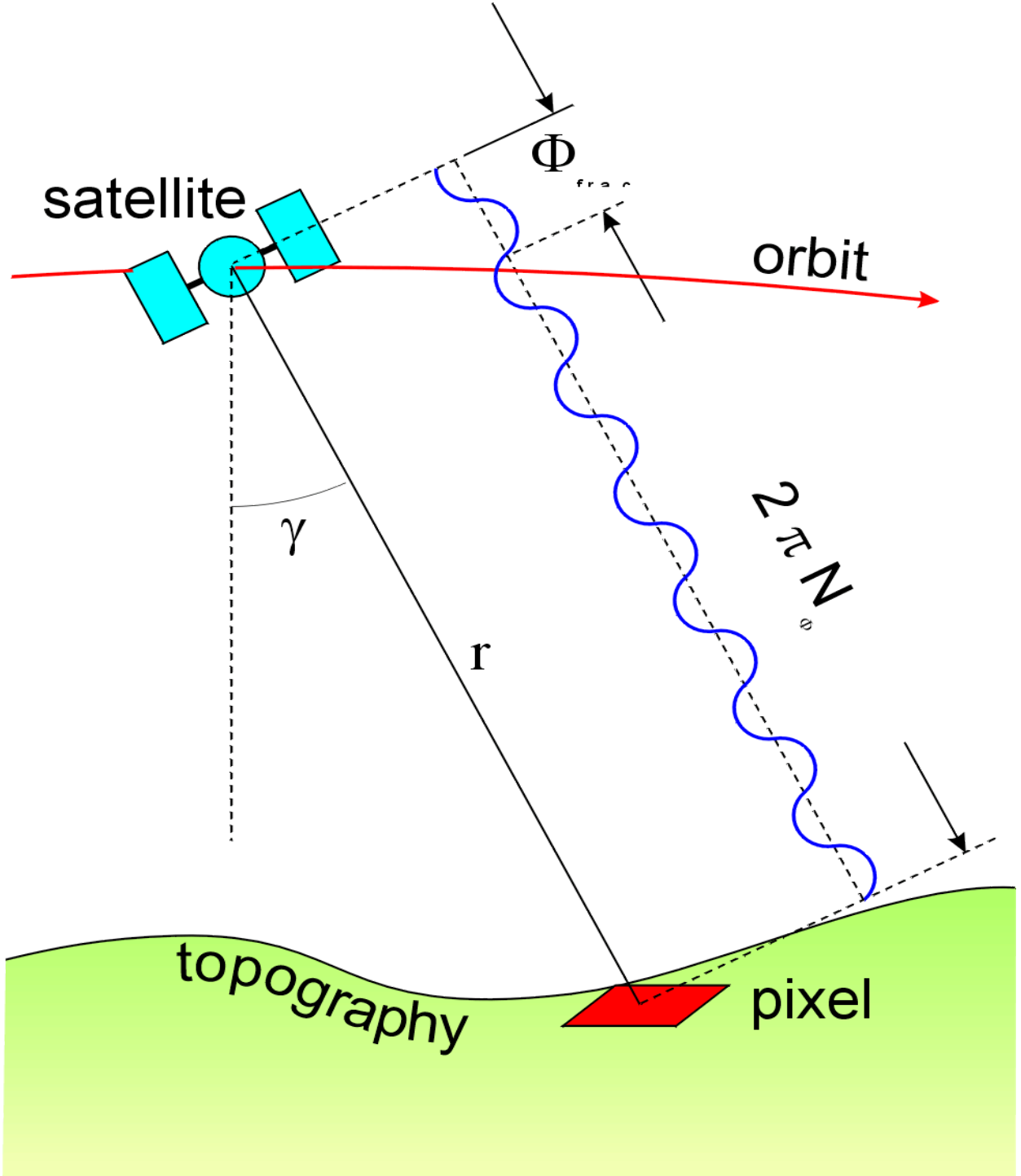

Phase-range relationship

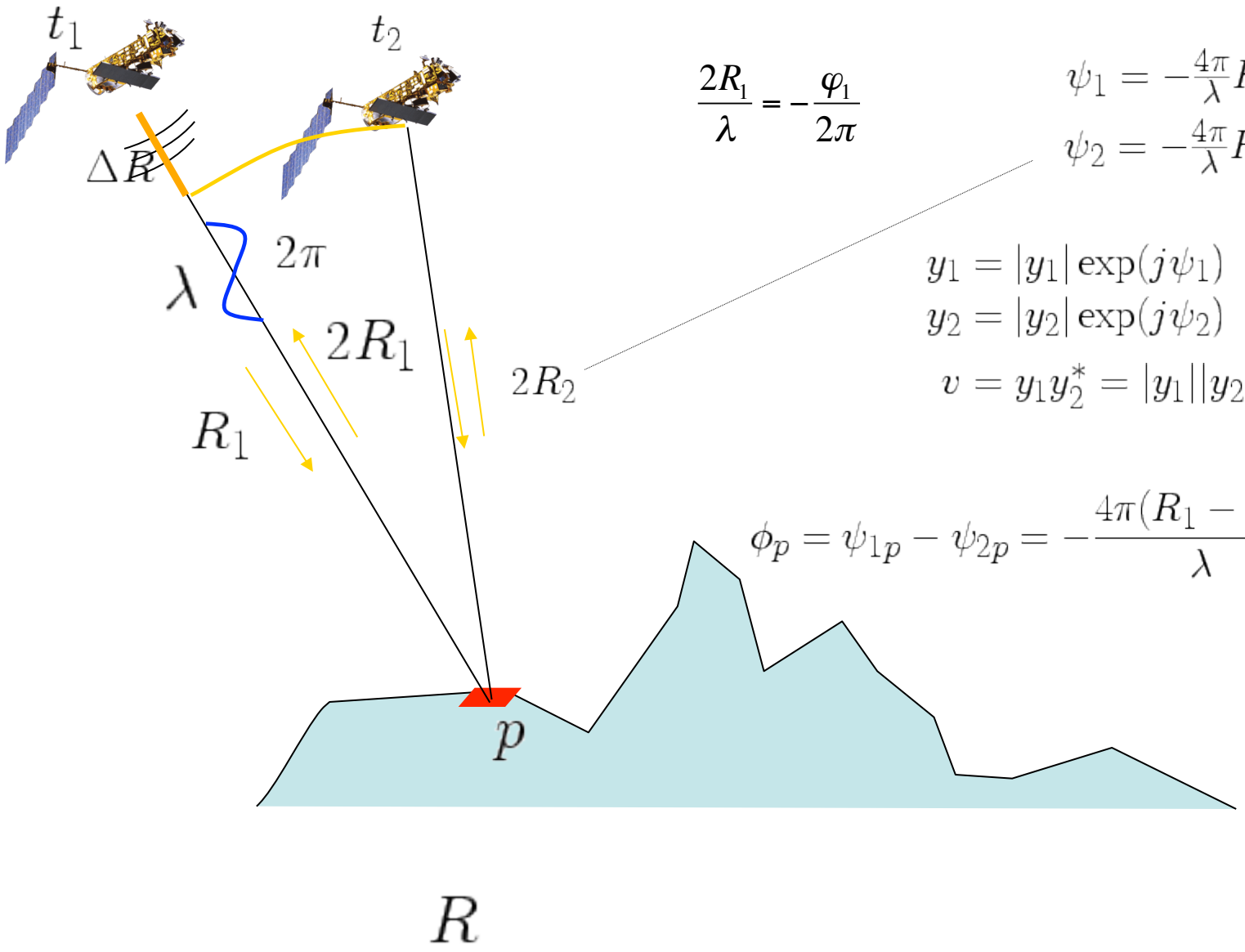

$$\frac{2R_1}{\lambda} = -\frac{\varphi_1}{2\pi}$$

$$\psi_1 = -\frac{4\pi}{\lambda}R_1$$

$$\psi_2 = -\frac{4\pi}{\lambda}R_2$$

$$y_1 = |y_1|\exp(j\psi_1)$$

$$y_2 = |y_2|\exp(j\psi_2)$$

$$v = y_1 y_2^* = |y_1||y_2|\exp(j(\psi_1 - \psi_2))$$

$$\phi_p = \psi_{1p} - \psi_{2p} = -\frac{4\pi(R_1 - R_2)}{\lambda} = -\frac{4\pi\Delta R}{\lambda}$$

Phase-height relationship

(Far-field approximation)

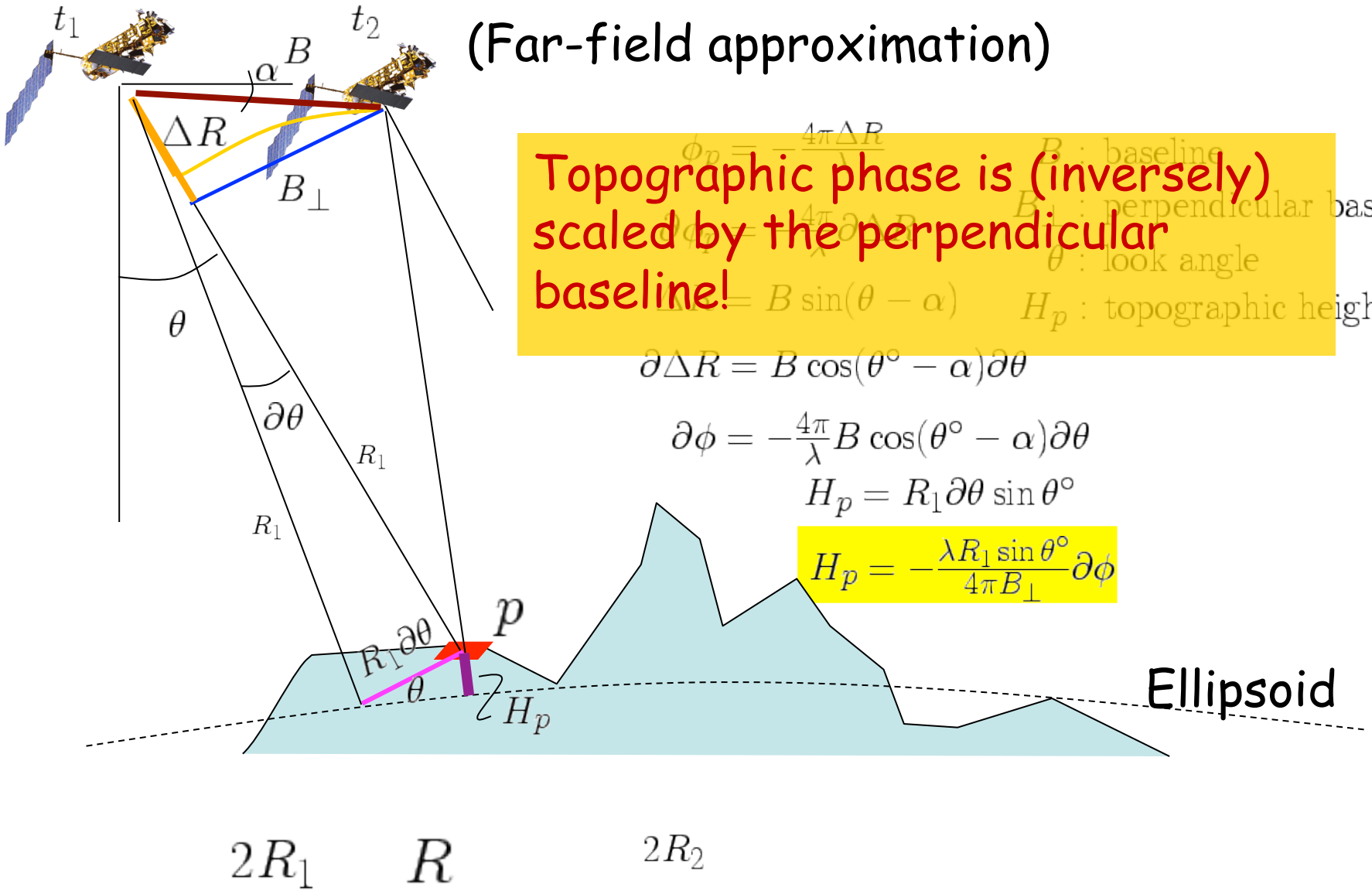

Topographic phase is (inversely) scaled by the perpendicular baseline!

$\phi_p = -\frac{4\pi\Delta R}{\lambda}$ B : baseline

$\Delta R = B\sin(\theta - \alpha)$ $B_\perp$: perpendicular baseline

θ : look angle

H_p : topographic height

$$\partial\Delta R = B\cos(\theta^\circ - \alpha)\partial\theta$$

$$\partial\phi = -\frac{4\pi}{\lambda}B\cos(\theta^\circ - \alpha)\partial\theta$$

$$H_p = R_1\partial\theta\sin\theta^\circ$$

$$H_p = -\frac{\lambda R_1\sin\theta^\circ}{4\pi B_\perp}\partial\phi$$

Height ambiguity

$$H_p = -\frac{\lambda R_1 \sin\theta^\circ}{4\pi B_\perp}\partial\phi$$

Height difference related to 1 phase cycle:

$$H_{2\pi} = \frac{-\lambda R_1 \sin\theta^\circ}{4\pi B_\perp} 2\pi = \frac{-\lambda R_1 \sin\theta^\circ}{2B_\perp}$$

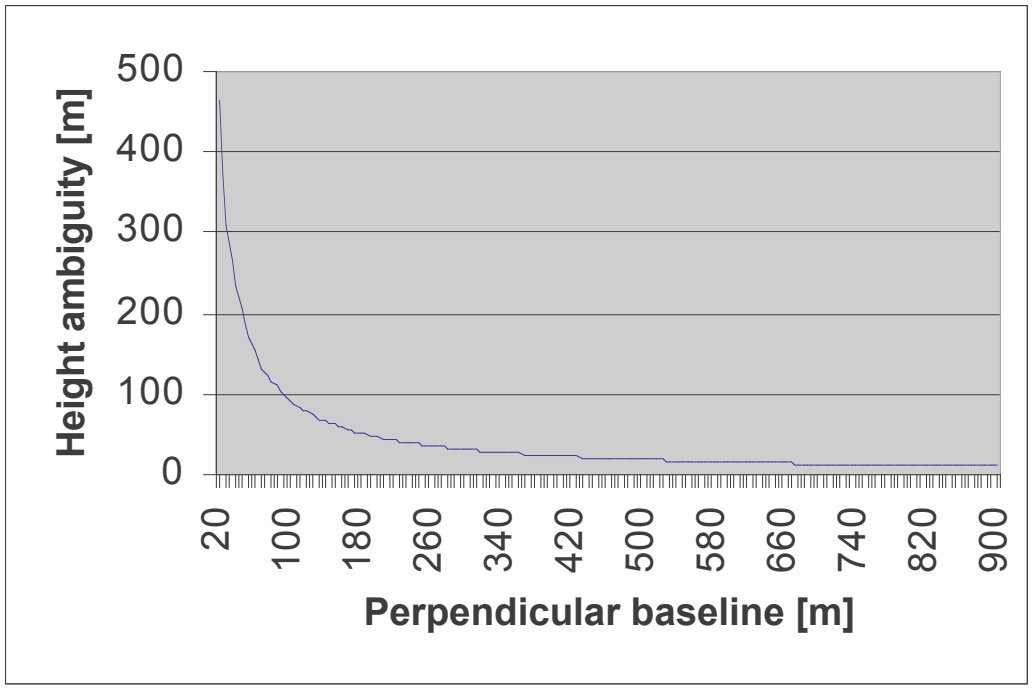

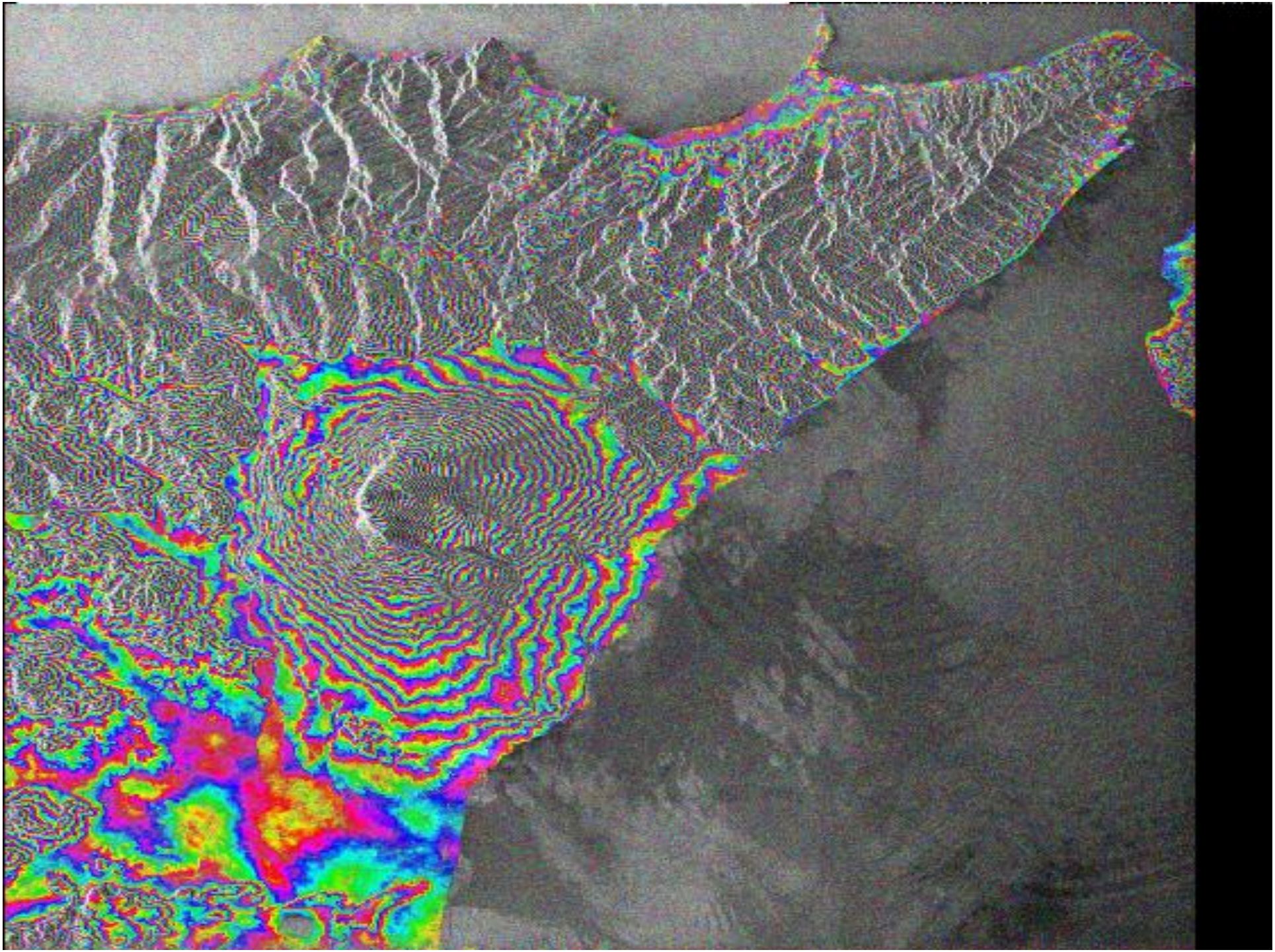

Baseline dependency, height ambiguity

Bperp 173 m, Bt= 1day

H_{2pi}=45m

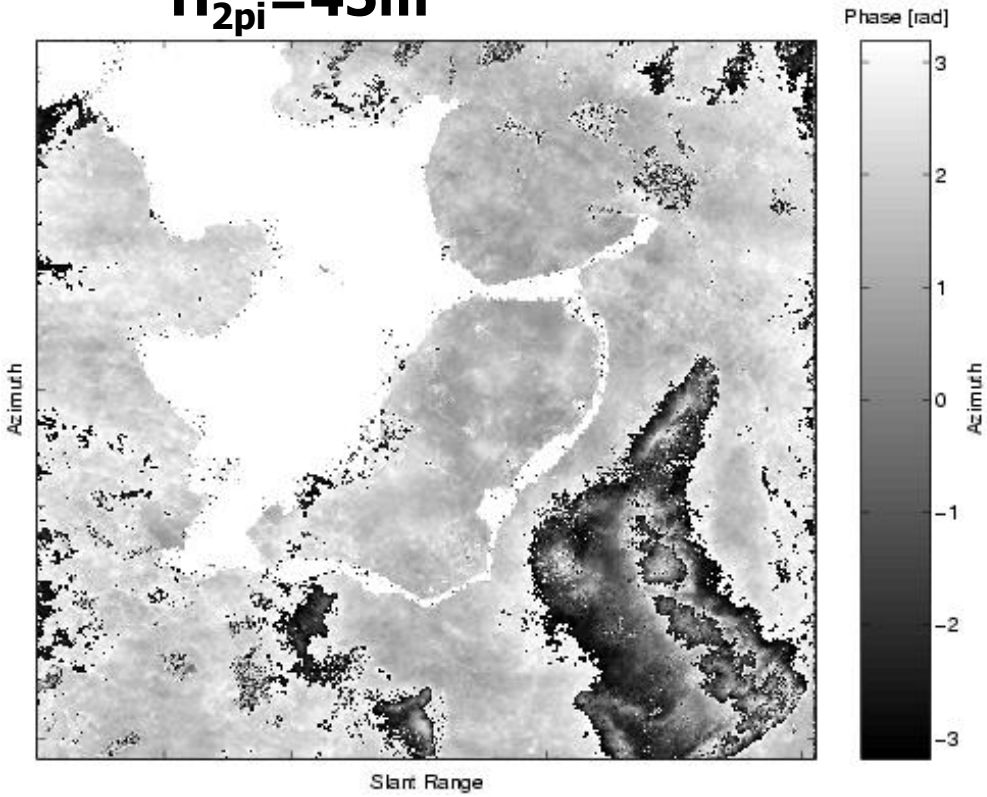

Bperp 531 m, Bt= 1 day

H_{2pi}=16m

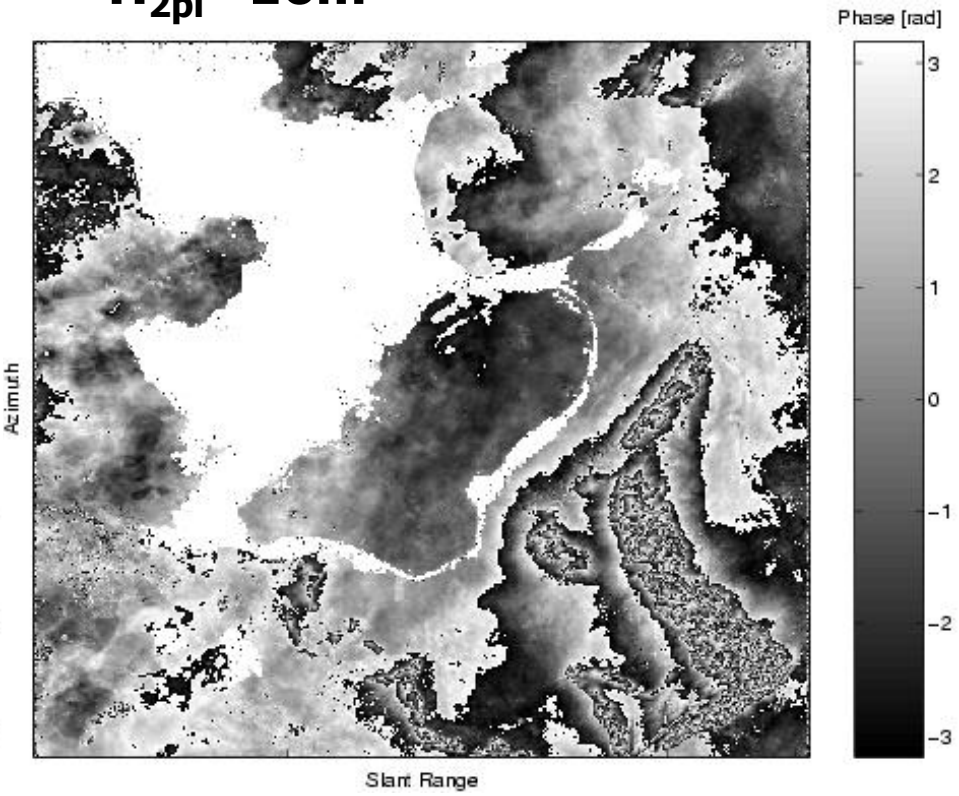

Phase-deformation relationship

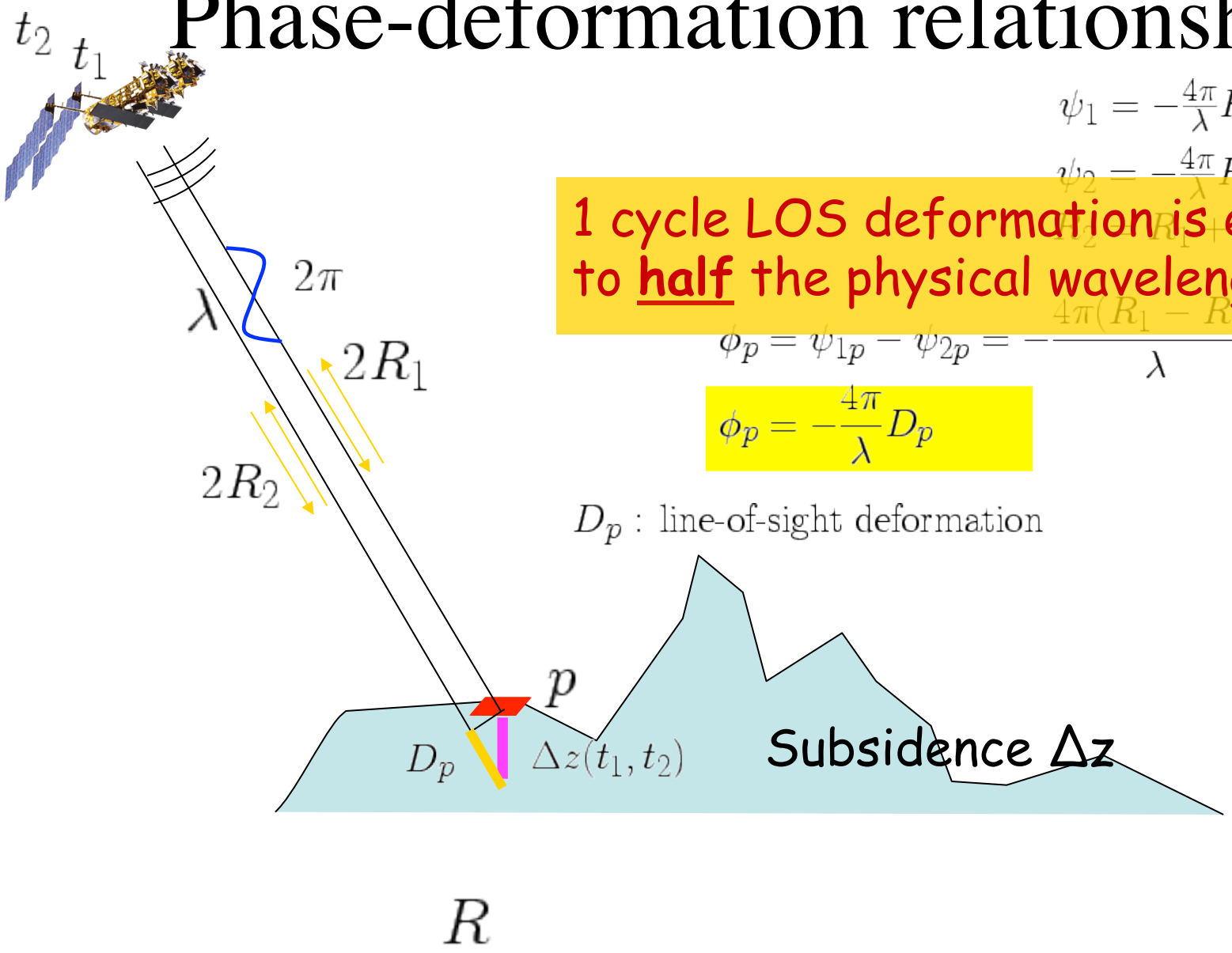

$$\psi_1 = -\frac{4\pi}{\lambda} R_1$$

$$\psi_2 = -\frac{4\pi}{\lambda} R_2$$

1 cycle LOS deformation is equal to **half** the physical wavelength

$$\phi_p = \psi_{1p} - \psi_{2p} = -\frac{4\pi(R_1 - R_2)}{\lambda} =$$

$$\phi_p = -\frac{4\pi}{\lambda} D_p$$

D_p : line-of-sight deformation

Interferometric phase - deformation

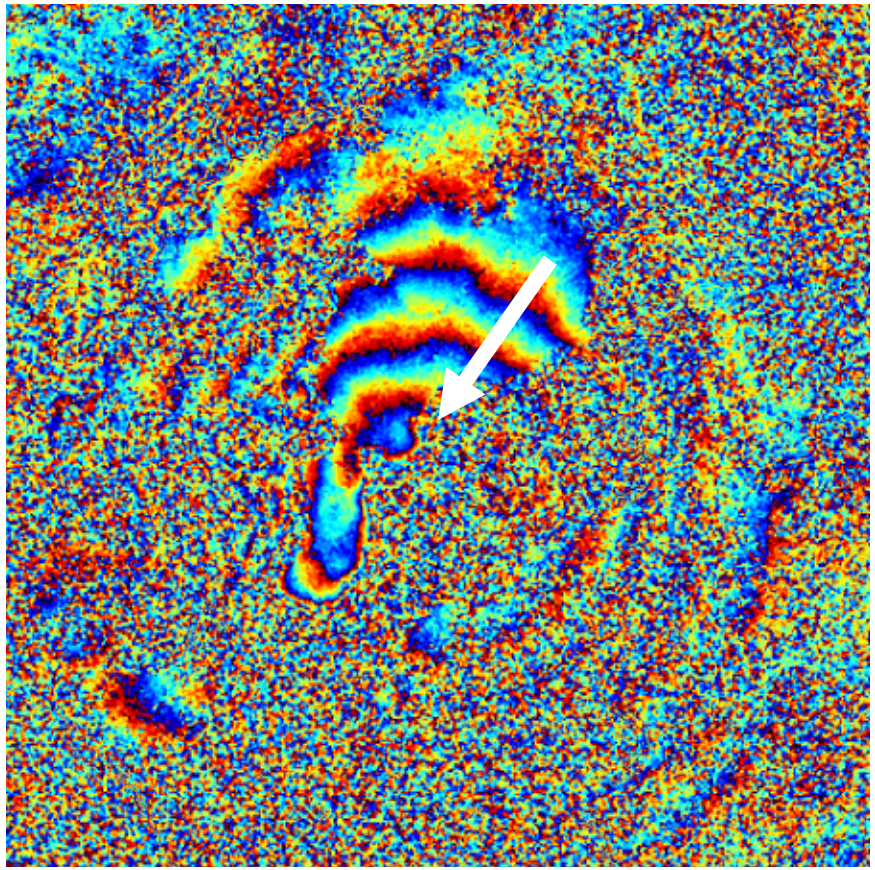

Interferometric phase decreases towards center

⇩

Distance satellite-ground has become shorter towards center

⇩

Relative uplift of the center (9 cm)

Topography and deformation

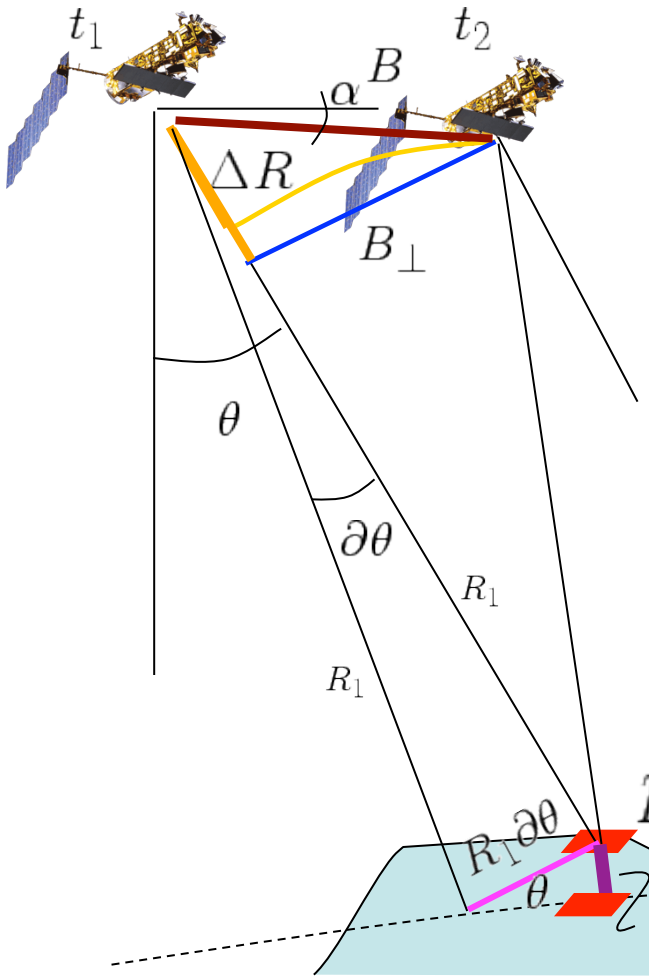

$$H_p = -\frac{\lambda R_1 \sin\theta^\circ}{4\pi B_\perp}\partial\phi$$

$$D_p = -\frac{\lambda}{4\pi}\partial\phi_p$$

$$\partial\phi_p = -\frac{4\pi}{\lambda}\left(D_p + \frac{B_\perp}{R_1 \sin\theta^\circ}H_p\right)$$

B : baseline

$B_\perp$: perpendicular baseline

θ : look angle

H_p : topographic height

Sensitivity to deformation 1000x higher than for topography

Ellipsoid

$2R_1$ R $2R_2$

One interferogram (igram) only provides one component (LOS) of the displacement field - pay attention to LOS vector.

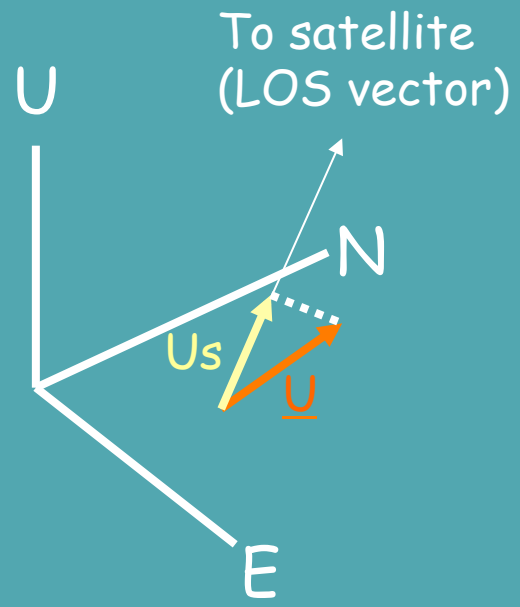

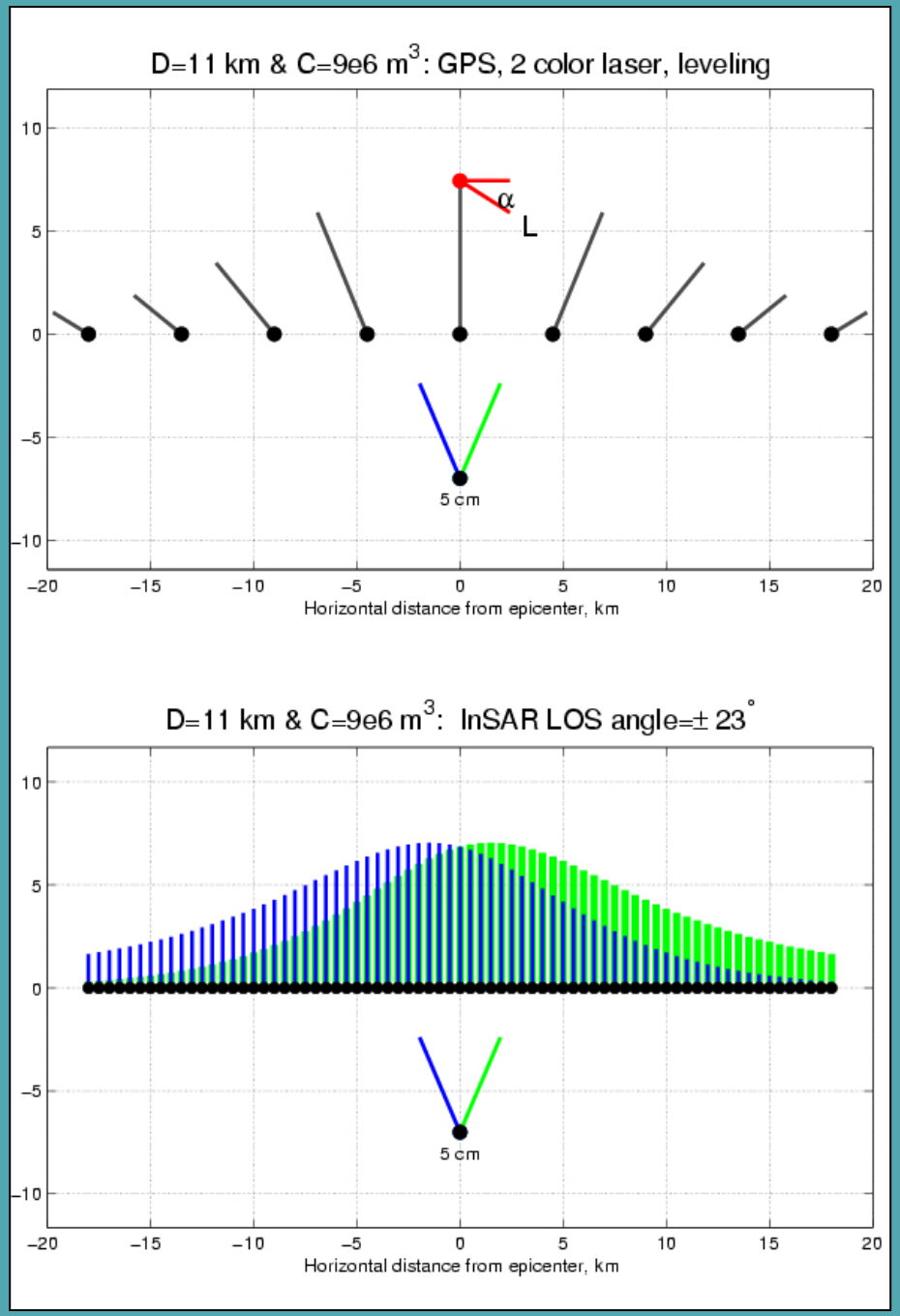

Atmospheric disturbance

- Spatially varying disturbance signal
- Can be ~5 cm over 20 km
- Spatially correlated but temporally uncorrelated ($\Delta t > 1$ day)
- Introduces covariances in stochastic model

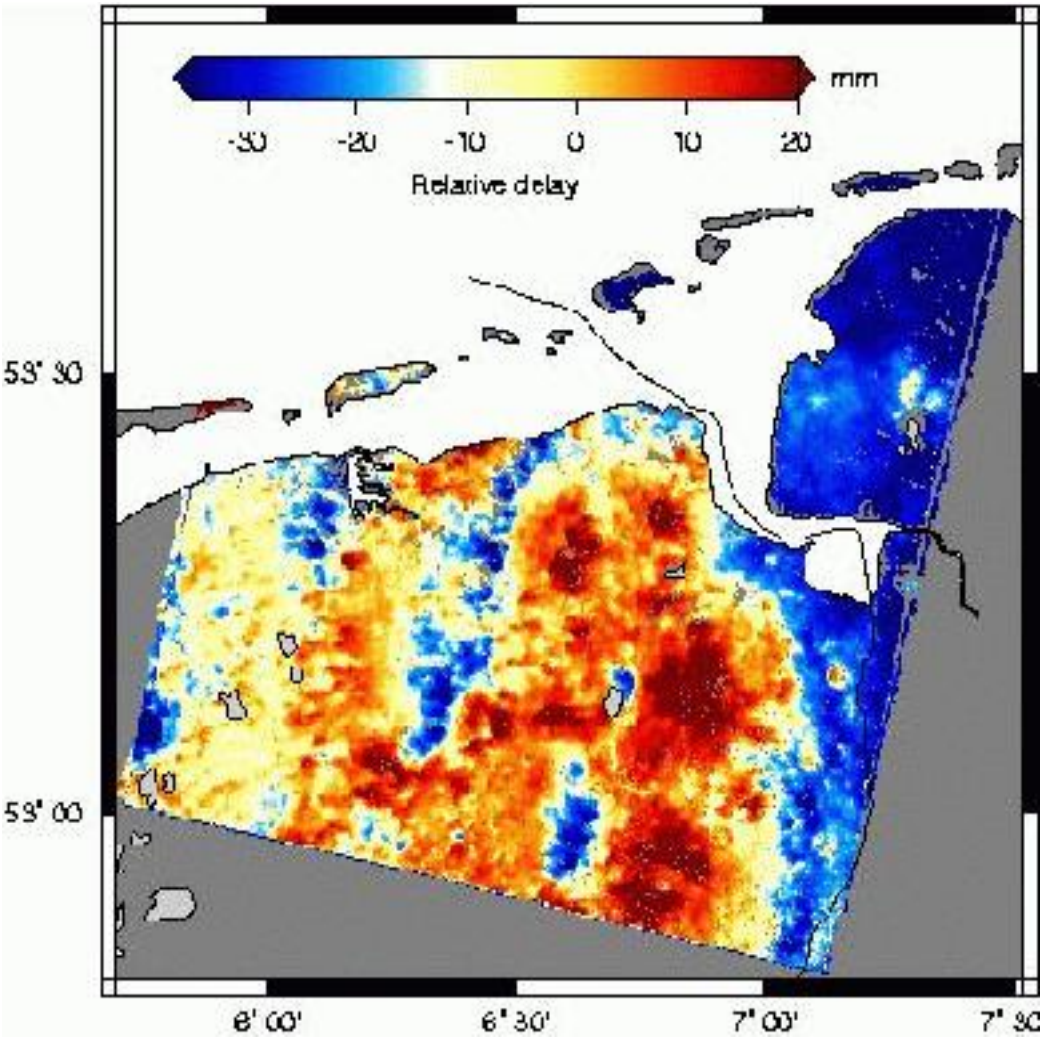

Example Interferometric Radar Meteorology

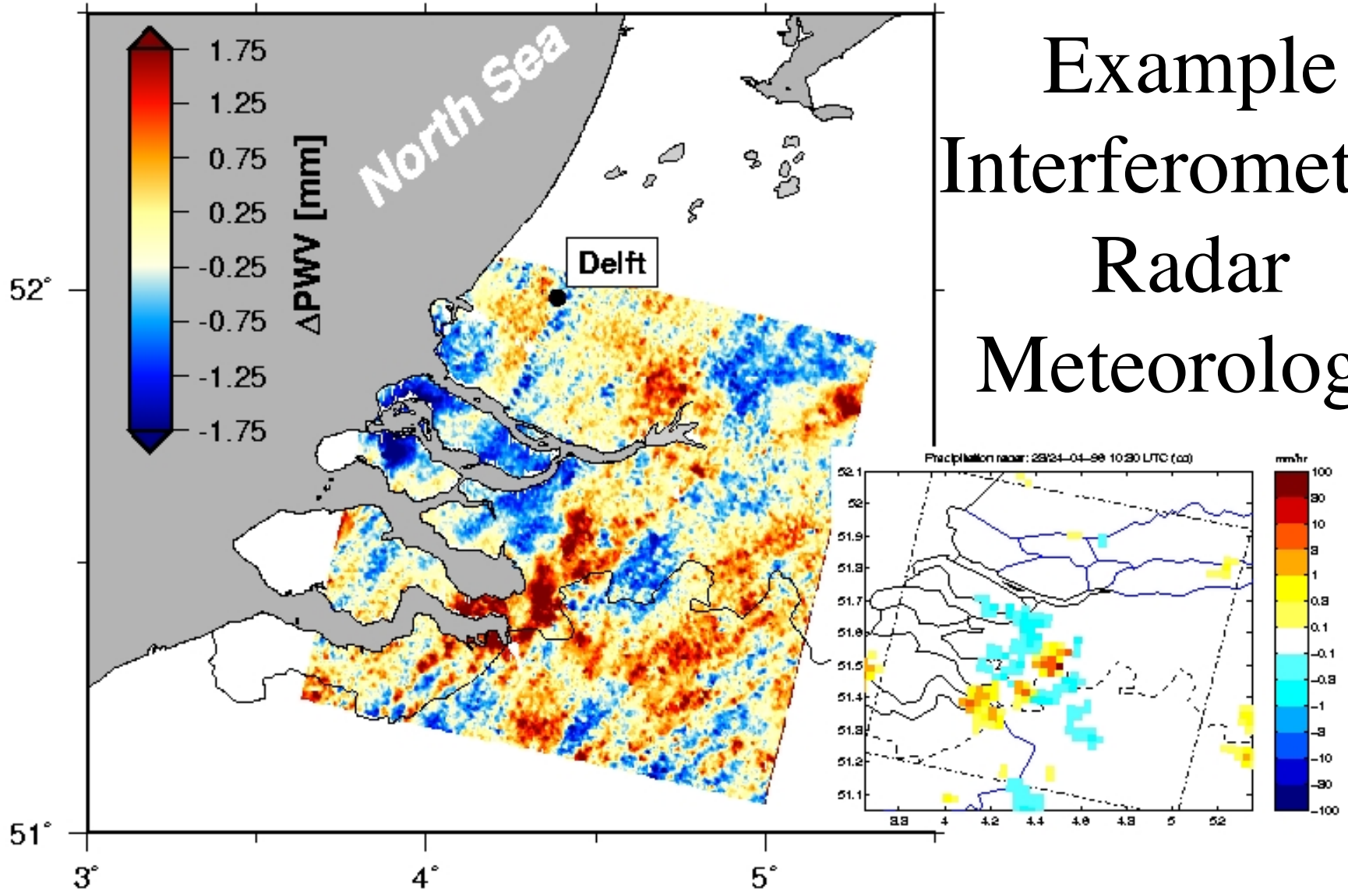

Geometric decorrelation

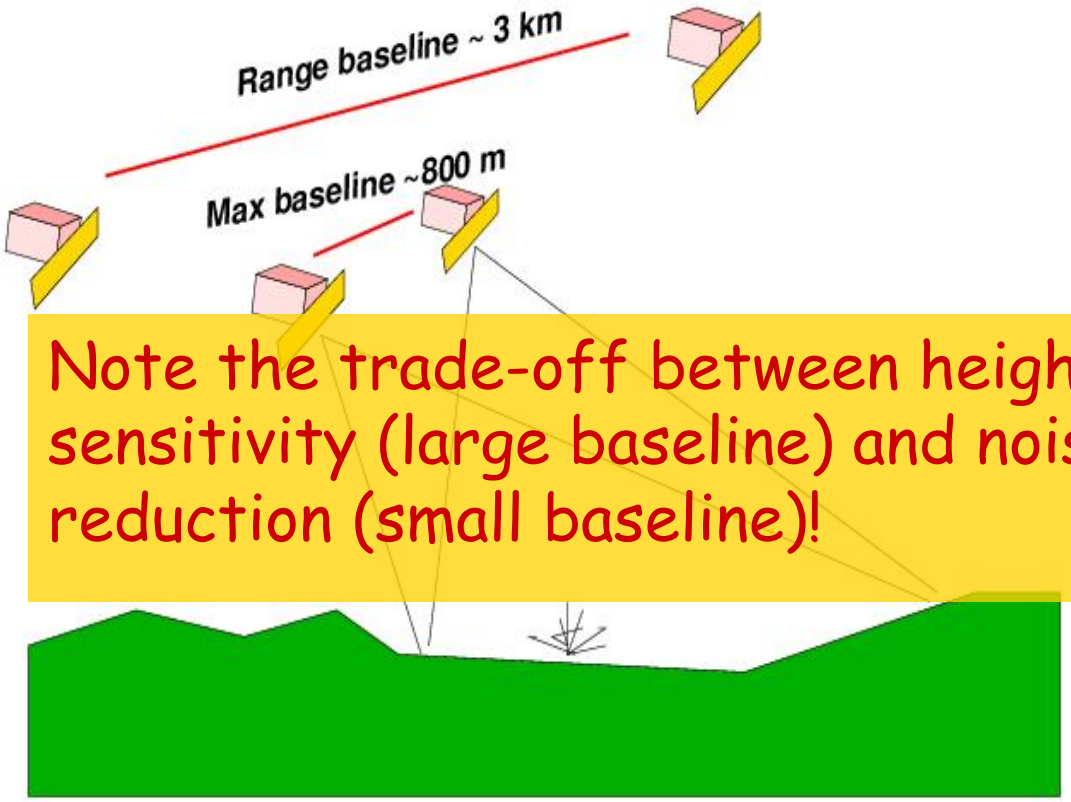

Note the trade-off between height sensitivity (large baseline) and noise reduction (small baseline)!

- Baselines vary
- Relative scattering mechanisms change
- Images become uncomparable
- Function of baseline, Doppler centroid, and terrain slope

Temporal decorrelation

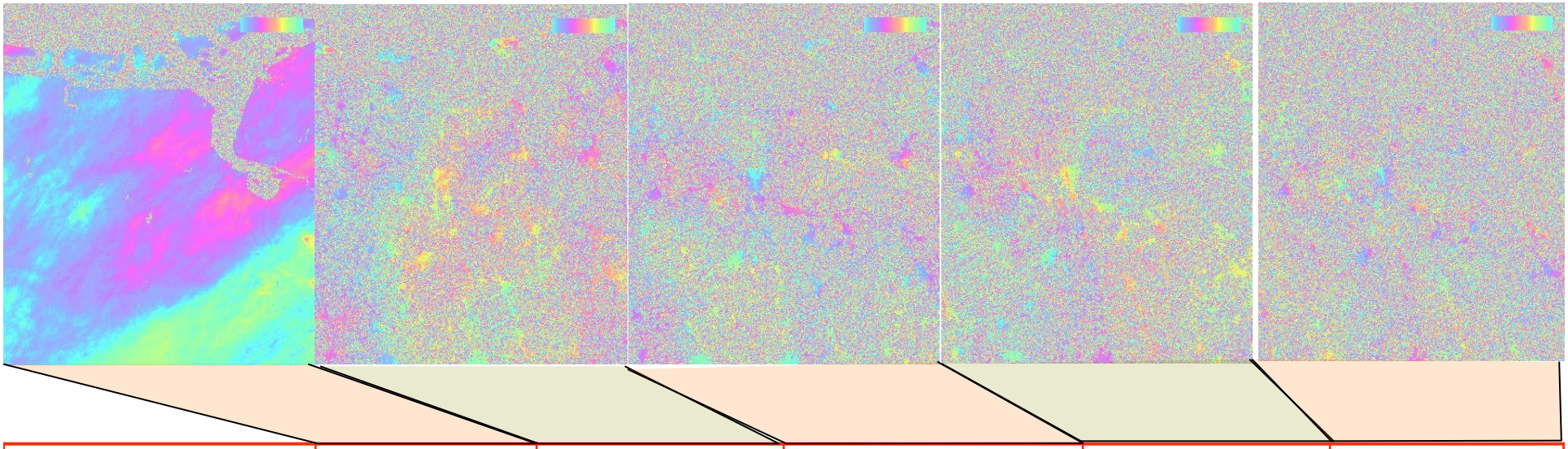

Temporal baseline	1 day	1 year	2 years	3 years	6 years
Perpendicular baseline (m)	29	112	93	185	166

Envisat interferograms (single master)

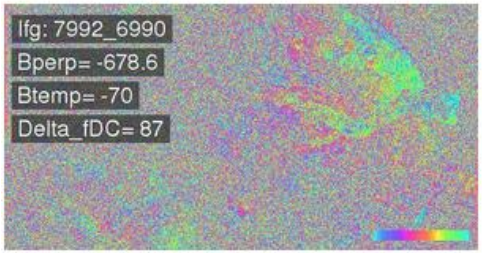

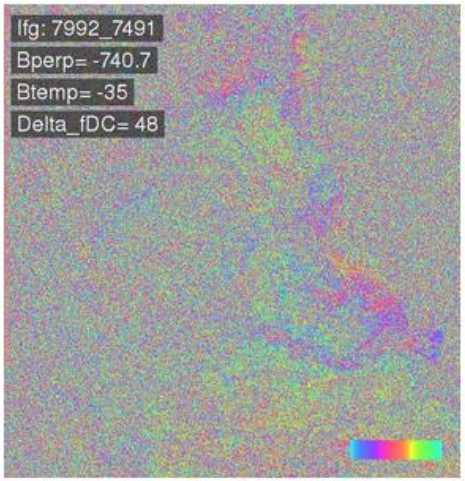

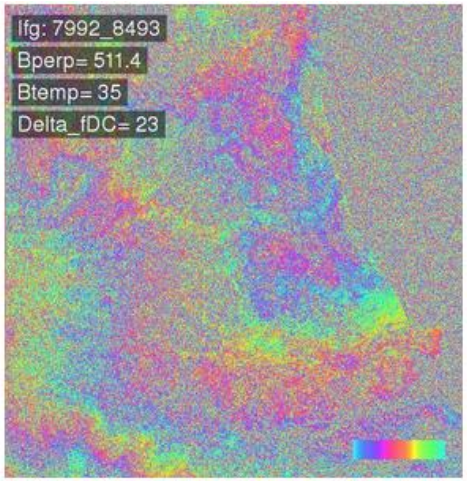

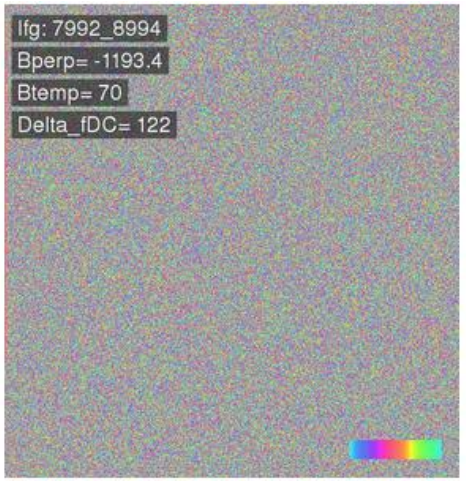

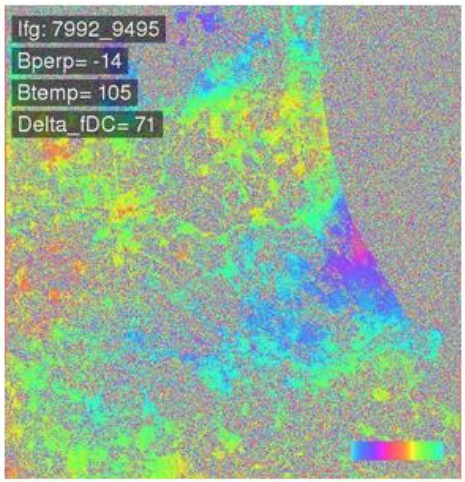

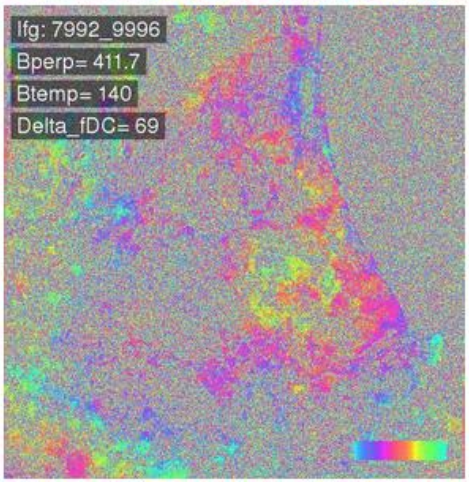

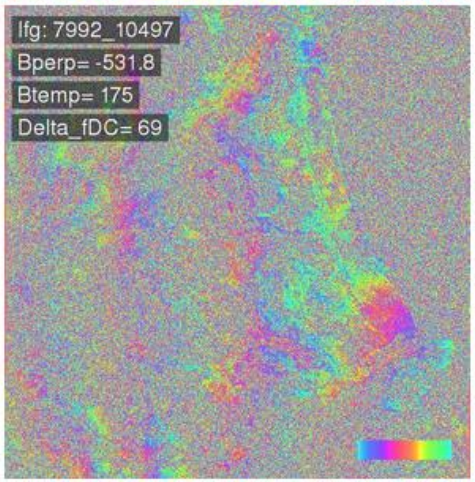

Volcanoes

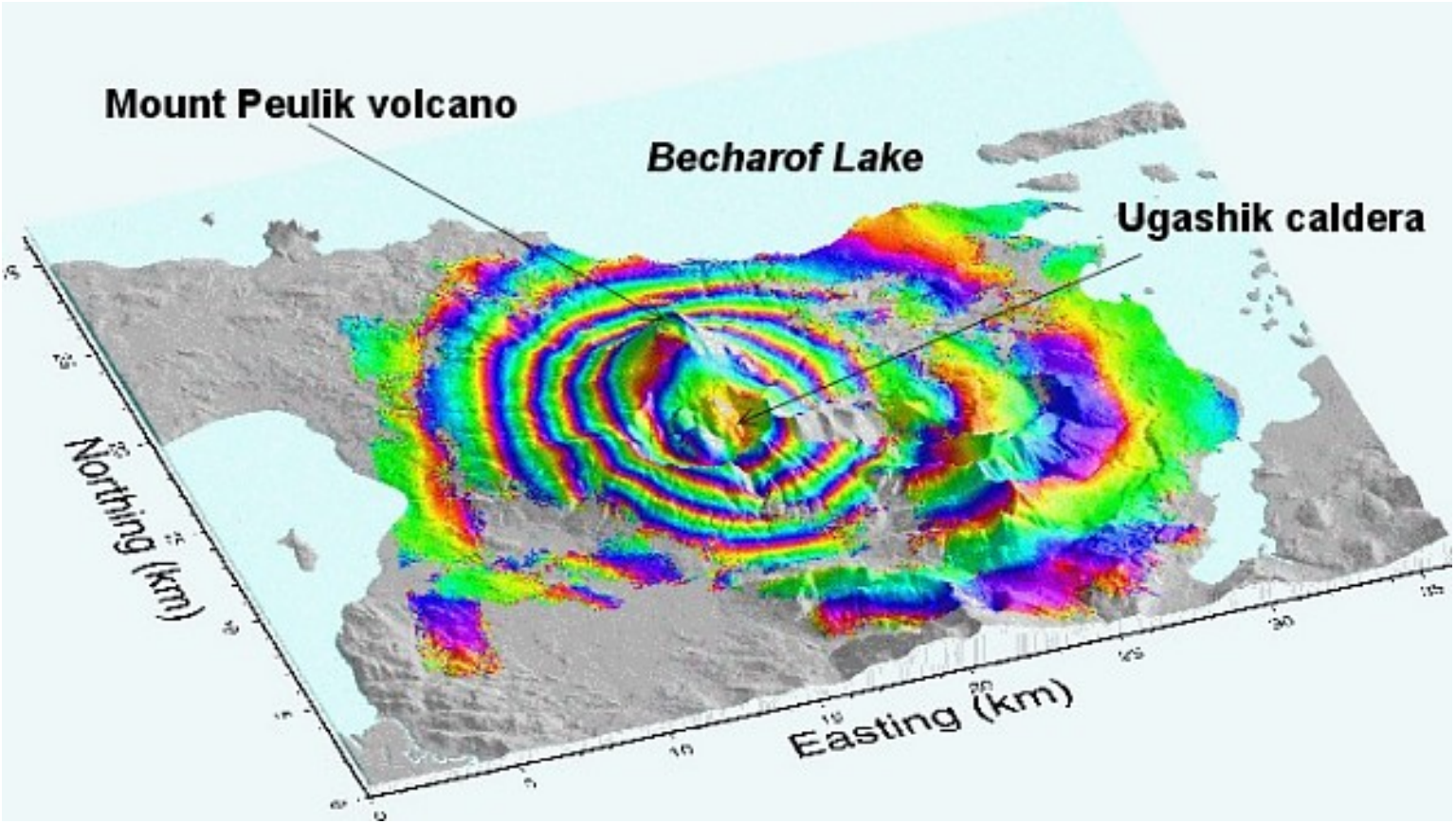
Mount Peulik volcano
Becharof Lake
Ugashik caldera
Northing (km)
Easting (km)

Mapping Out Large Swaths

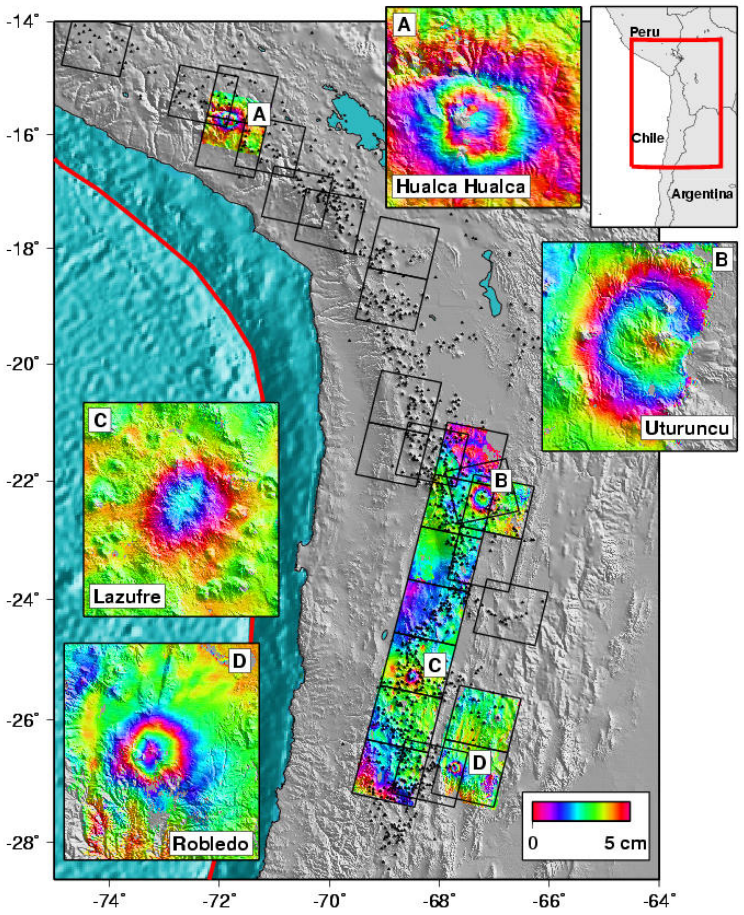

- From Pritchard and Simons (2002)
- Found inflation at 4 volcanic centers in Andes
- None were really expected

Volcanic source models

Point inflation source
(Mogi, 1958)

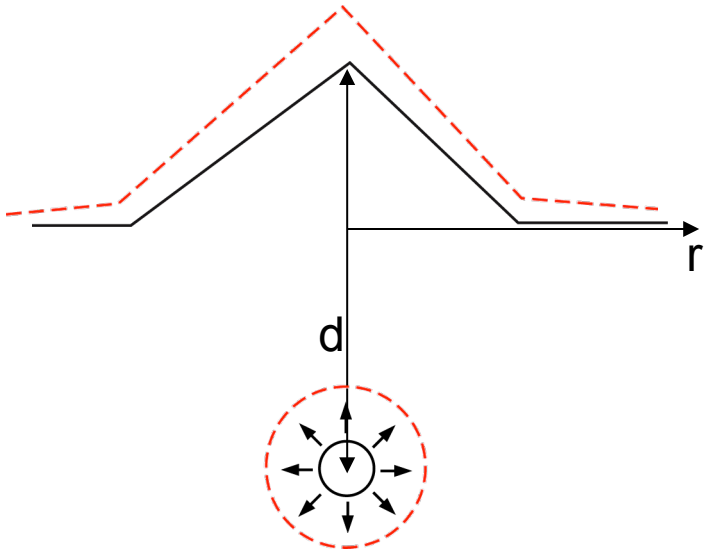

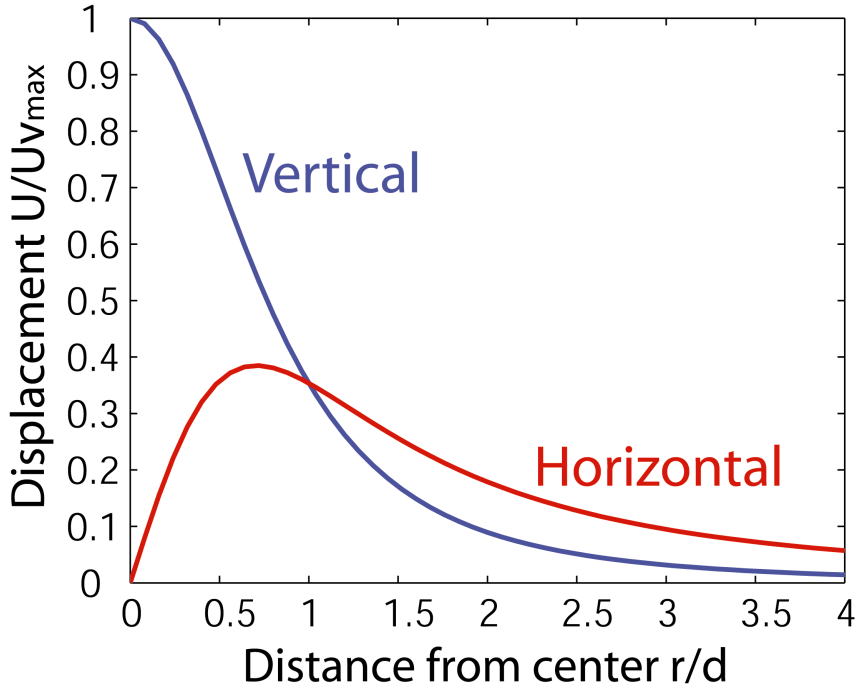

Uvmax: max. vertical displacement
d: source depth

Okmok Volcano, Alaska-Aleutian arc

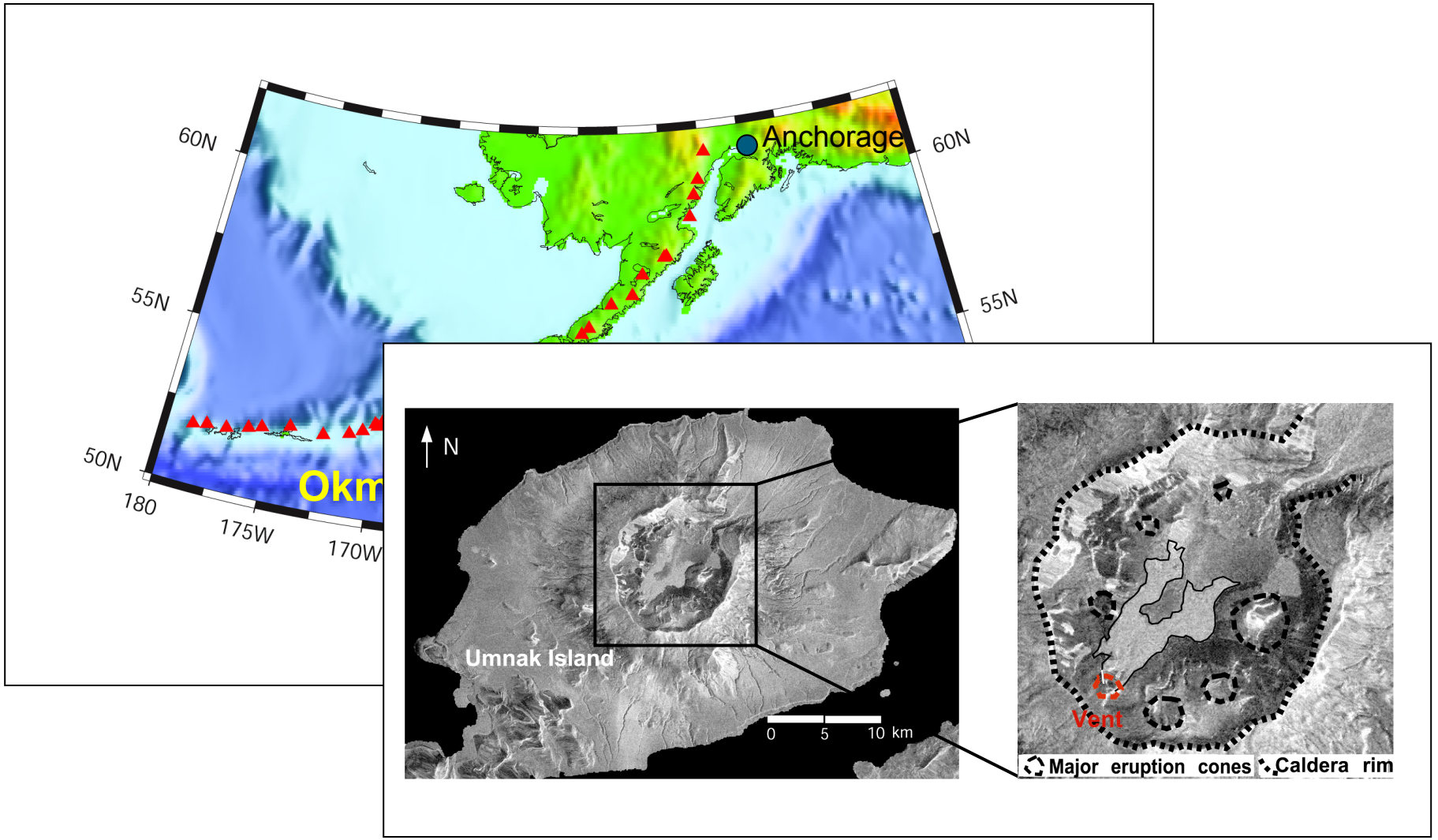

Deformation

1992 - 1993

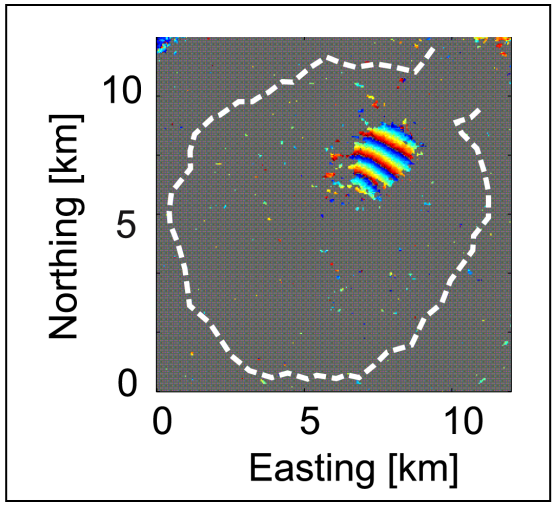

1995 - 1997

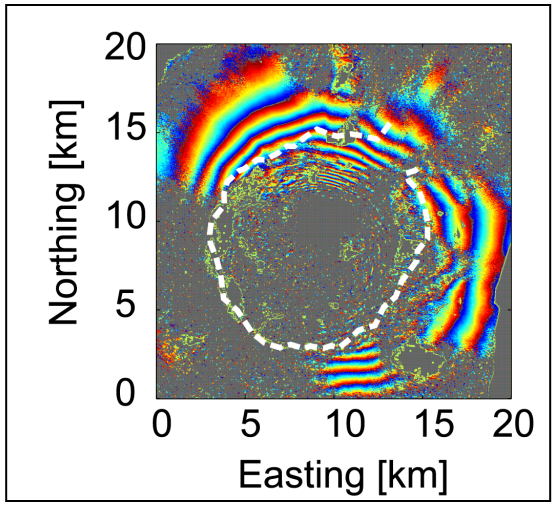

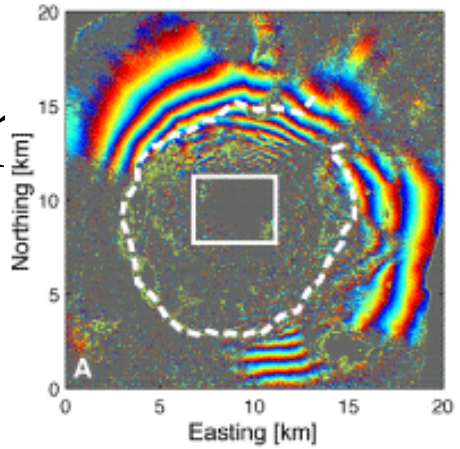

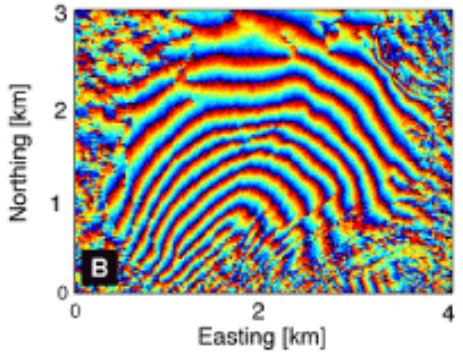

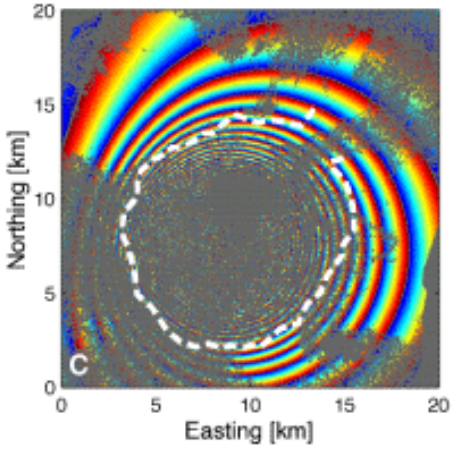

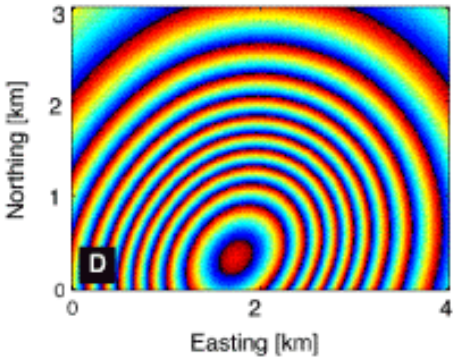

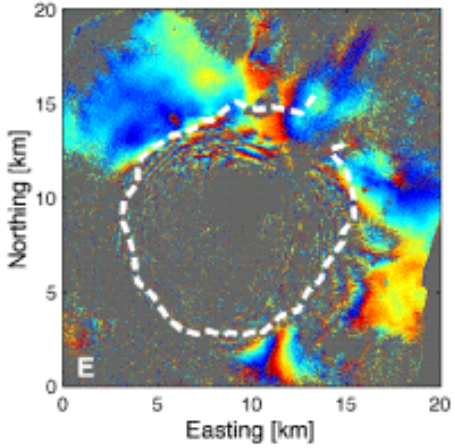

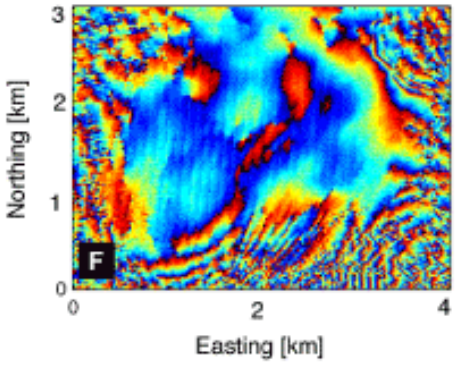

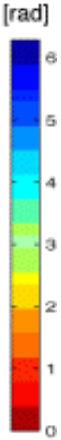

Source locations and depths

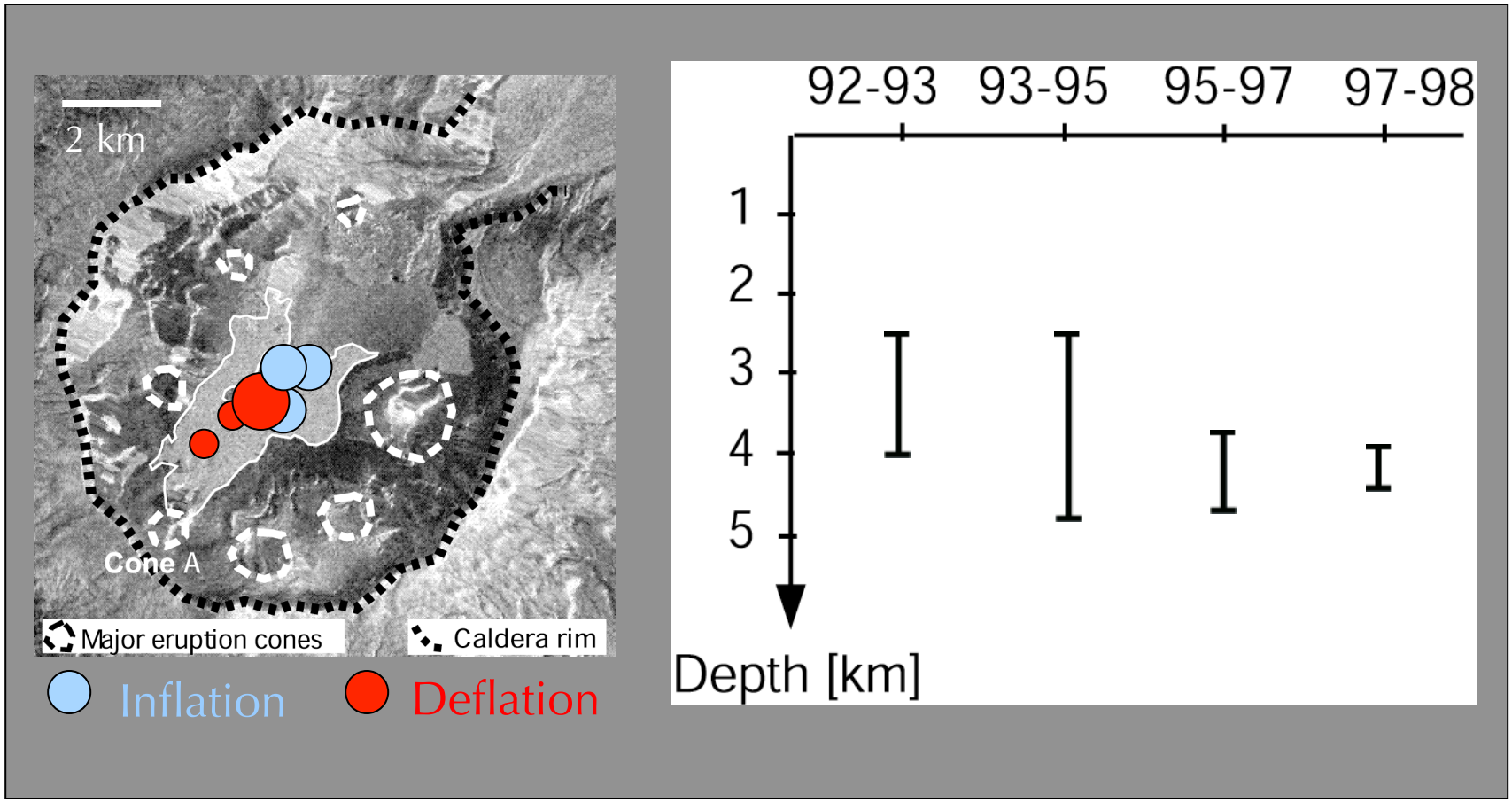

Time dependence of deformation

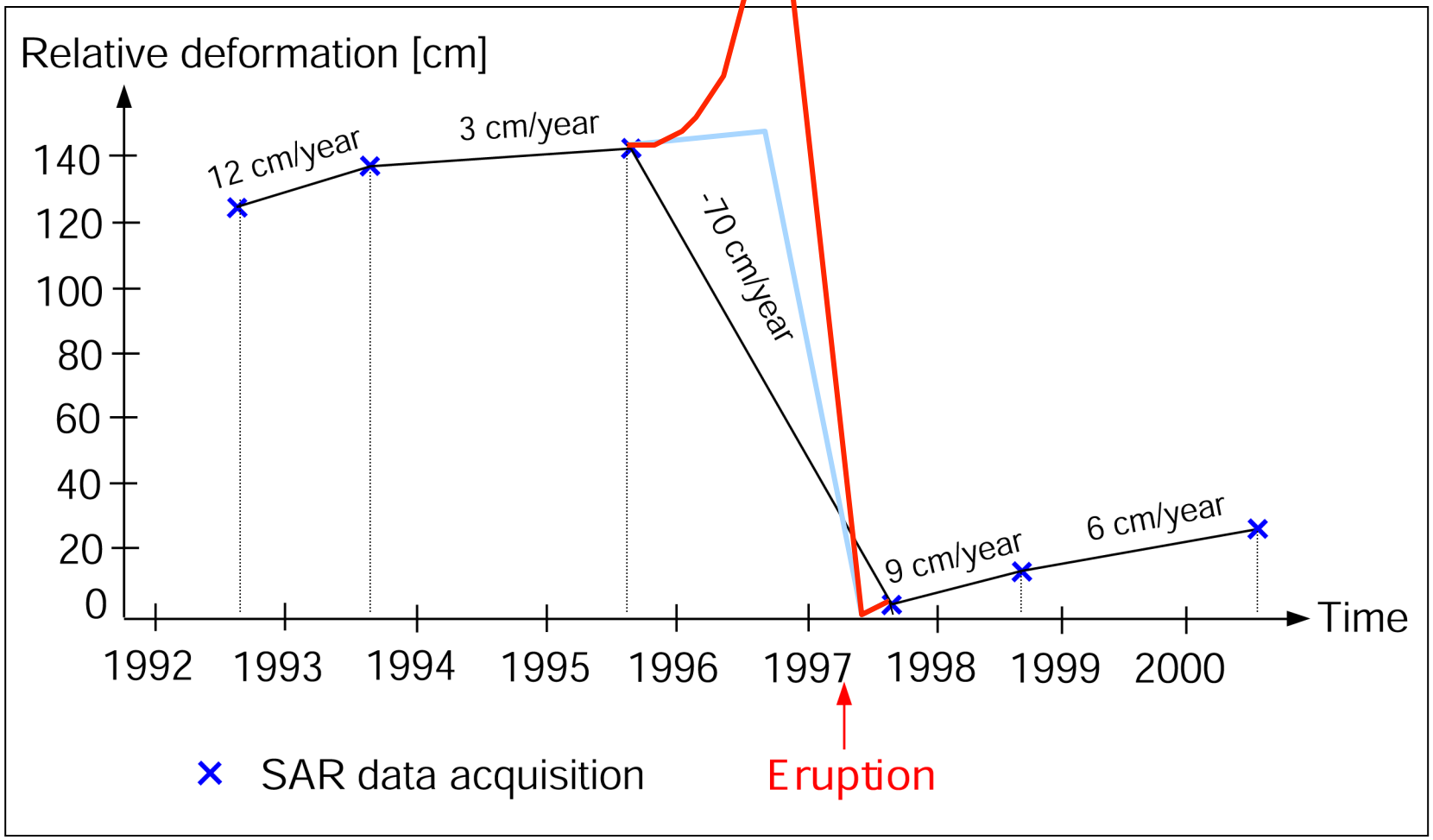

Magma Volume and Eruption Frequency

- Eruption volume in 1997: 70×10^6 m^3

- Average magma accumulation rate during inflation periods: $3\text{-}6 \times 10^6$ m^3/yr

Estimated recurrence time : 15 years

- Eruptive history:

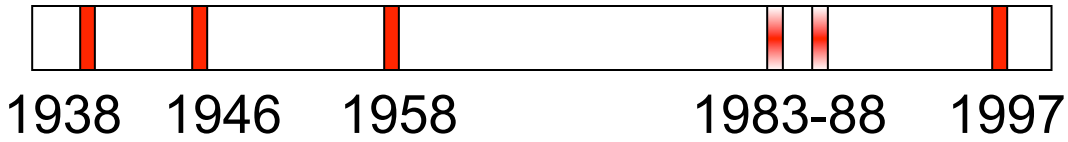

Observed magma accumulation rate is typical for the long term, suggesting continuous supply from a deeper source

Mann et al. (2002)

1992 Mw 7.3 Landers
1999 Mw 7.1 Hector Mine

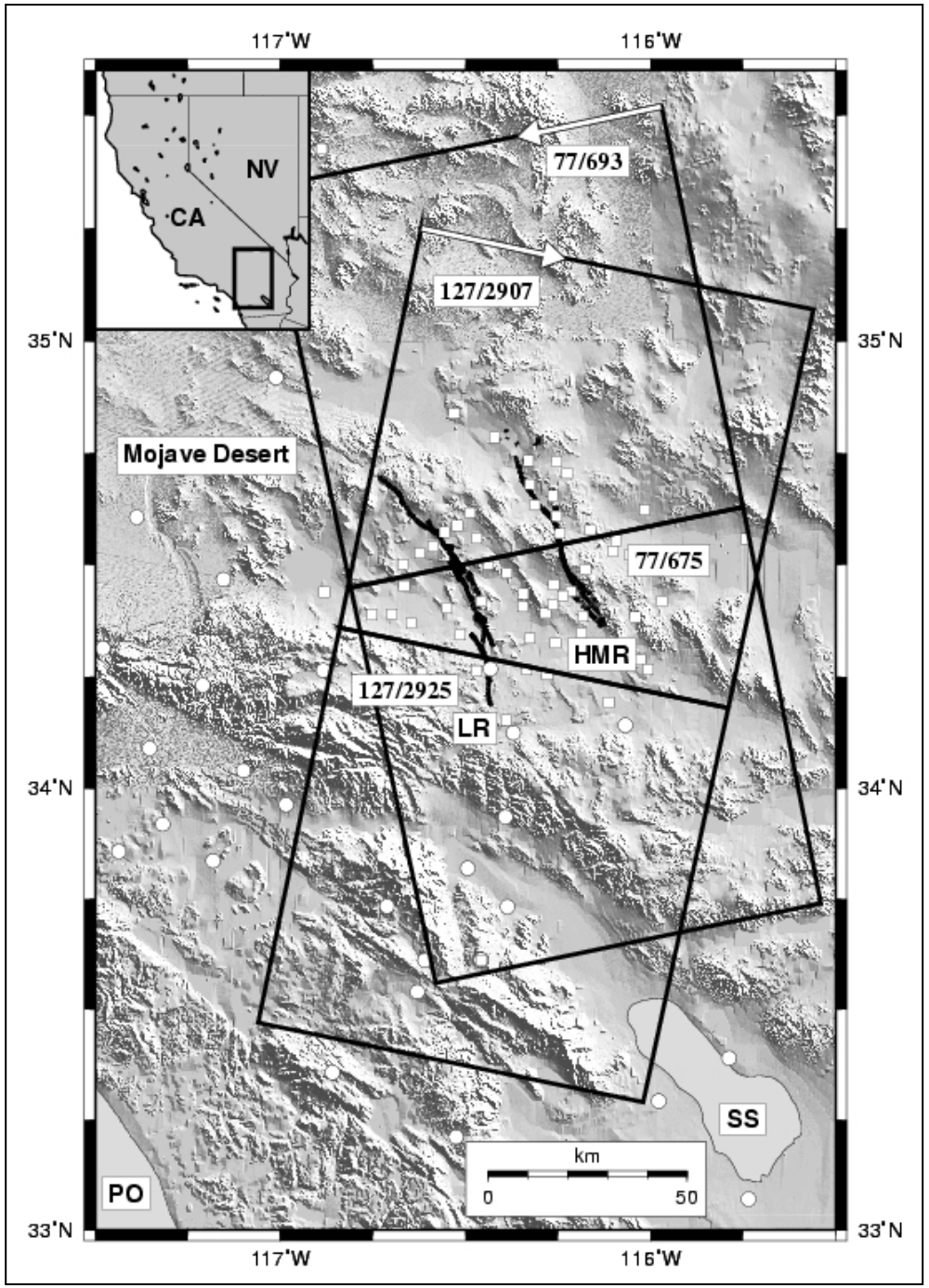

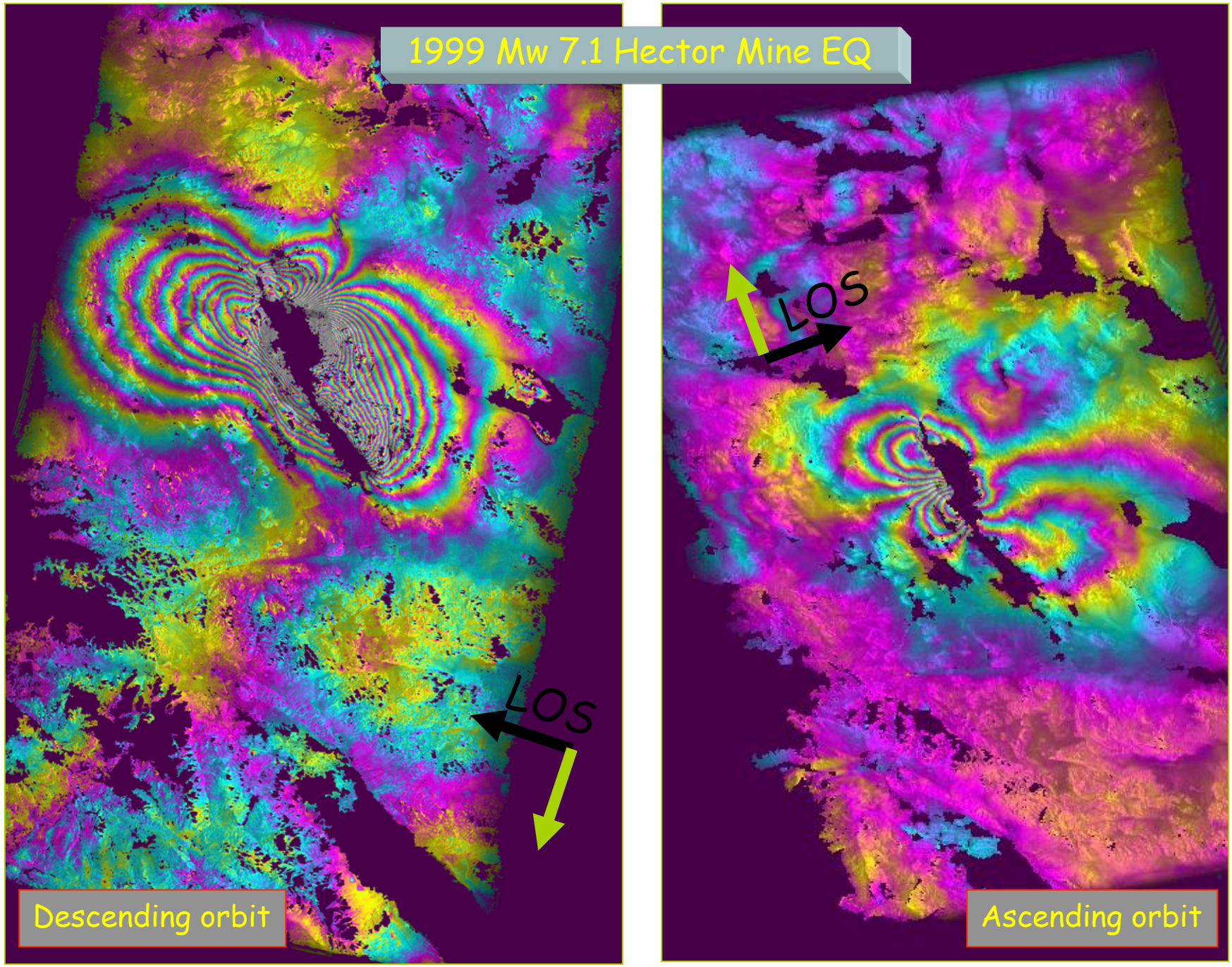
1999 Mw 7.1 Hector Mine EQ
LOS
LOS
Descending orbit
Ascending orbit

1999, Mw 7.1 Hector Mine, CA Earthquake

Tracking features in imagery:
How much did a boulder/cactus move?

- Find shift (offset) that maximizes cross-correlation of small ensembles of pixels in two (before/after) images
- With radar data, along track component of offsets is perpendicular to LOS phase
- Does not need to be phase unwrapped
- Sensitivity much less than InSAR
- Can use optical data too (satellite and airphotos)
- Other applications (glaciers, …)

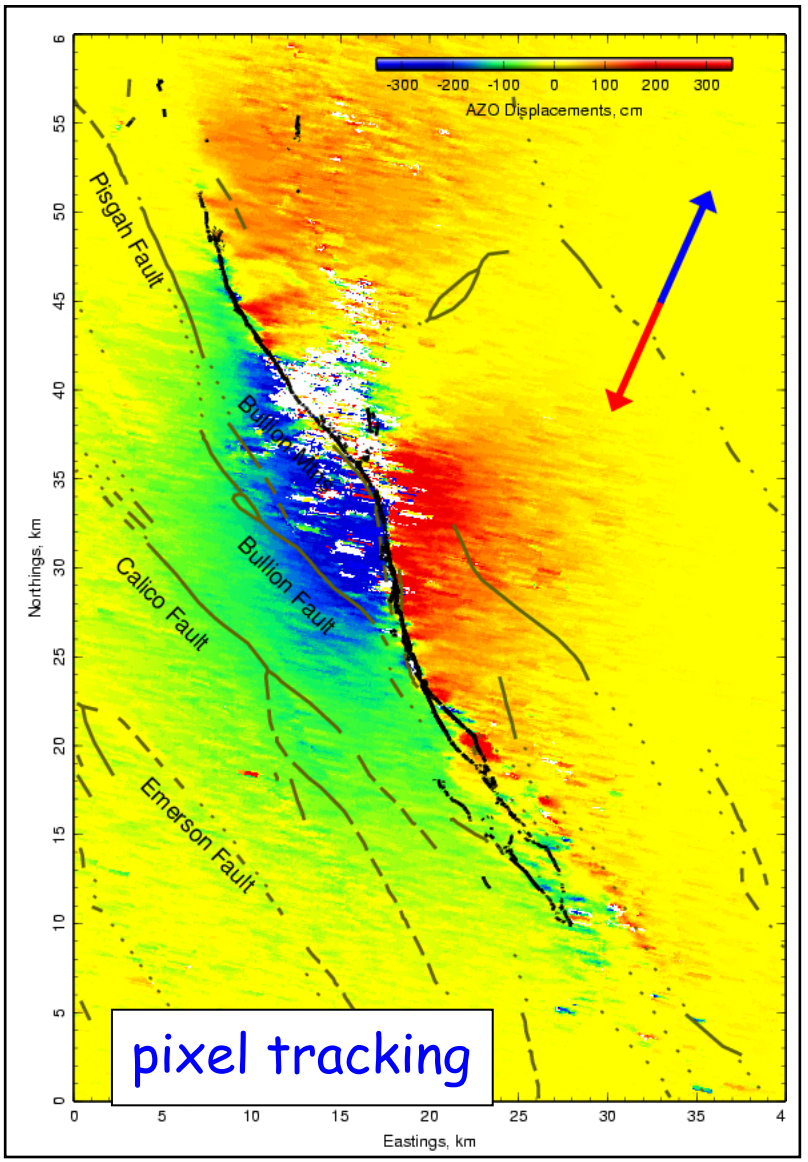

1999 Mw 7.1 Hector Mine EQ

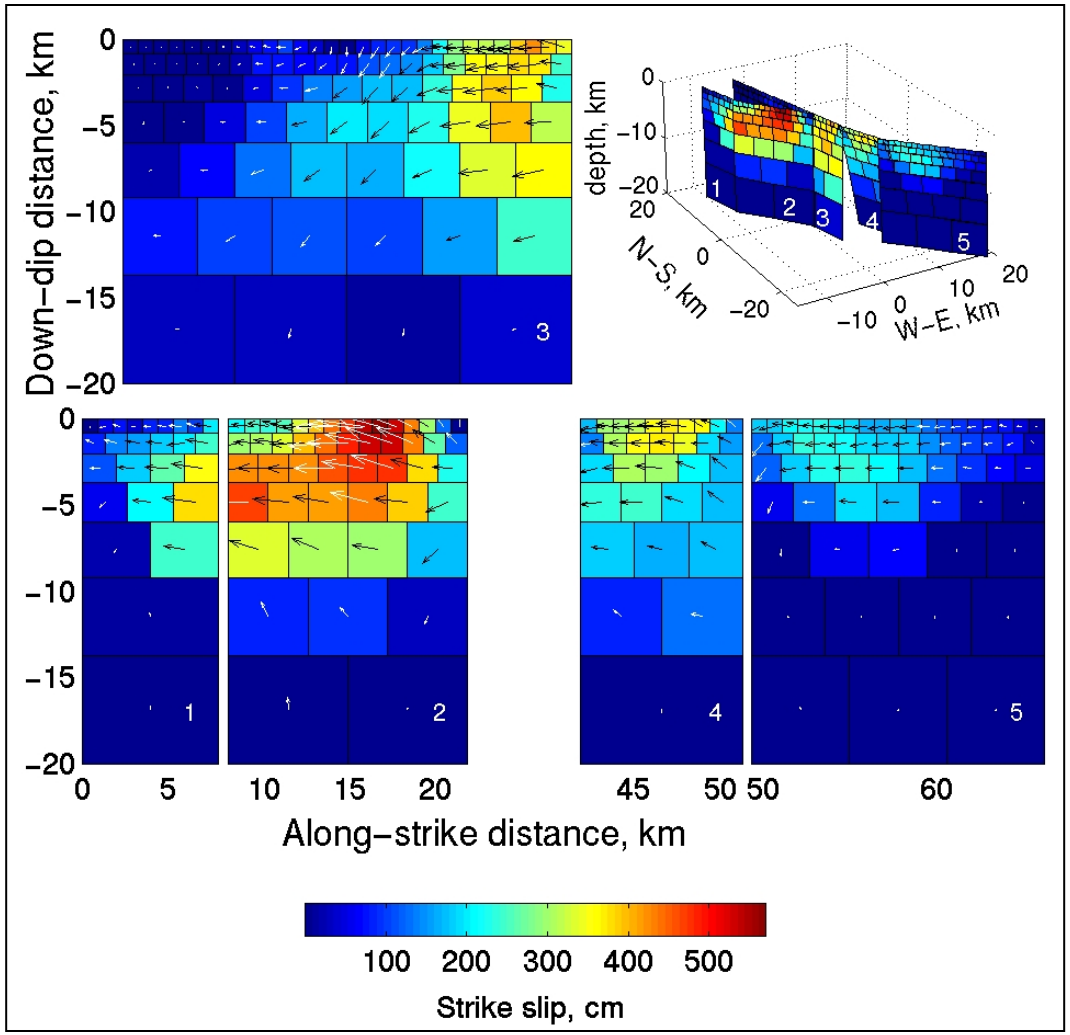

Inferred subsurface coseismic fault slip

3D displacement field

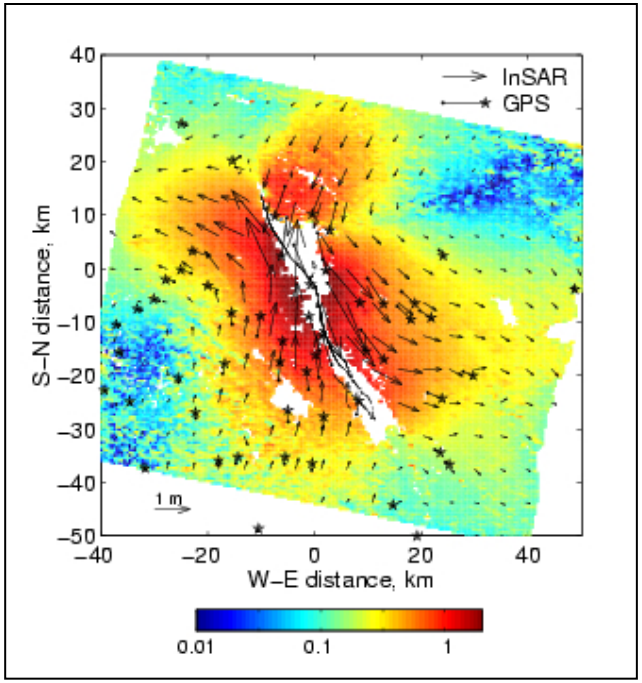

- Significant vertical fault slip
- Fault slip concentrated at shallow depth (7 to 10 km)
- Use as input into post-seismic models

Flow of Rutford Ice Stream

6 days of displacement, each fringe ~28 mm LOS

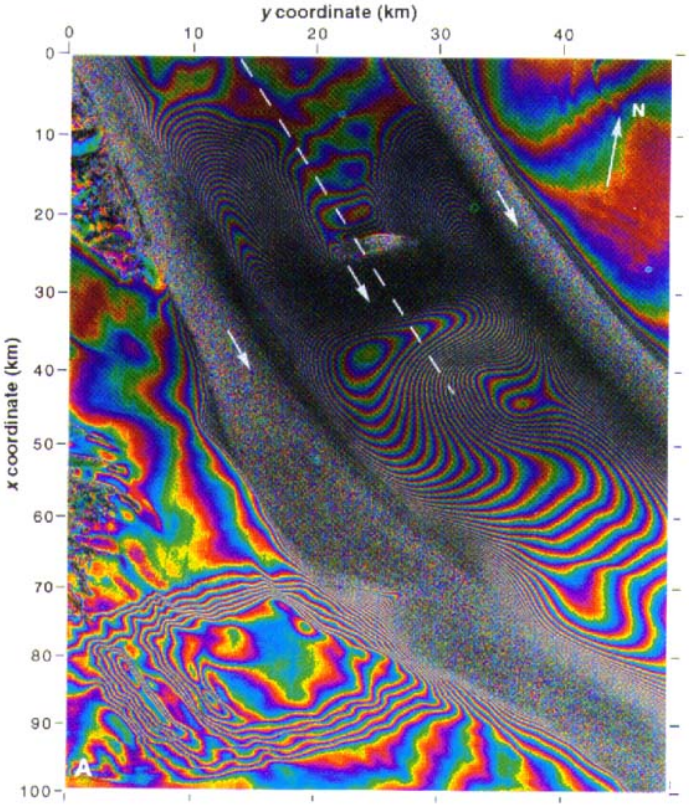

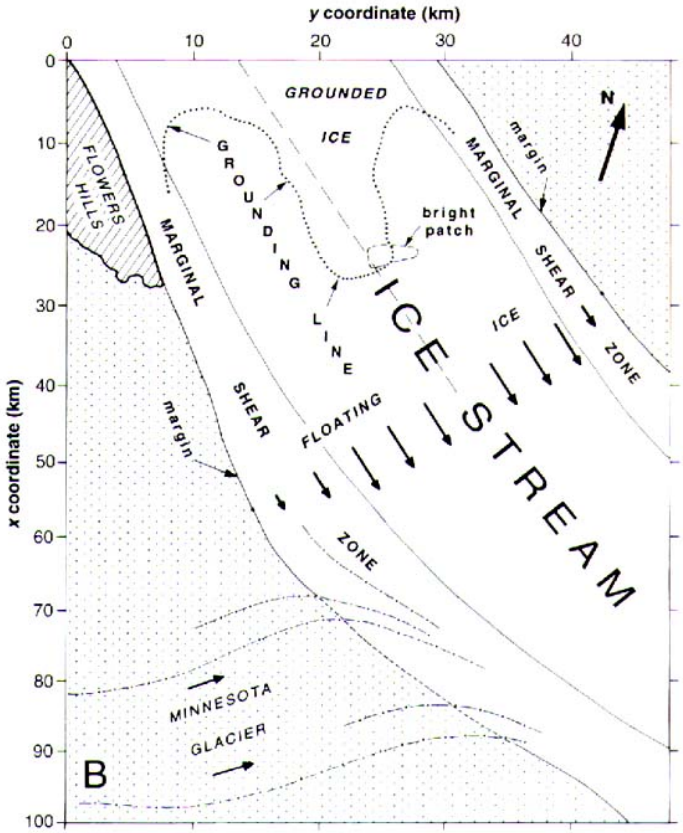

D. Goldstein, JPL

Patagonia Ice Velocities

from Shuttle Imaging Radar (SIR-C)

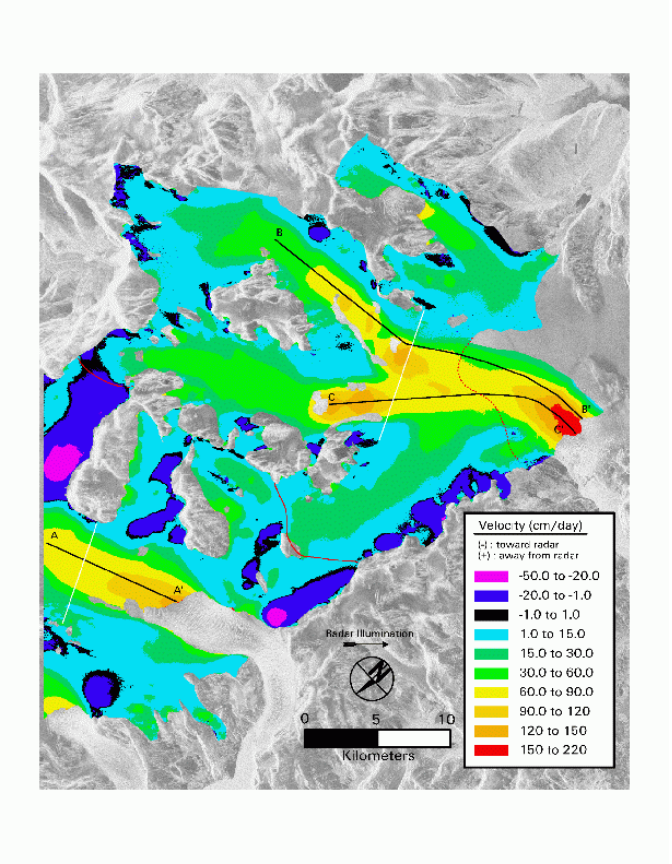

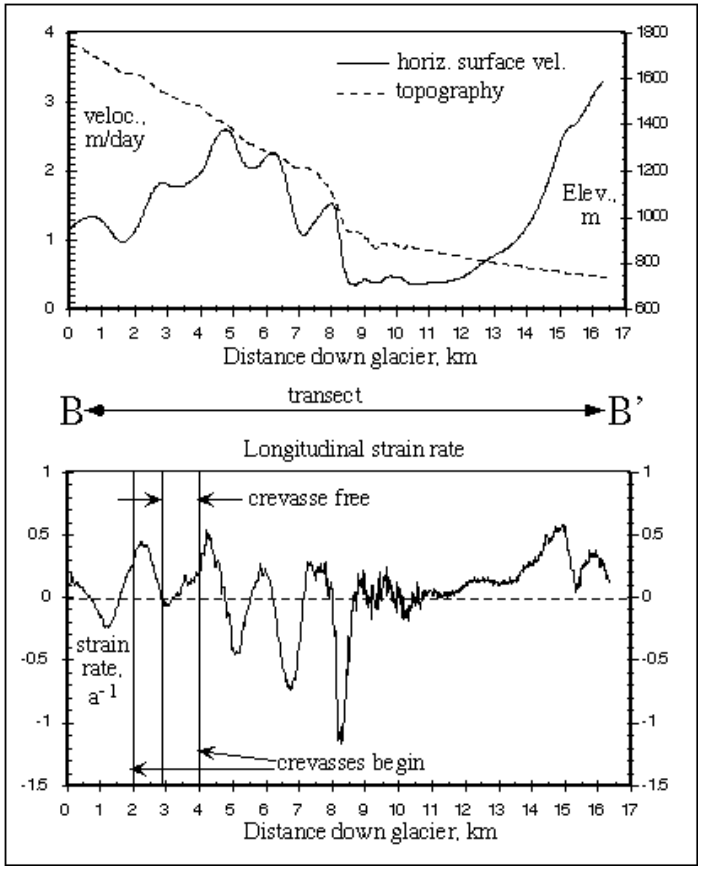

Isacks et al. (1997)
http://www.geo.cornell.edu/geology/SIRC_Pat/patagonia.html

InSAR Glacier Velocity

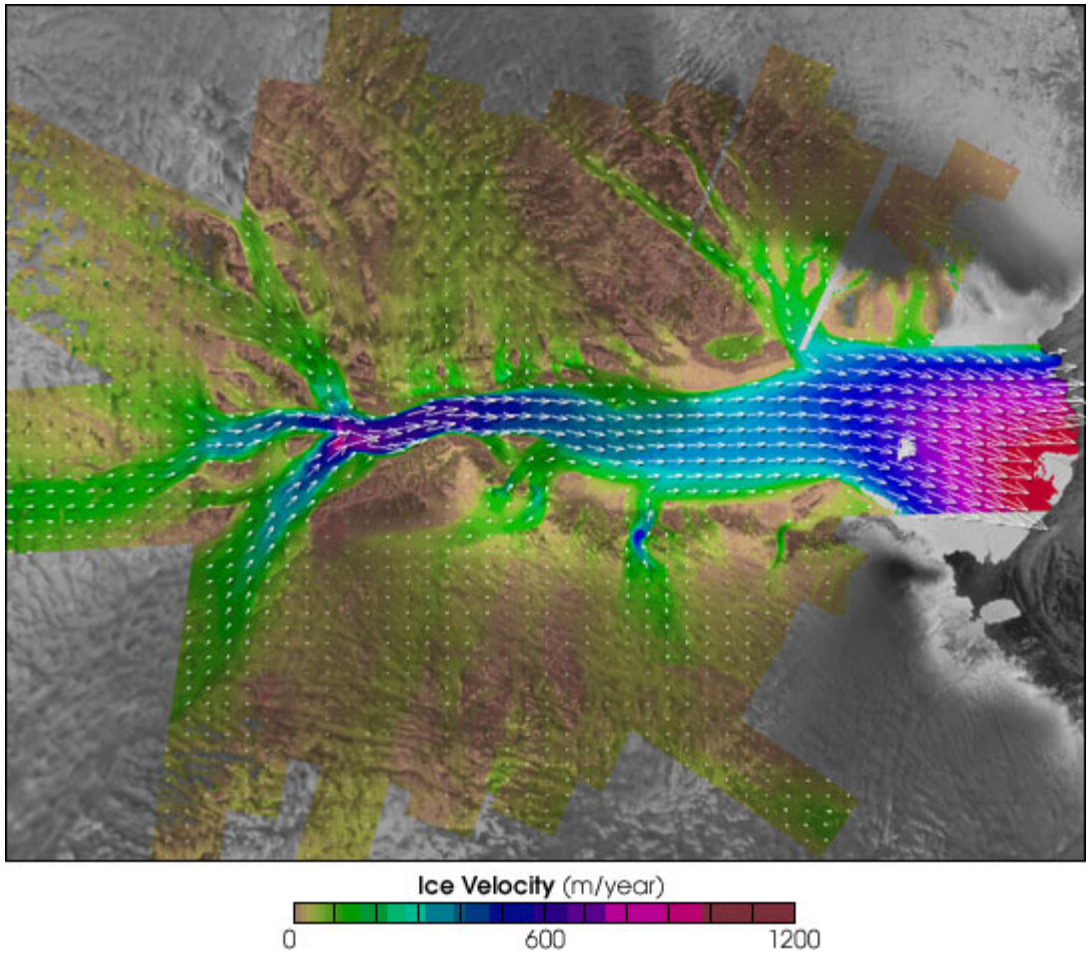

DInSAR

Land Subsidence

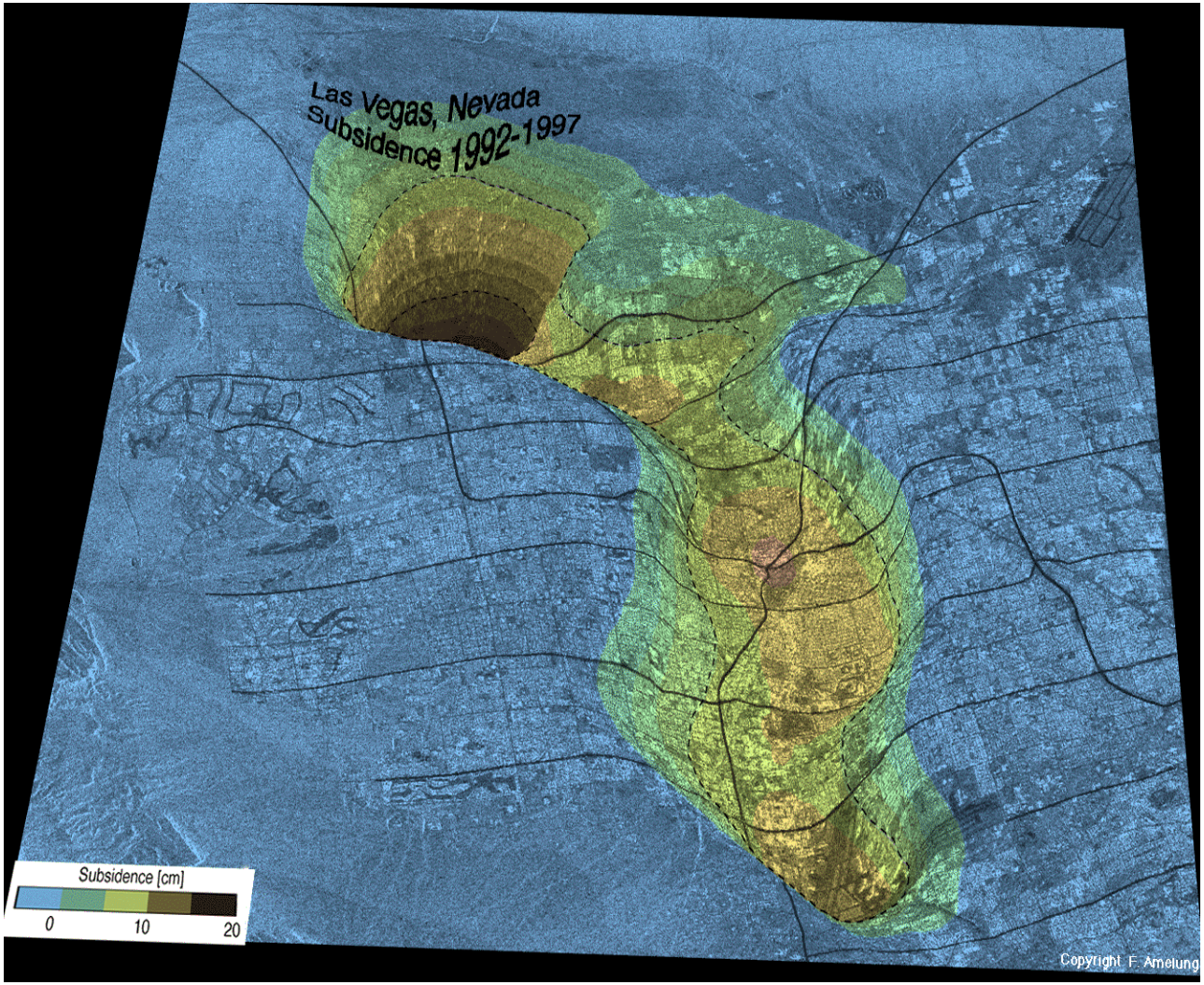

PS principle

- Pixels with strong and consistent reflections in time.
- Multi-pass InSAR – time series necessary.
- Estimate atmospheric signal:
  - Spatially, not temporally correlated.

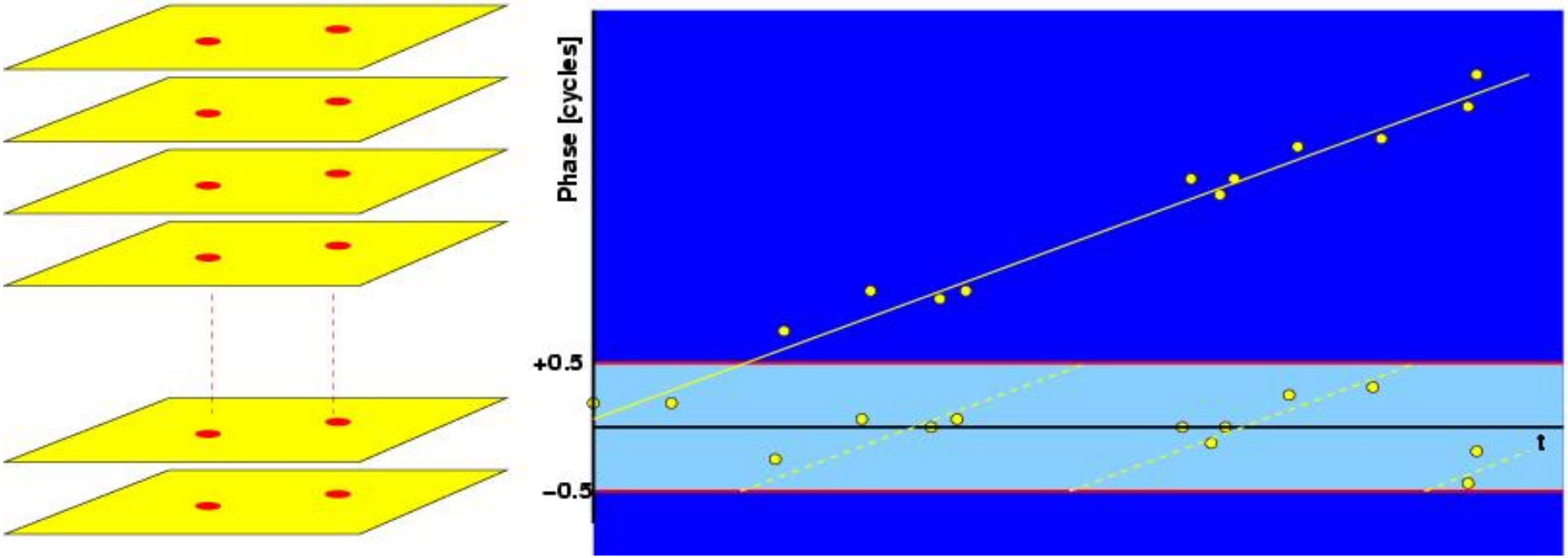

Persistent Scatterers processing

Preprocessing: Selection test areas

Selection potential PS points

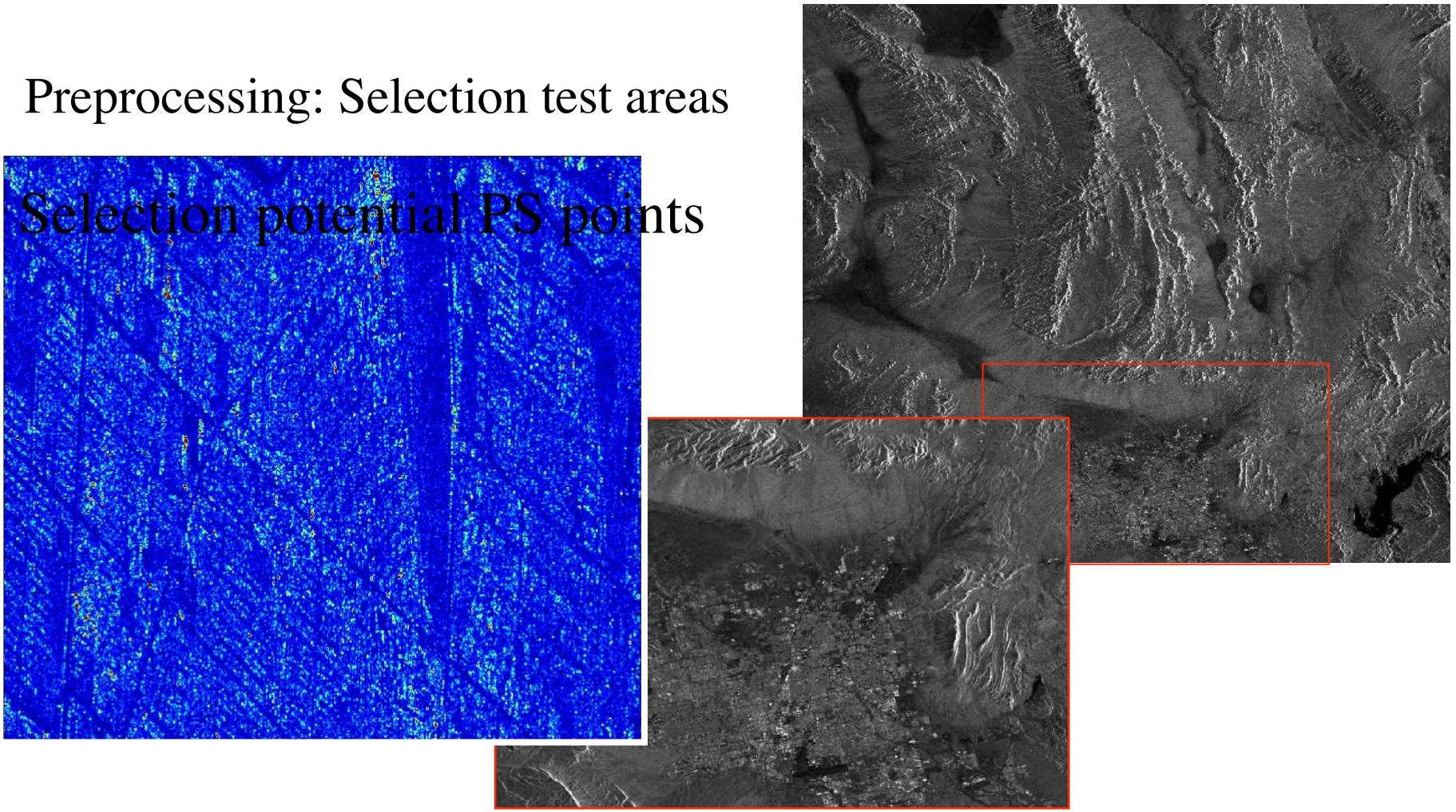

Persistent Scatterers processing chain

- Persistent Scatterer Candidates selection, based on amplitude dispersion (Ferretti et al., 2001)
- Construction network by Delaunay triangulation

- Integer LSQ estimation of ambiguities and parameters
- Testing of residuals
- Spatial unwrapping (path integration)
- Separation of atmosphere and residual deformation by filtering and Kriging
- Removal Atmospheric Phase Screen
- Selection of Persistent Scatterers

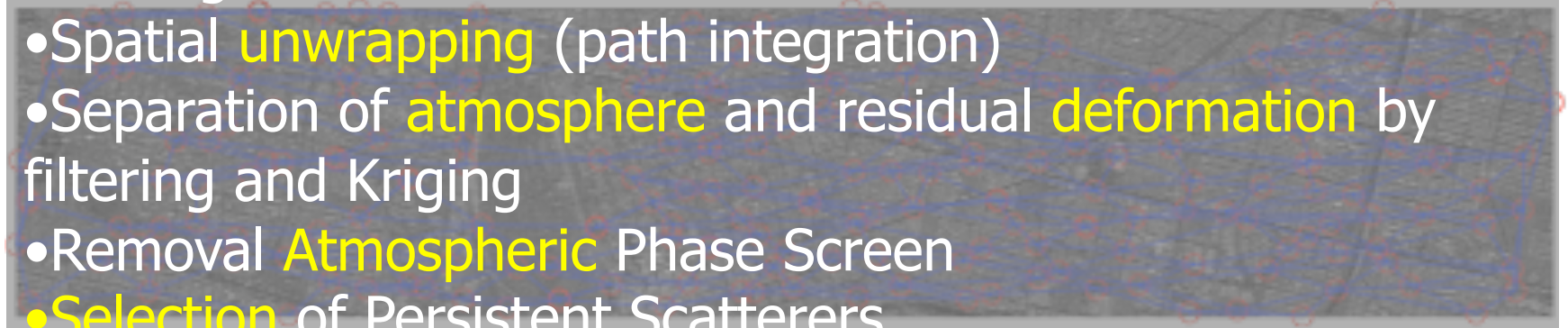
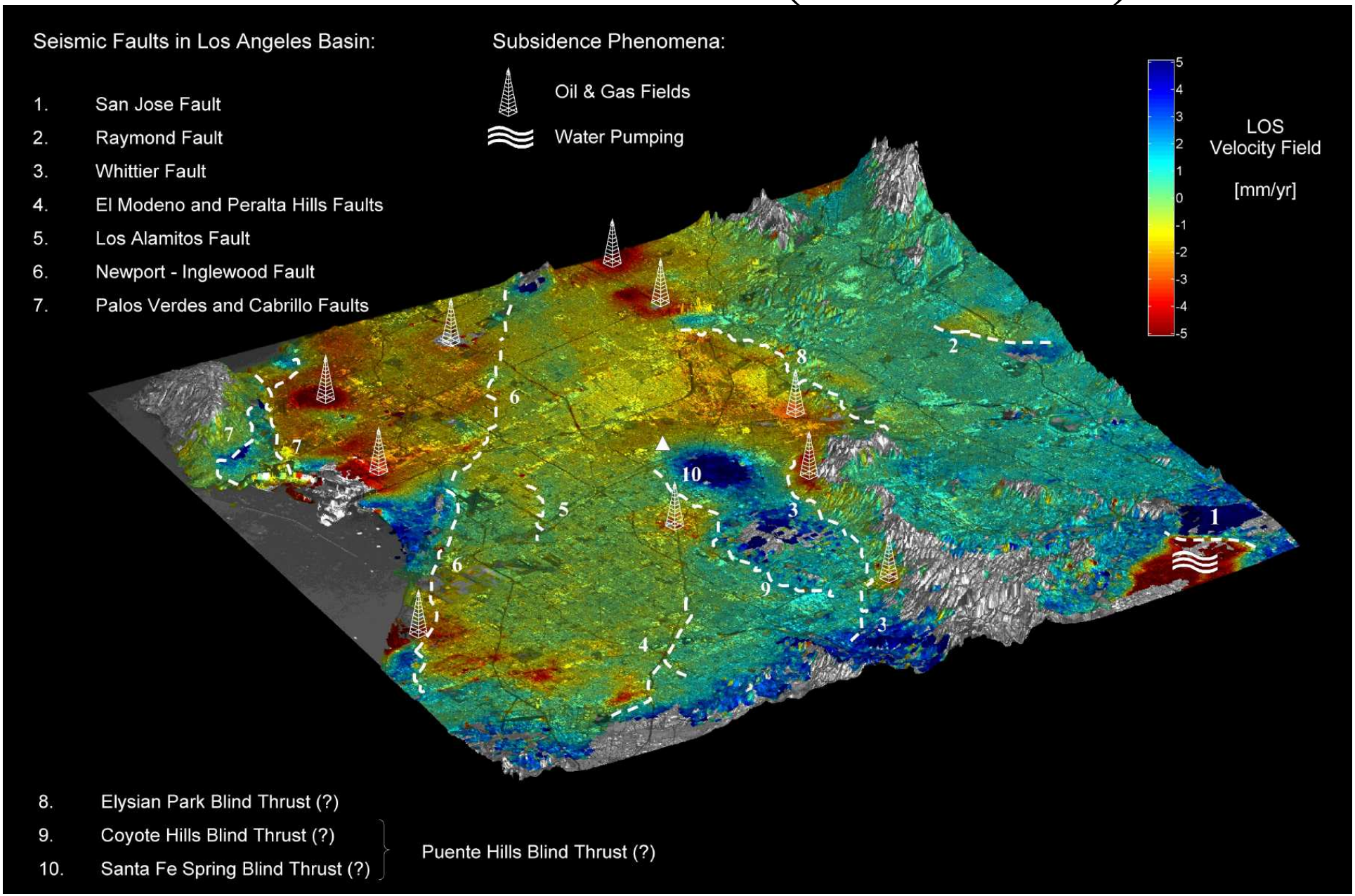
PS Result for L.A. (U. Milano)